

# Zero-Delay Multiple-Descriptions Source Coding of Stationary AR( $p$ ) Sources Using Feedback

Kristian Sjøgaard

Mathematical Engineering

Aalborg University

Department of Electronic Systems &  
Department of Mathematical Sciences

Master's Thesis



Copyright © Aalborg University 2021

This project has been written in  $\text{\LaTeX}$  with figures produced in  $\text{\textit{TikZ}}$  and Python 3.8. Scripts have been made using Python 3.8.



**AALBORG UNIVERSITY**  
STUDENT REPORT

**Mathematical Engineering**  
Aalborg University  
<http://www.aau.dk>

**Title:**

Zero-Delay Multiple-Descriptions  
Source Coding of Stationary  
 $AR(p)$  Sources Using Feedback

**Project Period:**

September 2021 - June 2022

**Participants:**

Kristian Søgaaard

**Supervisors:**

Jan Østergaard  
Andreas Jonas Fuglsig

**Copies:** 1

**Number of Pages:** 100

**Date of Completion:**

June 3, 2022

**Abstract:**

This thesis considers zero-delay multiple-descriptions (ZDMD) coding of stationary scalar  $AR(p)$  sources and mean square error (MSE) distortion constraints. Specifically, the symmetric two-descriptions case is considered for transmission over unreliable channels.

A novel operational ZDMD coding scheme is developed based on index assignment and differential pulse code modulation (DPCM) quantization assuming feedback from the decoder. A prediction error sample is quantized and mapped to two descriptions using a non-linear one-to-many map. The decoder produces a reconstruction based on the received packets, where the fidelity is higher when both packets are received.

The developed scheme can be applied to any assumption on the model order of the source. In the DPCM quantization, the MMSE predictors are used.

The theoretical performance of the codes are assessed, and their practical performances are demonstrated in a simulation study.

It is shown that the novel ZDMD scheme achieves a smaller MSE distortion compared to existing ZDMD coding schemes. Furthermore, the robustness against packet losses is demonstrated.

*The content of this project is freely available, but publication (with reference) may only be pursued with the explicit agreement of the authors.*



# Dansk Resumé

Ved trådløs kommunikation over en kanal med pakke-tab kan der opleves store forsinkelser, som skyldes et behov for retransmission af tabte pakker. I applikationer, såsom trådløse mikrofoner og højttalere samt trådløs transmission af tale mellem høreapparater på hver sit øre, kan der ofte være krav til lav eller næsten ingen forsinkelse. Til at fjerne forsinkelser på grund af pakke-tab betragter vi i denne afhandling zero-delay multiple-descriptions (ZDMD) kodning. Specifikt betragter vi indkodning af stationære skalare  $AR(p)$  kilder med mean square error (MSE) distortion ved brug af ZDMD kodning.

ZDMD kodning er en kombination af multiple-descriptions (MD) kodning og zero-delay (ZD) kodning. Med ZD kodning kræves det, at dekoderen kan producere rekonstruktioner så snart beskrivelsen er modtaget. ZD kodning er kausal, hvilket betyder, at rekonstruktioner kun afhænger af det nuværende og tidligere samples af kilden. I MD kodning indkodes kilden til flere forskellige beskrivelser. Disse beskrivelser transmitteres over hver sin kanal. På dekodersiden kombineres de modtagne beskrivelser til en rekonstruktion af kilden. Beskrivelserne designes sådan, at hver beskrivelse kan bruges hver for sig som rekonstruktion af kilden, og hvis alle beskrivelser er modtaget, opnås en bedre rekonstruktion.

I denne afhandling betragter vi symmetrisk ZDMD kodning med to beskrivelser, hvilket betyder, at den samme rate bruges til begge beskrivelser, og at nøjagtigheden af rekonstruktionen kun afhænger af hvor mange beskrivelser, der er modtaget og ikke hvilke. Vi foreslår et nyt operationel ZDMD kvantiseringsystem baseret på index assignment og differential pulse code modulation (DPCM). Systemet består i, at en prædiktionsfejl af kilden indkodes ved brug af uniform kvantisering, hvorefter to beskrivelser er formet ved brug af en ikke-lineær index assignment funktion. Hvis begge beskrivelser modtages af dekoderen, bruges den inverse index assignment funktion til at fremskaffe den kvantiserede prædiktionsfejl, ellers bruges den modtagne beskrivelse som estimat af den kvantiserede prædiktionsfejl.

Vi vurderer den teoretiske rate-distortion performance og sammenligner med eksisterende ZDMD kvantiseringsystem samt den teoretiske nedre grænse. Derudover demonstreres den praktiske rate-distortion performance gennem simuleringer af ind-

kodning af stationære skalare AR(2) kilder. Dette viser, at det foreslåede ZDMD kvantiseringsystem, ved brug af den optimale prædiktor for AR(1) modellering af kilden, opnår en operationel distortion performance omkring 3.5 dB fra den teoretiske nedre grænse for ZDMD kodning af AR(1) kilder. Desuden demonstreres det, at ved at bruge AR(2) prædiktor i kvantiseringsystemet opnås en lavere distortion end ved brug af AR(1) prædiktor.

Endeligt demonstreres kvantiseringssystemets robusthed over pakketab gennem simuleringer.

# Preface

This Master's Thesis (60 ECTS) is written by Kristian Søgaaard of the Master program Mathematical Engineering at Aalborg University, Department of Mathematical Sciences in the period September 2021 - June 2022. The thesis has been made in collaboration with the Department of Mathematical Sciences at Aalborg University, Department of Electronic Systems at Aalborg University and RTX A/S.

The topic of interest in this thesis is *Zero-Delay Multiple-Descriptions Source Coding of Stationary AR(p) Sources Using Feedback*.

Citations follow the IEEE-style guide, meaning that references are numbered after order of appearance and optionally specify the location in the source by specification of pages, sections or chapters, etc. Additional information about the references can be seen in the bibliography. Theorems, definitions, examples, etc. share a common counter for referencing, e.g., Theorem 1.2 follows Definition 1.1. Figures, tables and algorithms have individual counters.

All figures and tables throughout the report have been created by the author and are generated with Python 3.8 and the Tikz-package in L<sup>A</sup>T<sub>E</sub>X. In addition, Python 3.8 is used to develop software used to perform the numerical calculations related to the report. The scripts developed for this project can be found using the link <https://github.com/ksagaa17/ZDMD-Masters-Thesis>.

The author would like to thank Jan Østergaard (Department of Electronic Systems), Andreas Jonas Fuglsig (Department of Electronic Systems and RTX A/S), and Jens Toftgaard Petersen (RTX A/S) for their supervision throughout the project period.

Aalborg University, June 3, 2022



---

Kristian Søgaaard

<ksagaa17@student.aau.dk>



# Nomenclature

Symbols in boldface denote vectors or matrices, e.g.  $\mathbf{x} \in \mathbb{R}^n$  or  $\mathbf{A} \in \mathbb{R}^{n \times m}$ . All vectors are considered as column vectors unless otherwise specified. We use uppercase letters to denote random variables. However, matrices will also be denoted with uppercase letters even if the elements are not random. It will be clear from the context whether a uppercase boldface symbol denotes a random vector a deterministic matrix.

## List of Symbols

$\mathbb{E}[\cdot]$	Expected value operator.
$\text{Var}(\cdot)$	Variance operator.
$\mathbb{N}$ ( $\mathbb{N}_0$ )	The set of natural numbers (including 0).
$\mathbb{Z}$	The set of integers.
$\mathbb{R}$	The set of real numbers.
$\text{AR}(p)$	Autoregressive process of order $p$ .
$\log(\cdot)$	Logarithm to base 2.
$\ln(\cdot)$	Natural logarithm.

## List of Abbreviations

ACF	Autocorrelation function.
AWGN	Additive white Gaussian noise.
dB	Decibel.
i.i.d.	Independent and identically distributed.
MD	Multiple-descriptions.
MSE	Mean square error.
MMSE	Minimum mean square error.
RDF	Rate-distortion function.
ZD	Zero-delay.
ZDMD	Zero-delay multiple-descriptions.



# Contents

Dansk Resumé	v
Preface	vii
Nomenclature	ix
<b>1 Introduction</b>	<b>1</b>
1.1 Research Question . . . . .	2
1.1.1 Delimitations . . . . .	3
<b>2 Multiple-Descriptions Coding</b>	<b>5</b>
2.1 Multiple-Descriptions Source Code . . . . .	5
2.2 Gaussian Source and Squared Error Distortion . . . . .	7
2.2.1 Test-Channel . . . . .	9
2.3 Symmetric Distortions . . . . .	13
<b>3 Zero-Delay Coding</b>	<b>15</b>
3.1 Zero-Delay Source Code . . . . .	15
3.2 Directed Information . . . . .	17
3.3 Lower Bound on Gaussian ZD RDF . . . . .	18
3.4 Test-Channel Realization . . . . .	19
3.4.1 Test-Channel for Scalar Source . . . . .	22
<b>4 Zero-Delay Multiple-Descriptions</b>	<b>25</b>
4.1 ZDMD Source Coding . . . . .	25
4.2 Lower Bounds on Average Rates . . . . .	29
4.2.1 Distributions . . . . .	29
4.2.2 Lower Bounds . . . . .	30
4.2.3 Gaussian Lower Bound for Scalar Gaussian Sources . . . . .	32
4.3 Characterization of Symmetric ZDMD RDF . . . . .	35
4.3.1 Side Reconstructions . . . . .	35
4.3.2 Central Decoder . . . . .	37
4.3.3 Rates . . . . .	38

<b>5</b>	<b>Operational ZDMD coding</b>	<b>41</b>
5.1	Schemes Based on Staggered Quantizers . . . . .	42
5.1.1	Staggered Quantization . . . . .	42
5.1.2	Staggered DPCM Quantization . . . . .	43
5.2	DPCM Index Assignment . . . . .	50
5.2.1	Design of Index Assignment Map . . . . .	51
5.2.2	Rates and Distortion Performance . . . . .	54
5.3	Theoretical Rate-Distortion Performance . . . . .	55
5.3.1	Theoretical Lower Bound . . . . .	56
5.3.2	Schemes Using Staggered Quantizers . . . . .	56
5.3.3	Index Assignment Schemes . . . . .	56
<b>6</b>	<b>Simulation Study</b>	<b>59</b>
6.1	Simulation Setup . . . . .	59
6.1.1	Index Assignment Scheme . . . . .	60
6.1.2	Staggered Quantization Schemes . . . . .	62
6.1.3	Lower bound . . . . .	63
6.2	Rate-Distortion Performance with no Packet Loss . . . . .	64
6.2.1	Correlation of Quantization Noise . . . . .	66
6.3	Performance Versus Packet Loss Probability . . . . .	66
<b>7</b>	<b>Discussion</b>	<b>69</b>
7.1	Operational ZDMD Coder Design . . . . .	69
7.1.1	Trade-off between Central and Side Distortion . . . . .	70
7.1.2	Feedback Assumption . . . . .	70
7.2	Simulation Results . . . . .	71
7.2.1	Using AR(1) Predictors . . . . .	71
7.2.2	Using AR(2) Predictors . . . . .	71
7.2.3	Packet Loss . . . . .	72
<b>8</b>	<b>Conclusion</b>	<b>73</b>
8.1	Future Work . . . . .	74
	<b>Bibliography</b>	<b>75</b>
<b>A</b>	<b>Information Theory</b>	<b>79</b>
A.1	Entropy and Mutual Information . . . . .	79
A.2	Differential Entropy . . . . .	86
<b>B</b>	<b>WS: Source Coding</b>	<b>91</b>
B.1	Bound on Natural Logarithm . . . . .	95
<b>C</b>	<b>WS: Rate-Distortion Theory</b>	<b>97</b>
C.1	Distortion . . . . .	97
C.2	Rate-Distortion Function . . . . .	99

# 1. Introduction

Wireless communication over unreliable channels can lead to arbitrarily long delays due to the need of retransmission of lost packets. In applications where near real-time communication is desired such as wireless speakers or wireless microphones [1] or audio transmission between microphones in an hearing aid [2], small delays are required. To decrease the delay, the bandwidth of the channel code can be increased to ensure the desired delay and performance, which on the other hand will increase the cost.

Alternatively, the type of joint source and channel coding known as multiple descriptions (MD) coding can be applied [3]–[5]. In MD coding, the source is encoded into  $L \geq 2$  descriptions or representations and sent over  $L$  separate channels. Let us conceptualize with  $L = 2$  descriptions which is illustrated in Fig. 1.1. Each of the two descriptions represents the source to a certain level of distortion, and when the two descriptions are combined, the distortion should be lower. In this way, if a packet is lost in one of the channels, the receiver decodes the source using only one of the descriptions. Thus no further delay occurs due to packet loss. [6]

The problem is to design a coding scheme such that distortion of the center reconstruction is smaller than the distortion of the side reconstructions [6]. How this is done, depends on the situation. E.g., if the packet loss probability is high, then good representations should be available using the side decoders, but if the packet loss probability is low, the information can be spread across the two channels, meaning that each side reconstruction would have a larger distortion.

In general, the source coding schemes that achieves the best performance are computationally expensive, non-causal, and tends to impose long delays on the end-to-end processing of information [7]. In order to remove the delays and achieve near instantaneous encoding and decoding, it is necessary that the encoder and decoder of a communication system are causal, meaning that the reconstruction of the current source sample only depends on past and present source samples [7]. In the ideal case, where both instantaneous encoding and decoding are required, it is common to use the term zero-delay (ZD) source coding [7].

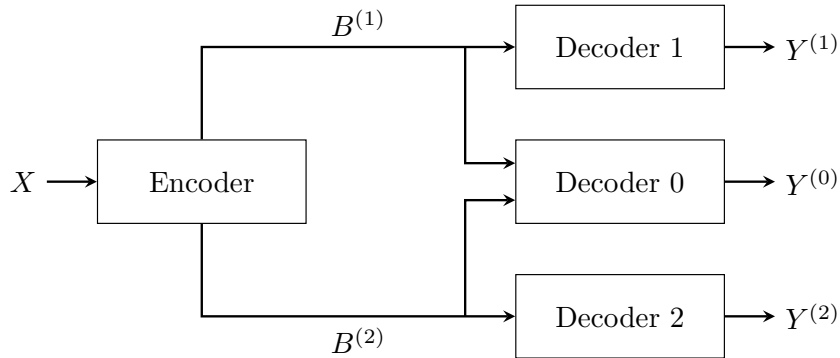


**Figure 1.1:** MD communication system. The source symbol  $X$  is encoded into two descriptions  $B^{(1)}, B^{(2)}$  which are transmitted over separate channels. Each side decoder (Decoder 1 and Decoder 2) reconstruct the source using only one of the descriptions, while the central decoder (Decoder 0) uses both descriptions. [4]

Recently, in [8], they proposed to combine MD coding with ZD coding referred to as zero-delay multiple-descriptions (ZDMD) coding. They developed a theoretical lower bound of ZDMD codes and illustrated the applicability using a simple scheme based on staggered quantization [9]. In particular, the two description case with feedback of the side reconstructions was considered with stationary scalar first order autoregressive (AR(1)) sources subject to mean square error (MSE) distortion constraints. The setup is illustrated in Fig. 1.2.

The main results of [8] constitute a lower bound on the sum-rate and a characterization of this lower bound for the symmetric case, i.e., both side channels operate at the same rate. Furthermore, a test-channel realization scheme was derived. The operational achievable results were obtained using a simple quantization scheme developed in [9] in a high-rate scenario.

This thesis is concerned with the development of operational ZDMD coders achieving better performance than the simple quantization scheme. Furthermore, when encoding audio or speech signals, it is common to assume local stationarity and model the signals as AR( $p$ ) processes of order  $p = 2$  or order  $p = 10$  [10, pp. 270-271]. Therefore, we will develop an operational ZDMD coding scheme which can use the modeling of the source.

## 1.1 Research Question

Only a single operational ZDMD coding scheme has been proposed [8]. Furthermore, the development in [8] restricted the source to first order AR sources. In this thesis, we will extend upon the work in [8] by designing an operational ZDMD coding scheme which can exploit the structure of AR( $p$ ) sources. In addition, since MD coding is designed to combat packet losses without inducing delay due to packet losses, the

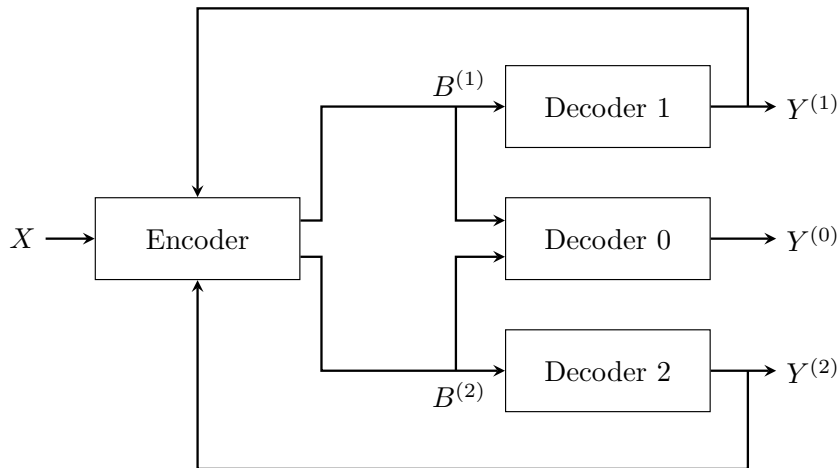


**Figure 1.2:** ZDMD communication system. The source symbol  $X$  is encoded into two descriptions  $B^{(1)}, B^{(2)}$  which are transmitted over separate channels. Each side decoder (Decoder 1 and Decoder 2) reconstruct the source using only one of the descriptions, while the central decoder (Decoder 0) uses both descriptions. The previous side reconstructions are available at the encoder through a feedback channel. [8]

performance under packet loss will be studied. Hence, the thesis work around the following research question:

*How can an operational ZDMD source coding scheme be designed for scalar autoregressive sources subject to MSE distortion constraints such that the optimal rates are achieved? Furthermore, how does such a scheme perform when packet losses occur?*

To answer the research question, the follow questions will be treated throughout the thesis.

- What is an operational quantization scheme that extends upon the optimum test-channel developed in [8] which provides achievable rates and distortions?
- What is the gab between the theoretical lower bound and operational achievable rates and distortions, and what can be attributed to such a gab?
- How does the operational quantization scheme perform under packet losses?

### 1.1.1 Delimitations

To simplify the problem, we will consider the two-descriptions case of MD coding and further restrict the design of operational ZDMD coding schemes to be symmetric, i.e., the rate is the same for both descriptions and the distortion does not depend on which packets are received, but the number of packets. Throughout the thesis, we will assume stationary sources.



## 2. Multiple-Descriptions Coding

While for the classical single description communication, we are interested in finding the achievable rate-distortion pairs  $(R, D)$ , we are for the MD coding in the two-descriptions case interested in characterizing the region of achievable quintuples  $(R_1, R_2, D_0, D_1, D_2)$ , referred to as the MD region, where  $R_i$ ,  $i = 1, 2$  denote the rate per description while  $D_0$  and  $D_1, D_2$  denote central distortion and side distortions, respectively. It is however only in very few cases that the MD region is characterized.

The achievable region for two-descriptions and memoryless sources is presented in [5]. This region was shown to be tight for white Gaussian sources and squared error distortion in [4]. In [11], the MD region is characterized for time-correlated stationary Gaussian sources. It was shown in [11] that the MD region forms a closed and convex set and the minimal description rates can be found by minimizing over all distortion spectra satisfying the side and central distortion constraints [6].

In this chapter, we first define MD coding in the two-descriptions case. Then we present a characterization of the MD region for a white Gaussian source and the MSE distortion. Finally, we will simplify the problem to the symmetric distortions case, meaning that both descriptions are communicated with the same rate  $R$  yielding the same side distortion  $D_S$ .

### 2.1 Multiple-Descriptions Source Code

In this section, we define MD source coding for a scalar zero-mean discrete-time stationary sources. Therefore, consider a zero-mean discrete-time stationary process  $\{X_t\}_{t \in \mathbb{N}} = \{X_t\}$  with  $X_t \in \mathcal{X}$ . A sequence of source variables is denoted by  $X_r^t = (X_r, X_{r+1}, \dots, X_t)$ ,  $(r, t) \in \mathbb{Z} \times \mathbb{Z}$  and  $r \leq t$ . For simplicity, if  $r = 1$  we use  $X_1^t = X^t$ . In a MD coding scheme with  $L = 2$  descriptions, we have two side reconstruction processes denoted  $\{Y_t^{(i)}\}_{t \in \mathbb{N}}$ ,  $i = 1, 2$  and one central reconstruction process denoted  $\{Y_t^{(0)}\}_{t \in \mathbb{N}}$ . The samples of the reconstruction processes takes values in the alphabets  $Y_t^{(i)} \in \mathcal{Y}^{(i)}$ ,  $i = 0, 1, 2$ . We denote by  $\mathbb{E}[\cdot]$  the expectation operator.

**Definition 2.1 (Multiple-Descriptions Source Code [6])**

Let  $\{X_t\}$  be a scalar zero-mean discrete-time stationary process and let  $d_i : \mathcal{X} \times \mathcal{Y}^{(i)} \rightarrow \mathbb{R}_+$ ,  $i = 0, 1, 2$  be distortion measures. A rate- $(R_1, R_2)$  two-descriptions source code consists of two encoding functions and three decoding functions. The encoding functions maps from an  $n$ -block  $X^n = (X_1, \dots, X_n)$  to a set of indices, i.e.,

$$f_i^{(n)} : \mathcal{X}^n \rightarrow \{1, 2, \dots, 2^{nR_i}\}, \quad i = 1, 2. \quad (2.1)$$

The two decoding functions

$$g_i^{(n)} : \{1, 2, \dots, 2^{nR_i}\} \rightarrow \mathcal{Y}^{(i),n}, \quad i = 1, 2, \quad (2.2)$$

are referred to as side decoding functions and

$$g_0^{(n)} : \{1, 2, \dots, 2^{nR_1}\} \times \{1, 2, \dots, 2^{nR_2}\} \rightarrow \mathcal{Y}^{(i),n} \quad (2.3)$$

is the central decoding function. The resulting  $n$ -block reconstructions are  $Y^{(i),n} = g_i^{(n)}(f_i^{(n)}(X^n))$  for  $i = 1, 2$  and  $Y^{(0),n} = g_0^{(n)}(f_1^{(n)}(X^n), f_2^{(n)}(X^n))$ . The distortion associated with the rate- $(R_1, R_2)$  two-descriptions source code is the triplet  $(D_0, D_1, D_2)$ , where

$$D_i = \frac{1}{n} \sum_{t=1}^n \mathbb{E} \left[ d_i \left( X_t, Y_t^{(i)} \right) \right] \quad i = 0, 1, 2. \quad (2.4)$$

The sets of indices  $\{1, 2, \dots, 2^{nR_i}\}$ ,  $i = 1, 2$  can be associated with the codebooks  $\mathcal{B}_i$ ,  $i = 1, 2$ , with cardinality  $|\mathcal{B}_i^{(i)}| = 2^{nR_i}$ . Each codeword  $B_n^{(i)}$  has a corresponding length  $\ell_n^{(i)}$  in bits which may vary between the codewords. The rates  $R_i$  describes the average expected codeword length, i.e.,

$$R_i = \lim_{n \rightarrow \infty} \frac{1}{n} \sum_{t=1}^n \mathbb{E} \left[ \ell_n^{(i)} \right]. \quad (2.5)$$

The two-descriptions problem consists of determining the achievable rate pairs  $(R_1, R_2)$  subject to the distortion constraints  $(D_0, D_1, D_2)$  for a given source. The formal definition of achievability is as follows:

**Definition 2.2 (Achievability [6])**

Given a zero-mean discrete-time stationary source  $\{X_t\}$ , a rate pair  $(R_1, R_2)$  is said to be achievable with respect to the distortion triple  $(D_0, D_1, D_2)$  if there for a sufficiently large  $n$  exists a coding scheme  $(f_1^{(n)}, f_2^{(n)}, g_0^{(n)}, g_1^{(n)}, g_2^{(n)})$  such that

$$\frac{1}{n} \sum_{t=1}^n \mathbb{E} \left[ d_i \left( X_t, Y_t^{(i)} \right) \right] \leq D_i \quad i = 0, 1, 2. \quad (2.6)$$

The convex closure of all achievable quintuples  $(R_1, R_2, D_0, D_1, D_2)$  is referred to as the MD region, denoted by  $\mathcal{R}_X(R_1, R_2, D_0, D_1, D_2)$ .

Since the MD region is a closed convex set, a characterization of the region can be obtained by determining the bounds of the region. These bounds are typically given in terms of lower bounds on the marginal rates  $R_i$ ,  $i = 1, 2$  and the sum-rate  $R_1 + R_2$  [5], [11].

As mentioned, characterizations of the MD region has been developed for both white Gaussian sources and stationary Gaussian sources with memory. However, for this thesis, it suffices to cover the results for white Gaussian sources.

## 2.2 Gaussian Source and Squared Error Distortion

For the remainder of this chapter, we will consider a white Gaussian process  $\{X_t\}$  with  $X_t \stackrel{\text{i.i.d.}}{\sim} \mathcal{N}(0, \sigma_X^2)$ . Furthermore, we will restrict the distortion measure to the squared-error distortion measure

$$d(x, y) = (x - y)^2. \quad (2.7)$$

When the squared error distortion and a stationary source process is considered, we will always consider distortions smaller than the variance of source process, since a distortion equal to the variance is achieved by letting the reconstructions be the mean of the process. This can be seen from

$$\begin{aligned} \frac{1}{n} \sum_{t=1}^n \mathbb{E} [(X_t - Y_t)^2] &= \frac{1}{n} \sum_{t=1}^n \mathbb{E} [(X_t - \mu_x)^2] \\ &= \frac{1}{n} \sum_{t=1}^n \sigma_X^2 \\ &= \sigma_X^2. \end{aligned} \quad (2.8)$$

Since the mean of the source does not tell anything of a given realization of the source, we will restrict the distortions to be less than the variance of the process, i.e.,  $D_i \leq \sigma_X^2$ . Furthermore, as mentioned, we also want the central distortion to be less than either the side distortions, as the combination of the two reconstructions should refine the estimate of the source and therefore decrease the distortion. Therefore, we will consider distortions  $0 < D_0 \leq D_i \leq \sigma_X^2$  for both  $i = 1, 2$ .

In [5], El Gamal and Cover presented an information theoretic characterization of the MD region in the case of memoryless sources and two descriptions. The characterization was given as bounds on the marginal rates  $R_i$ ,  $i = 1, 2$  and the sum-rate  $R_1 + R_2$ . These bounds are given the following theorem.

**Theorem 2.3 (Information Theoretic Bounds on MD Region [5], [4])**

Consider a white Gaussian process  $\{X_t\}$  with  $X_t = X \stackrel{\text{i.i.d.}}{\sim} \mathcal{N}(0, \sigma_X^2)$  and let  $(U^{(1)}, U^{(2)})$  be a pair of arbitrary random variable jointly distributed given  $X$  by  $p(u^{(1)}, u^{(2)}|x)$ . Then, an achievable rate region for distortions  $(D_0, D_1, D_2)$  is given by the convex closure of all rate pairs  $(R_1, R_2)$  satisfying

$$R_i \geq I(X; U^{(i)}), \quad i = 1, 2, \quad (2.9a)$$

$$R_1 + R_2 \geq I(X; U^{(1)}, U^{(2)}) + I(U^{(1)}; U^{(2)}), \quad (2.9b)$$

such that

$$D_i \geq \mathbb{E} \left[ \left( X - \mathbb{E} \left[ X | U^{(i)} \right] \right)^2 \right], \quad i = 1, 2,$$

$$D_0 \geq \mathbb{E} \left[ \left( X - \mathbb{E} \left[ X | U^{(1)}, U^{(2)} \right] \right)^2 \right].$$

For general sources, these bounds are not tight, but in the case of a memoryless Gaussian source subject to MSE distortion constraints, the bounds are shown to be tight in [4]. The characterization of the MD region for memoryless Gaussian source subject to MSE distortion constraints is given in the following theorem.

**Theorem 2.4 (MD Region for White Gaussian Source [4], [11])**

Consider a white Gaussian process  $\{X_t\}$  with  $X_t \stackrel{\text{i.i.d.}}{\sim} \mathcal{N}(0, \sigma_X^2)$  and the MSE distortion constraints. The MD region  $\mathcal{R}_X(R_1, R_2, D_0, D_1, D_2)$  is the set of points  $(R_1, R_2, D_0, D_1, D_2)$  given by

$$\mathcal{R}(\sigma_X^2, D_0, D_1, D_2) = \left\{ (R_1, R_2) : R_i \geq \frac{1}{2} \log \left( \frac{\sigma_X^2}{D_i} \right), i = 1, 2, \right. \\ \left. R_1 + R_2 \geq \frac{1}{2} \psi(\sigma_X^2, D_0, D_1, D_2) \right\}, \quad (2.11)$$

where

$$\psi = \begin{cases} \log \left( \frac{\sigma_X^2}{D_0} \right) & D_0 < D_1 + D_2 - \sigma_X^2 \\ \log \left( \frac{\sigma_X^4}{D_1 D_2} \right) & D_0 > \left( \frac{1}{D_1} + \frac{1}{D_2} - \frac{1}{\sigma_X^2} \right)^{-1} \\ \log \left( \frac{\sigma_X^2 \pi_0}{D_0 \left( \pi_0^2 - (\sqrt{\pi_1 \pi_2} - \sqrt{\lambda})^2 \right)} \right) & \text{otherwise} \end{cases} \quad (2.12)$$

with

$$\pi_i = (\sigma_X^2 - D_i), \quad i = 0, 1, 2 \quad (2.13)$$

$$\lambda = (D_1 - D_0)(D_2 - D_0) \quad (2.14)$$

When the logarithms in Theorem 2.3 are to base 2, the rates are in bits. If not otherwise stated,  $\log(\cdot)$  denotes the logarithm to base 2 throughout this thesis.

A proof of Theorem 2.4 is given in [4]. We will address the essentials of the forward part of the proof, i.e., the constructions of a reconstruction distribution achieving the lower bound. Such a reconstruction distribution is referred to as a test-channel [12].

### 2.2.1 Test-Channel

We will now present a test-channel which achieves the lower bound of the MD region for the white Gaussian source. We consider the test-channel developed in [4], and this is depicted in the block diagram in Fig. 2.1.

The white Gaussian source  $X_t \stackrel{\text{i.i.d.}}{\sim} \mathcal{N}(0, \sigma_X^2)$  is given as input to two additive white Gaussian noise (AWGN) channels, where the noises of the two channels are correlated. The two descriptions of the test-channel are the output of the two AWGN channels

$$U^{(i)} = X + Z^{(i)}, \quad i = 1, 2 \quad (2.15)$$

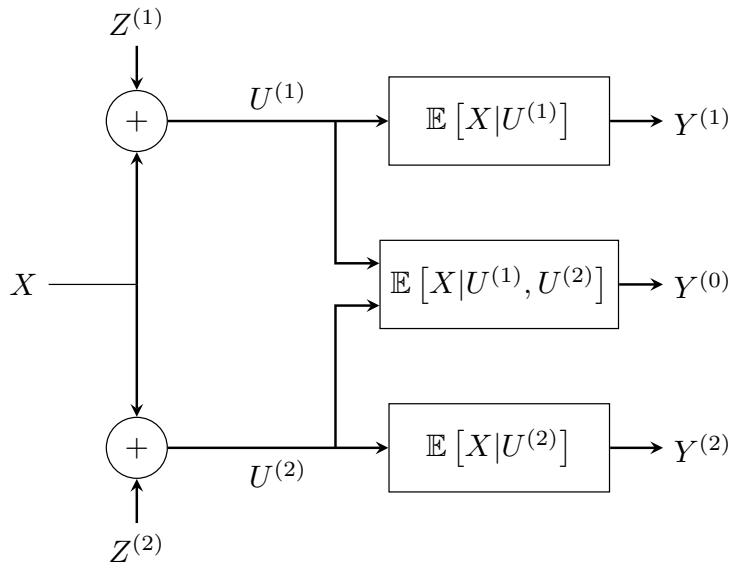


**Figure 2.1:** Illustration of the test-channel for two-description coding described in [4].

where  $Z^{(1)}$  and  $Z^{(2)}$  are jointly distributed by

$$\begin{bmatrix} Z^{(1)} \\ Z^{(2)} \end{bmatrix} \sim \mathcal{N} \left( \mathbf{0}, \begin{bmatrix} \sigma_{Z^{(1)}}^2 & \rho \sigma_{Z^{(1)}} \sigma_{Z^{(2)}} \\ \rho \sigma_{Z^{(1)}} \sigma_{Z^{(2)}} & \sigma_{Z^{(2)}}^2 \end{bmatrix} \right). \quad (2.16)$$

The reconstructions are given by the minimum MSE (MMSE) estimate given the respective descriptions, i.e.,

$$Y^{(i)} = \mathbb{E} [X|U^{(i)}], \quad i = 1, 2 \quad (2.17a)$$

$$Y^{(0)} = \mathbb{E} [X|U^{(1)}, U^{(2)}]. \quad (2.17b)$$

Since  $(X, U^{(i)})$ ,  $i = 1, 2$  and  $(X, (U^{(1)}, U^{(2)}))$  are jointly Gaussian, the MMSE estimates are linear [13, p. 447]. Thus, if we let  $\mathbf{U} = [U^{(1)}, U^{(2)}]^T$

$$Y^{(i)} = \theta_i U^{(i)}, \quad i = 1, 2 \quad (2.18a)$$

$$Y^{(0)} = \Theta_C \mathbf{U}, \quad (2.18b)$$

where

$$\theta_i = \mathbb{E} [XU^{(i)}] \mathbb{E} [U^{(i)}]^{-1} = \frac{\sigma_X^2}{\sigma_X^2 + \sigma_{Z^{(i)}}^2}, \quad i = 1, 2 \quad (2.19)$$

$$\Theta_C = [\theta_{C,1} \quad \theta_{C,2}] = \mathbb{E} [X\mathbf{U}^T] \mathbb{E} [\mathbf{U}\mathbf{U}^T]^{-1} \quad (2.20)$$

with

$$\theta_{C,i} = \frac{\sigma_X^2 (\sigma_{Z^{(j)}}^2 - \rho \sigma_{Z^{(1)}} \sigma_{Z^{(2)}})}{(\sigma_X^2 + \sigma_{Z^{(1)}}^2)(\sigma_X^2 + \sigma_{Z^{(2)}}^2) - (\sigma_X^2 + \rho \sigma_{Z^{(1)}} \sigma_{Z^{(2)}})^2}, \quad i, j \in \{1, 2\}, i \neq j. \quad (2.21)$$

Computing the MSE distortions yields

$$D_i = \frac{\sigma_X^2 \sigma_{Z^{(i)}}^2}{(\sigma_X^2 + \sigma_{Z^{(i)}}^2)}, \quad i = 1, 2, \quad (2.22)$$

$$D_0 = \frac{\sigma_X^2 \sigma_{Z^{(1)}}^2 \sigma_{Z^{(2)}}^2 (1 - \rho^2)}{\sigma_{Z^{(1)}}^2 \sigma_{Z^{(2)}}^2 (1 - \rho^2) + \sigma_X^2 (\sigma_{Z^{(1)}}^2 + \sigma_{Z^{(2)}}^2 - 2\rho \sigma_{Z^{(1)}} \sigma_{Z^{(2)}})}. \quad (2.23)$$

Then computing the mutual informations in Theorem 2.3, the bound in Theorem 2.4 is obtained if we during the derivation, choose [4], [14]

$$\rho = -\frac{\sqrt{D_1 D_2 - \sigma_X^4 2^{-2(R_1 + R_2)}}}{\sqrt{D_1 D_2}}. \quad (2.24)$$

As seen in (2.12), the MD region for white Gaussian sources is partitioned into three three distortion regions. The first two cases are so-called degenerate. These are the trivial lower bounds on the sum-rate [14]. We illustrate these cases in the

following two examples. First we note that, we can formulate the bounds in terms of the distortions such that the MD region for a white Gaussian source consists of the points  $(R_1, R_2, D_0, D_1, D_2)$  satisfying

$$D_i \geq \sigma_X^2 2^{-2R_i}, \quad i = 1, 2 \quad (2.25)$$

$$D_0 \geq \sigma_X^4 2^{-2(R_1+R_2)} \gamma_D(R_1, R_2, D_1, D_2), \quad (2.26)$$

where  $\gamma_D = 1$  if  $D_1 + D_2 > \sigma_X^2 + D_0$  and

$$\gamma_D = \frac{1}{1 - \left( \sqrt{(1-D_1)(1-D_2)} - \sqrt{D_1 D_2 - 2^{-2(R_1+R_2)}} \right)^2} \quad (2.27)$$

otherwise [4].

### Example 2.5 (First case of (2.12))

In this case we assume that  $\sigma_X^2 = 1$  and that the coding scheme ensures that the central decoder provide the best performance as possible, i.e.,  $D_0 = 2^{-2(R_1+R_2)}$ . By (2.26),

$$1 - \left( \sqrt{(1-D_1)(1-D_2)} - \sqrt{D_1 D_2 - 2^{-2(R_1+R_2)}} \right)^2 = 1 \quad (2.28)$$

which implies that

$$(1-D_1)(1-D_2) = D_1 D_2 - 2^{-2(R_1+R_2)}. \quad (2.29)$$

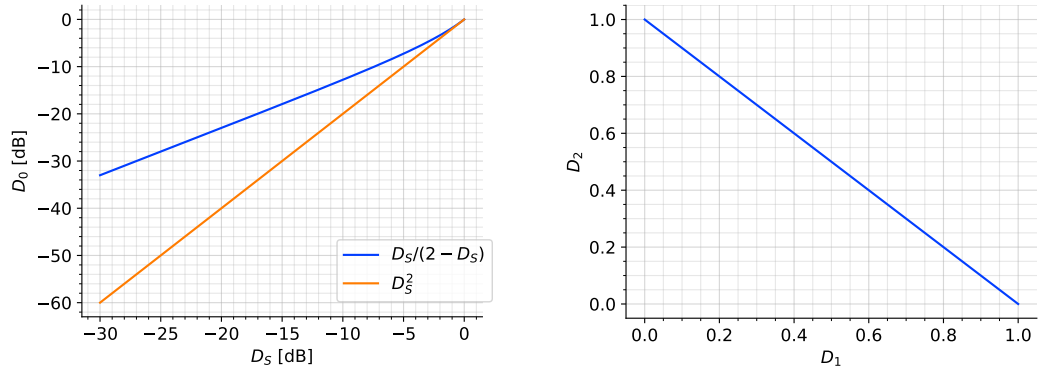
Expanding the right hand side and isolating  $D_1 + D_2$  yields

$$D_1 + D_2 = 1 + 2^{-2(R_1+R_2)}. \quad (2.30)$$

As mentioned in the beginning of this section, a distortion of  $D = \sigma_X^2 = 1$  can be achieved by always estimating the source by its mean. By (2.30) which is plotted in Fig. 2.2b, if either  $D_1$  or  $D_2$  is small, the other side distortion will be close to one, which means that the latter reconstruction. [4, p. 1913]

### Example 2.6 (Second case of (2.12))

We consider the symmetric case (which we will focus on later) where  $R = R_1 = R_2$  and  $D_S = D_1 = D_2$  and we consider a source with  $\sigma_X^2 = 1$ . Furthermore, we let  $D_S = \sigma_X^2 2^{-2R} = 2^{-2R}$ , i.e., we let the side distortions be on the rate-distortion



(a) Central distortion as function of side distortion in the case of Example 2.6

(b) Second side distortion as function of first side distortion in the case of Example 2.5

**Figure 2.2:** Plots of the lower bounds on the distortion described in Examples 2.5 and 2.6.

curve for a single description coding scheme. In this case the central distortion is

$$\begin{aligned}
 D_0 &\geq 2^{-4R} \frac{1}{1 - \left( (1 - D_S) - \sqrt{D_S^2 - 2^{-4R}} \right)^2} \\
 &= D_S^2 \frac{1}{1 - (1 - D_S)^2} \\
 &= D_S^2 \frac{1}{2D_S - D_S^2} \\
 &= \frac{D_S}{2 - D_S}. \tag{2.31}
 \end{aligned}$$

This means that the central distortion is greater than half the side distortion. Hence when using the central decoder, which corresponds to doubling the rate compared to the side decoders, the distortion is at best halved compared to the side distortion.

The achievable distortion using single description coding with rate  $2R$  is

$$D \geq 2^{-2(2R)} = D_S^2 \tag{2.32}$$

which for small values of  $D_S$  is much better than (2.31) [4, p. 1912]. This is illustrated in Fig. 2.2a.

In the cases described in the examples, the rate is not affected by all the distortion constraints simultaneously. This is however the case in the non-degenerate case, i.e., the third case of (2.12). Therefore, we will focus on the non-degenerate case for the remainder of the thesis. Using the expressions for the distortion in (2.22) and (2.23),

the bound on the sum-rate can be expressed as [4]

$$R_1 + R_2 \geq \frac{1}{2} \log\left(\frac{\sigma_X^4}{D_1 D_2}\right) - \frac{1}{2} \log(1 - \rho^2), \quad (2.33)$$

for non-degenerate distortions. From (2.23), it is seen that when  $\rho \rightarrow -1$ , the central distortion becomes smaller. However, from (2.33) it can be seen that when  $\rho \rightarrow -1$ , the sum-rate becomes larger. Therefore, it is not possible to obtain a smaller central distortion  $D_0$  by making the descriptions more correlated, without sacrificing the fidelity on the side descriptions or using a higher rate. This illustrates the trade-off between the side distortions and the central distortion. Good descriptions of the same source are similar, and therefore the combination of these do not add much. The fundamental problem of MD coding can be framed as making individual descriptions good, yet not too similar. [3, p. 81]

How to deal with the trade-off between the central distortion and the side distortions depends on the situation. If for example the probability of packet losses is high, then it may be a good idea to sacrifice on the central distortion to make the side reconstructions more accurate. If on the other hand, the packet loss probability is low, it may not be necessary with highly accurate side reconstructions, and the fidelity of these can be sacrificed on behalf of a better central distortion.

The test-channel developed in [4] suggests how to construct optimal operational MD coding schemes. In an operational MD coding scheme, the quantization noise should be approximately distributed as  $Z^{(i)}$ ,  $i = 1, 2$ . However, it is not an easy task to generate highly negatively correlated quantization noises in practice [15]. We will in Chapter 5 consider the design of operational ZDMD quantization schemes. To this end we will consider the use of staggered uniform quantization and index assignment. With the staggered uniform quantizers, it is not possible to obtain correlations below  $-\frac{1}{2}$ , but index assignment can achieve a high negative correlation by using a fine-grained uniform quantizer together with a non-linear function, mapping each point in the fine-grained quantizer to a pair of outputs of two coarser identical quantizers [15], [16]. We will elaborate further on these methods in Chapter 5.

## 2.3 Symmetric Distortions

In a special case of two-descriptions coding, the source is encoded at the same rate in both encoders which yields the same distortion of the side reconstructions. This coding scheme is referred to as the symmetric case. This means that the symmetric two-descriptions coding can be described by a single rate  $R = R_1 = R_2$  and a pair of distortions  $(D_0, D_S)$  where  $D_S = D_1 = D_2$ .

### Definition 2.7 (Symmetric MD RDF)

The symmetric MD rate-distortion function (RDF) is defined as the minimum rate  $R$ , which is achievable with respect to the distortion pair  $(D_0, D_S)$ .

In the case of a white Gaussian source process, we get from Theorem 2.4 the following symmetric MD RDF in the non-degenerate case.

**Corollary 2.8**

The symmetric MD RDF for a white Gaussian source process with variance  $\sigma_X^2$  with respect to the MSE distortions  $(D_0, D_S)$  is given the minimum achievable rate and it is given by

$$R(\sigma_X^2, D_C, D_S) = \frac{1}{4} \log \left( \frac{\sigma_X^2 (\sigma_X^2 - D_C)}{4D_C (D_S - D_C) (\sigma_X^2 - D_S)} \right). \quad (2.34)$$

*Proof.*

We will prove that the third case of (2.12) has the form of (2.34) in the symmetric case. This follows from substitution of  $D_1$  and  $D_2$  with  $D_S$ . Making the substitutions in the last case of (2.12) and expanding the quadratic terms we obtain

$$\begin{aligned} \psi &= \log \left( \frac{\sigma_X^2 (\sigma_X^2 - D_0)}{D_0 \left( (\sigma_X^2 - D_0)^2 - \left( \sqrt{(\sigma_X^2 - D_1)(\sigma_X^2 - D_2)} - \sqrt{(D_1 - D_0)(D_2 - D_0)} \right)^2 \right)} \right) \\ &= \log \left( \frac{\sigma_X^2 (\sigma_X^2 - D_C)}{D_C \left( (\sigma_X^2 - D_C)^2 - ((\sigma_X^2 - D_S) - (D_S - D_C))^2 \right)} \right) \\ &= \log \left( \frac{\sigma_X^2 (\sigma_X^2 - D_C)}{D_C (4D_S \sigma_X^2 + 4D_S D_C - 4D_S^2 - 4\sigma_X^2 D_C)} \right) \\ &= \log \left( \frac{\sigma_X^2 (\sigma_X^2 - D_C)}{4D_C (D_S - D_C) (\sigma_X^2 - D_S)} \right). \end{aligned} \quad (2.35)$$

Since the sum-rate in the symmetric case is  $2R$ , we have by (2.11) that

$$R \geq \frac{1}{4} \psi, \quad (2.36) \quad \blacksquare$$

and since the MD RDF is the minimum of the rates, the result follows.

## 3. Zero-Delay Coding

In this chapter we will review the basic theory concerning zero-delay (ZD) coding. This includes the relevant definitions and the results regarding the rate-distortion function for zero-delay coding schemes. First we define ZD source coding stationary vector valued AR(1) source processes. Then we present the information theoretic zero-delay rate-distortion function (ZD RDF) as well as a the test-channel realization scheme developed in [7]. Finally, we cover the special case of a scalar stationary AR(1) source.

When designing a coding scheme, the lower bound on the rate-distortion performance is described by the RDF, for a given source and distortion measure. In general, the source coding schemes that get close to achieving the RDF are generally computationally expensive, non-causal, and tends to impose long delays on the end-to-end processing of information [7, p. 841]. If we require near instantaneous encoding and decoding, the coding scheme must be causal. It is common to use the term ZD source coding in applications where both instantaneous encoding and decoding are required [7]. We will in the following define ZD source codes and discuss some necessities on these codes.

In general non-causal source coding, when establishing the achievability of a certain rate-distortion performance, the technique is often based on random codebooks, which requires asymptotically large source vector dimensions [7, p. 841]. This technique is however in general not applicable in the case of ZD source coding.

### 3.1 Zero-Delay Source Code

We will in this chapter consider ZD source coding of a vector valued source. To this end, we let  $\{\mathbf{X}_t\}_{t \in \mathbb{N}_0} = \{\mathbf{X}_t\}$  denote the stochastic process modeling a source and a realization of the process is denoted by  $\{\mathbf{x}_t\}$ . The elements of the process are random vectors  $\mathbf{X}_t \in \mathcal{X} \subseteq \mathbb{R}^p$  with  $\mathcal{X}$  being the alphabet of  $\mathbf{X}_t$ . As in Chapter 2, we use the notation  $\mathbf{X}^t = (\mathbf{X}_0, \mathbf{X}_1, \dots, \mathbf{X}_t)$ .

The source process we will consider in this worksheet is the vector-valued AR(1) source process described by the following discrete-time linear time-invariant Gaussian state-space model

$$\mathbf{X}_t = \mathbf{A}\mathbf{X}_{t-1} + \mathbf{C}\mathbf{W}_t, \quad t \in \mathbb{N}, \quad (3.1)$$

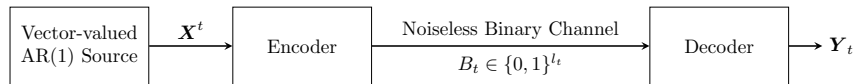


**Figure 3.1:** Illustration of the ZD source coding scenario. [7]

where  $\mathbf{A} \in \mathbb{R}^{p \times p}$  and  $\mathbf{C} \in \mathbb{R}^{p \times q}$  are deterministic matrices,  $\mathbf{X}_0 \in \mathbb{R}^p \sim \mathcal{N}(\mathbf{0}, \boldsymbol{\Sigma}_{\mathbf{X}_1})$  is the initial state and  $\mathbf{W}_t \in \mathbb{R}^q \sim \mathcal{N}(\mathbf{0}, \boldsymbol{\Sigma}_{\mathbf{W}})$ ,  $\boldsymbol{\Sigma}_{\mathbf{W}} = \mathbf{I}$  is an i.i.d. Gaussian sequence, independent of  $\mathbf{X}_0$ . We will further assume that the source process is stationary. In [7] they assume that the process is asymptotic stationary and state a result in the asymptotic regime. By assuming stationarity, this result applies for the entire source process.

The setting for the ZD source coding is depicted in Fig. 3.1. At each time  $t \in \mathbb{N}_0$ , the encoder observes  $\mathbf{X}^t$ , i.e., the random sequence observed by the encoder grows with time. The encoder produces a single binary codeword  $B_t$  of length  $\ell_t$  (in bits) from a predefined set of codewords  $\mathcal{B}_t$  of at most a countable number of codewords. The codeword  $B_t$  and its length  $\ell_t$  are assumed random since the source is random. At the decoder side, the decoder receives  $B_t$  assuming that it has already received  $B^{t-1} \in \mathcal{B}^{t-1} = \times_{i=0}^{t-1} \mathcal{B}_i$ . Given  $B^t$ , the decoder produces an estimate  $\mathbf{Y}_t$  of  $\mathbf{X}_t$ , under the assumption that  $\mathbf{Y}^{t-1}$  has already been produced. It is assumed that the encoder and decoder process information without delay.

We will in the following formally define a ZD source code.

### Definition 3.1 (Zero-Delay Source Code [7])

Consider the source process  $\{\mathbf{X}_t\}$  given by (3.1). The encoder is specified by a sequence of functions  $\{f_t\}_{t \in \mathbb{N}_0}$  given by

$$f_t : \mathcal{B}^{t-1} \times \mathcal{X}_t \rightarrow \mathcal{B}_t, \quad t \in \mathbb{N}_0, \quad (3.2)$$

i.e., the function  $f_t$  maps the sequence of past codewords and the current source vector to the current codeword, such that the output at time  $t \in \mathbb{N}_0$  is  $B_t = f_t(B^{t-1}, \mathbf{X}_t)$  with  $B_0 = f_0(\mathbf{X}_0)$ . Likewise, the decoder is specified by a sequence of functions  $\{g_t\}_{t \in \mathbb{N}_0}$  given as

$$g_t : \mathcal{B}^t \rightarrow \mathcal{Y}_t, \quad (3.3)$$

i.e., the decoding function maps the sequence of all previous and the current codeword to the current estimate of the source vector such that the output of the decoder at time  $t \in \mathbb{N}_0$  is  $\mathbf{Y}_t = g_t(B^t)$  under the assumption that  $\mathbf{Y}^{t-1}$  has already been produced.

As is the goal of classical rate-distortion theory, we want to establish the RDF, which is the minimum of achievable rates given a distortion. However, the RDF is hard to establish for ZD source codes and it has not been found for general Gaussian sources subject to squared error distortion [7]. However, in [7], the operational

ZD RDF has been lower bounded by the so-called nonanticipative RDF (NRDF) for which the characterization also was given in [7]. If the source satisfies conditional independence given by (3.10), the NRDF is specified in terms of directed information, which will be introduced in the next section. We will however first define the operational ZD RDF for a Gaussian source subject to the following asymptotic MSE distortion constraint.

The goal of the design of the system in Fig. 3.1 is to achieve an asymptotic average expected distortion that satisfies

$$\lim_{n \rightarrow \infty} \frac{1}{n+1} \sum_{t=0}^n \mathbb{E} \left[ \|\mathbf{X}_t - \mathbf{Y}_t\|_2^2 \right] \leq D, \quad (3.4)$$

where  $D > 0$  is a predefined level of MSE distortion [7]. The operational ZD RDF, in the asymptotic regime, is the minimum over all ZD source codes of expected average codeword length, i.e.,

$$\limsup_{n \rightarrow \infty} \frac{1}{n+1} \sum_{t=0}^n \mathbb{E} [\ell_t]. \quad (3.5)$$

The accumulated number of bits received by the decoder at time  $n \in \mathbb{N}_0$  is denoted  $L_n = \sum_{t=0}^n \ell_t$ .

### Definition 3.2 (Operational Vector-Valued Gaussian ZD RDF [7])

For the source process defined by (3.1) and MSE distortion constraint  $D$ , the operational Gaussian ZD RDF is given by the following optimization problem

$$\begin{aligned} R_{ZD}^{op}(D) = & \inf_{\substack{B_t = f_t(B^{t-1}, \mathbf{X}_t), t \in \mathbb{N}_0 \\ \mathbf{Y}_t = g_t(B^t)}} \limsup_{n \rightarrow \infty} \frac{1}{n+1} \mathbb{E} [L_n] \\ & \text{s.t. } \lim_{n \rightarrow \infty} \frac{1}{n+1} \sum_{t=0}^n \mathbb{E} \left[ \|\mathbf{X}_t - \mathbf{Y}_t\|_2^2 \right] \leq D \end{aligned} \quad (3.6)$$

As the optimization is over all ZD codes, the solution is very hard to find. Later, a lower bound will be found in terms of information theoretic quantities.

## 3.2 Directed Information

We will in this section define directed information which is a measure of the information that causally flows from one random sequence to another [17]. The definition is as follows:

**Definition 3.3 (Directed Information [18])**

The directed information between sequences  $\mathbf{X}^n$  and  $\mathbf{Y}^n$  is defined by

$$I(\mathbf{X}^n \rightarrow \mathbf{Y}^n) = \sum_{t=0}^n I(\mathbf{X}^t; \mathbf{Y}_t | \mathbf{Y}^{t-1}) \quad (3.7)$$

Comparing the definition of directed information with mutual information, the causality of (3.7) is evident. By the chain rule for mutual information [12, Theo. 2.5.2], the mutual information between  $\mathbf{X}^n$  and  $\mathbf{Y}^n$  can be written as

$$I(\mathbf{X}^n; \mathbf{Y}^n) = \sum_{t=0}^n I(\mathbf{X}^n; \mathbf{Y}_t | \mathbf{Y}^{t-1}). \quad (3.8)$$

While the terms in (3.8) capture the mutual information between the whole sequence  $\mathbf{X}^n$  and  $\mathbf{Y}_t$  given the past observations of the second sequence  $\mathbf{Y}^{t-1}$ , it is only the past and current samples of  $\mathbf{X}^n$ , i.e.,  $\mathbf{X}^t$  which is considered in the terms in the directed information [17].

One of the properties of directed information is that  $I(\mathbf{X}^n \rightarrow \mathbf{Y}^n) \leq I(\mathbf{X}^n; \mathbf{Y}^n)$ , with equality if and only if  $\mathbf{Y}^n$  is causally related to  $\mathbf{X}^n$  [17], [18]. Another property, known as the conservation law of mutual and directed information, states that

$$I(\mathbf{X}^n \rightarrow \mathbf{Y}^n) + I(\mathbf{0} * \mathbf{Y}^{n-1} \rightarrow \mathbf{X}^n) = I(\mathbf{X}^n; \mathbf{Y}^n), \quad (3.9)$$

where  $\mathbf{0} * \mathbf{Y}^{n-1}$  denotes the concatenation  $\mathbf{0}, \mathbf{Y}_0, \dots, \mathbf{Y}_{n-1}$  [19].

**3.3 Lower Bound on Gaussian ZD RDF**

In this section, the lower bounds to the operational Gaussian ZD RDF presented in [7] will be presented. The key result of [7] is presented in Theorem 3.5 where  $R_{ZD}^I(D)$  denotes an information theoretic lower bound to the operational rate-distortion function which is specified in terms of directed information.

We assume that the source distribution satisfies conditional independence of the past reconstructions, i.e.,

$$P_{\mathbf{X}_t | \mathbf{X}^{t-1}, \mathbf{Y}^{t-1}} = P(\mathbf{x}_t | \mathbf{x}^{t-1}), \quad t \in \mathbb{N}_0. \quad (3.10)$$

This implies that  $\mathbf{W}_t$  in (3.1) is independent of  $\mathbf{Y}^{t-1}$ .

**Definition 3.4 (Information Theoretic ZD RDF [7])**

Consider a Gaussian source of the form (3.1) with the property in (3.10). Then the Gaussian information theoretic ZD RDF subject to an asymptotic MSE distortion

constraint is defined by

$$\begin{aligned}
 R_{ZD}^I(D) &= \inf \lim_{n \rightarrow \infty} \frac{1}{n+1} I(\mathbf{X}^n \rightarrow \mathbf{Y}^n) \\
 \text{s.t. } &\lim_{n \rightarrow \infty} \frac{1}{n+1} \sum_{t=0}^n \mathbb{E} \left[ \|\mathbf{X}_t - \mathbf{Y}_t\|_2^2 \right] \leq D,
 \end{aligned} \tag{3.11}$$

where the infimum is over all sequences of conditional probability distributions  $\{P(\mathbf{y}_t | \mathbf{y}_{t-1}, \mathbf{x}_t) : t \in \mathbb{N}_0\}$ .

For a Gaussian source, the MSE is minimized if  $(\mathbf{X}_t, \mathbf{Y}_t)$  is jointly Gaussian for  $t \in \mathbb{N}_0$ . Thus, the infimum in (3.11) can be restricted to be over Gaussian conditional probability distributions  $\{P^{GP}(\mathbf{y}_t | \mathbf{y}_{t-1}, \mathbf{x}_t) : t \in \mathbb{N}_0\}$  [7].

The next theorem, states that the operational ZD RDF is lower bounded by the information theoretic ZD RDF.

### Theorem 3.5 (Lower Bounds on Operational ZD RDF [7], [20])

For Gaussian sources with an asymptotic MSE constraint, the following bounds holds

$$R(D) \leq R_{ZD}^I(D) \leq R_{ZD}^{op}(D), \tag{3.12}$$

where  $R(D)$  is the classical non-causal RDF, i.e., the minimum achievable rate using any source coding scheme as defined in Definition C.6.

The first inequality follows from the definitions of  $R(D)$  and  $R_{ZD}^I(D)$  in Definition C.6 and Definition 3.4 and from the relation  $I(\mathbf{X}^n \rightarrow \mathbf{Y}^n) \leq I(\mathbf{X}^n; \mathbf{Y}^n)$ . The second inequality is established in [20].

## 3.4 Test-Channel Realization

In [7, Lemma 1, Theorem 2, Theorem 3], they give a characterization of the Gaussian information theoretic ZD RDF and a method to find the optimal test-channel distribution. In [7, Theorem 3], they consider the asymptotic characterization of the result in [7, Theorem 2]. They consider both characterizations as they assume the source is asymptotic stationary. We will in this worksheet consider sources of the form (3.1) which are stationary, thus the characterization of the Gaussian information theoretic ZD RDF reduces to the asymptotic characterization of [7, Theorem 3].

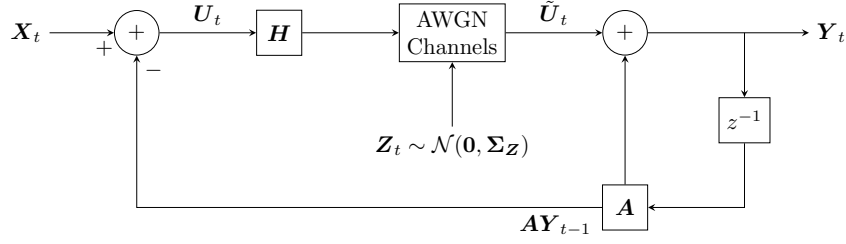


**Figure 3.2:** Block diagram of ZD test-channel.

### Theorem 3.6 (ZD Test-Channel Distribution [7])

Consider the setup in Definition 3.4 with the additional assumption that the source is stationary. Assume either  $\mathbf{A}$  has full rank or  $\mathbf{C}$  is square and has full rank in (3.1). Then the optimal test-channel distribution  $P(\mathbf{y}_t | \mathbf{y}_{t-1}, \mathbf{x}_t)$  is realized by

$$\mathbf{Y}_t = \mathbf{H}\mathbf{X}_t + (\mathbf{I} - \mathbf{H})\mathbf{A}\mathbf{Y}_{t-1} + \mathbf{Z}_t, \quad (3.13)$$

where  $\mathbf{Z}_t \in \mathbb{R}^p \sim \mathcal{N}(\mathbf{0}, \Sigma_Z)$  is a white Gaussian process independent of  $\{\mathbf{W}_t\}$

$$\mathbf{H} = \mathbf{I} - \mathbf{\Pi}\mathbf{\Lambda}^{-1} \succeq \mathbf{0}, \quad \mathbf{\Pi} \succeq \mathbf{0}, \quad \mathbf{\Lambda} \succeq \mathbf{0}, \quad (3.14)$$

$$\Sigma_Z = \mathbf{\Pi}\mathbf{H}^T \succeq \mathbf{0}, \quad (3.15)$$

$$\mathbf{\Lambda} = \mathbf{A}\mathbf{\Pi}\mathbf{A}^T + \mathbf{B}\mathbf{B}^T, \quad (3.16)$$

$$\mathbf{\Pi} = \mathbb{E} \left[ (\mathbf{X}_t - \mathbf{Y}_t) (\mathbf{X}_t - \mathbf{Y}_t)^T \right] \quad (3.17)$$

The characterization of  $R_{ZD}^I(D)$  is

$$\begin{aligned} R_{ZD}^I(D) &= \min_{\mathbf{\Pi}} \frac{1}{2} \log \left( \frac{|\mathbf{\Lambda}|}{|\mathbf{\Pi}|} \right) \\ &\text{s.t. } \mathbf{0} \prec \mathbf{\Pi} \preceq \mathbf{\Lambda} \\ &\text{tr}(\mathbf{\Pi}) \leq D, \end{aligned} \quad (3.18)$$

where  $|\cdot|$  denotes the determinant.

As it figures from the test-channel realization (3.13), in order to achieve the minimum rate, feedback is needed as  $\mathbf{Y}_{t-1}$  is used to obtain  $\mathbf{Y}_t$ . In Fig. 3.2, the realization scheme is illustrated. As it figures from the illustration, rather than directly transmitting the source samples  $\mathbf{X}_t$ ,  $t \in \mathbb{N}_0$ , the encoder transmit the prediction error process

$$\mathbf{U}_t = \mathbf{X}_t - \mathbb{E}[\mathbf{X}_t | \mathbf{Y}^{t-1}] = \mathbf{X}_t - \mathbf{A}\mathbf{Y}_{t-1}, \quad t \in \mathbb{N}_0 \quad (3.19)$$

which is Gaussian and has zero-mean and covariance

$$\begin{aligned}
\mathbb{E} [\mathbf{U}_t \mathbf{U}_t^T] &= \mathbb{E} [(\mathbf{X}_t - \mathbf{A}\mathbf{Y}_{t-1})(\mathbf{X}_t - \mathbf{A}\mathbf{Y}_{t-1})^T] \\
&= \mathbb{E} [(\mathbf{A}\mathbf{X}_{t-1} - \mathbf{A}\mathbf{Y}_{t-1} + \mathbf{C}\mathbf{W}_t)(\mathbf{A}\mathbf{X}_{t-1} - \mathbf{A}\mathbf{Y}_{t-1} + \mathbf{C}\mathbf{W}_t)^T] \\
&= \mathbb{E} [\mathbf{A}(\mathbf{X}_{t-1} - \mathbf{Y}_{t-1})(\mathbf{X}_{t-1} - \mathbf{Y}_{t-1})\mathbf{A}^T + \mathbf{C}\mathbf{W}_t\mathbf{W}_t^T\mathbf{C}^T] \\
&= \mathbf{A}\mathbf{\Pi}\mathbf{A}^T + \mathbf{B}\mathbf{B}^T \\
&= \mathbf{\Lambda}.
\end{aligned} \tag{3.20}$$

The process  $\{\tilde{\mathbf{U}}_t\}$  is called the innovation process [7] and is given as

$$\tilde{\mathbf{U}}_t = \mathbf{H}\mathbf{U}_t + \mathbf{Z}_t = \mathbf{H}(\mathbf{X}_t - \mathbf{A}\mathbf{Y}_{t-1}) + \mathbf{Z}_t, \tag{3.21}$$

which is also Gaussian with zero-mean and covariance

$$\begin{aligned}
\mathbb{E} [\tilde{\mathbf{U}}_t \tilde{\mathbf{U}}_t^T] &= \mathbb{E} [(\mathbf{H}\mathbf{U}_t + \mathbf{Z}_t)(\mathbf{H}\mathbf{U}_t + \mathbf{Z}_t)^T] \\
&= \mathbf{H}\mathbf{\Lambda}\mathbf{H}^T + \mathbf{\Sigma}_Z \\
&= \mathbf{H}\mathbf{\Lambda}\mathbf{H}^T + \mathbf{\Pi}\mathbf{H}^T.
\end{aligned} \tag{3.22}$$

We can consider  $\{\tilde{\mathbf{U}}_t\}$  as the reconstruction process of  $\{\mathbf{U}_t\}$  and we obtain the reconstruction of the source process by adding  $\mathbf{A}\mathbf{Y}_{t-1}$  to  $\tilde{\mathbf{U}}_t$ , i.e.,

$$\begin{aligned}
\mathbf{Y}_t &= \tilde{\mathbf{U}}_t + \mathbf{A}\mathbf{Y}_{t-1} \\
&= \mathbf{H}(\mathbf{X}_t - \mathbf{A}\mathbf{Y}_{t-1}) + \mathbf{Z}_t + \mathbf{A}\mathbf{Y}_{t-1}.
\end{aligned} \tag{3.23}$$

The error between the source and the source reconstruction  $\mathbf{Y}_t$  is equal to the error between  $\mathbf{U}_t$  and  $\tilde{\mathbf{U}}_t$ , as seen from

$$\begin{aligned}
\mathbf{X}_t - \mathbf{Y}_t &= \mathbf{X}_t - \mathbf{H}\mathbf{X}_t - (\mathbf{I} - \mathbf{H})\mathbf{A}\mathbf{Y}_{t-1} - \mathbf{Z}_t \\
&= \mathbf{X}_t - \mathbf{A}\mathbf{Y}_{t-1} - \mathbf{H}\mathbf{X}_t + \mathbf{H}\mathbf{A}\mathbf{Y}_{t-1} - \mathbf{Z}_t \\
&= \mathbf{U}_t - \tilde{\mathbf{U}}_t.
\end{aligned} \tag{3.24}$$

Thus,

$$\mathbf{\Pi} = \mathbb{E} [(\mathbf{X}_t - \mathbf{Y}_t)(\mathbf{X}_t - \mathbf{Y}_t)^T] = \mathbb{E} [(\mathbf{U}_t - \tilde{\mathbf{U}}_t)(\mathbf{U}_t - \tilde{\mathbf{U}}_t)^T]. \tag{3.25}$$

The minimization in (3.18) can be solved by e.g. semidefinite programming [21]. In [7] they found an approach of pre- and post scaling which reveals the reverse-waterfilling solution in the dimension of  $\mathbf{U}_t$ .

### 3.4.1 Test-Channel for Scalar Source

In this section, we consider the special case of a stationary scalar AR(1) source on the form

$$X_t = aX_{t-1} + W_t, \quad t \in \mathbb{N}, \quad (3.26)$$

where  $|a| < 1$ , and  $W_t \stackrel{\text{i.i.d.}}{\sim} \mathcal{N}(0, \sigma_W^2)$  is a white Gaussian process independent of  $X_0 \sim \mathcal{N}(0, \sigma_X^2)$  where  $\sigma_X^2 = \frac{\sigma_W^2}{1-a^2}$  is the stationary variance of the process. In the scalar case,  $\mathbf{\Pi} = \pi$  and  $\mathbf{\Lambda} = \lambda$  are scalars, and they are given by the quantities  $\pi = D$  and  $\lambda = a^2D + \sigma_W^2$ . The fact that  $\pi = D$  follows from (3.18) as the value of  $\pi$  that minimizes (3.18) is the maximum possible value of  $\pi$  which is  $D$  for  $D \leq \frac{\sigma_W^2}{1-a^2}$ . With these values of  $\pi$  and  $\lambda$ , (3.18) becomes

$$R_{ZD}^I(D) = \frac{1}{2} \log \left( \frac{a^2D + \sigma_W^2}{D} \right) = \frac{1}{2} \log \left( a^2 + \frac{\sigma_W^2}{D} \right). \quad (3.27)$$

The optimal test-channel is realized by

$$Y_t = hX_t + (1-h)aY_{t-1} + Z_t, \quad (3.28)$$

where  $Z_t \sim \mathcal{N}(0, \sigma_Z^2)$  and

$$h = 1 - \frac{D}{a^2D + \sigma_W^2}, \quad (3.29)$$

$$\sigma_Z^2 = hD = D - \frac{D^2}{a^2D + \sigma_W^2}. \quad (3.30)$$

In Fig. 3.3 we compare  $R_{ZD}^I(D)$  to the non-causal RDF of the AR(1) source, which is given by [22]

$$R(D) = \frac{1}{2} \log \left( \frac{\sigma_W^2(1-a^2)}{D} \right). \quad (3.31)$$

As seen from the figure, a loss in rate occurs when restricting the coding to be zero-delay. This rate loss can be explained by three factors, namely space-filling loss of causal encoders, increased distortion due to non-causal filtering, and entropy coding with memory [7], [8].

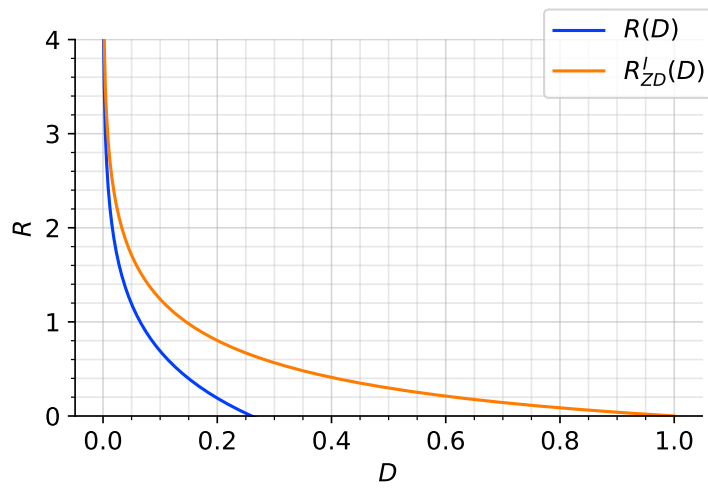


**Figure 3.3:** Non-causal RDF (blue) and Gaussian information theoretic ZD RDF (orange) for an AR(1) source with  $a = 0.7$  and  $\sigma_W^2 = 0.51$  with MSE distortion constraint  $D$ .



## 4. Zero-Delay Multiple-Descriptions

In this chapter, we cover zero-delay multiple-descriptions (ZDMD) coding, which was recently developed in [8]. As the name suggests, ZDMD coding is the combination of MD coding and ZD coding, i.e., we are considering MD encoders and decoders which are causal and has zero delay. First we define ZDMD coding in the case of two descriptions. Then, an information theoretic lower bound is presented and the bound will be characterized for stationary scalar AR(1) sources and MSE distortion constraints in the symmetric case. In relation to this, a test-channel realization scheme is presented. The content of this chapter is based on [8].

### 4.1 ZDMD Source Coding

We consider the setup for ZDMD coding described in [8], which is depicted in Fig. 4.1. The setup includes feedback from the side decoders. These feedback channels are assumed to be noiseless digital channels with a one-sample delay such that the operational feasibility of the system is ensured, i.e., the encoder output does not depend on current or future decoder output.

We will consider a stationary scalar AR(1) source process given by the discrete-time model in (3.26), i.e.,

$$X_t = aX_{t-1} + W_t, \quad t \in \mathbb{N}, \quad (4.1)$$

where  $|a| < 1$ ,  $X_0 \in \mathbb{R} \sim \mathcal{N}(0, \sigma_X^2)$  is the initial state,  $W_t \in \mathbb{R} \stackrel{\text{i.i.d.}}{\sim} \mathcal{N}(0, \sigma_W^2)$  is a white Gaussian process independent of  $X_0$ , and  $\sigma_X^2 = \frac{\sigma_W^2}{1-a^2}$ .

At each time step  $t \in \mathbb{N}_0$ , the encoder observes  $X_t$  assuming  $X^{t-1} = (X_0, \dots, X_{t-1})$  has already been observed. The encoder then produces descriptions  $B_t^{(1)}$  and  $B_t^{(2)}$  of length  $\ell_t^{(1)}$  and  $\ell_t^{(2)}$  from two predefined sets of binary codewords  $\mathcal{B}_t^{(1)}, \mathcal{B}_t^{(2)}$  of at most a countable number of codewords. The two descriptions are sent over two separate instantaneous digital noiseless channels and decoded without delay at three decoders. At the  $i$ 'th side decode,  $i = 1, 2$ , the reconstruction  $Y_t^{(i)}$  is produced when receiving  $B_t^{(i)}$  assuming that  $Y^{(i), t-1}$  has already been produced. Similar, at the central decoder, the reconstruction  $Y_t^{(0)}$  is produced when  $B_t^{(1)}$  and  $B_t^{(2)}$  are received assuming  $Y^{(0), t-1}$  has already been produced. Before the next descriptions

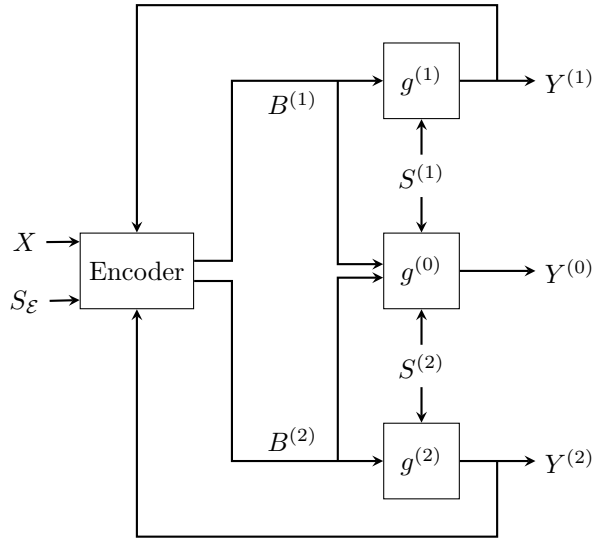


**Figure 4.1:** Block diagram of the ZDMD coding setup. [8]

are produced, the encoder receives  $Y_{t-1}^{(1)}$  and  $Y_{t-1}^{(2)}$  through the feedback channels, assuming that  $Y^{(1),t-2}$  and  $Y^{(2),t-1}$  has already been received. [8, pp. 4-5]

As it appears from Fig. 4.1, the central reconstruction is not fed back to the encoder. This is due to that all information about  $Y_t^{(0)}$  is contained in  $(Y_t^{(1)}, Y_t^{(2)})$  given the side information.

It is assumed that each sample is processed immediately for each time step  $t \in \mathbb{N}_0$  [8].

In the setup,  $S_{\mathcal{E}}^t$  denotes side information available at the encoder at time  $t$  and  $S^{(i),t}$ ,  $i = 1, 2$ , denotes the side information available at the decoders. The encoder and decoders are made dependent on the side information in order to allow for probabilistic encoding and decoding. Therefore, the side information processes are random processes independent of the source. This could for example be dithering signals. [8]

The setup is formalized in the following definition for scalar stationary sources.

**Definition 4.1 (ZDMD Source Code [8])**

Consider a stationary source process  $\{X_t\}$ . A ZDMD code consist of a encoder and three decoders. The encoder is specified by a sequence of functions  $\{f_t : t \in \mathbb{N}_0\}$  given by

$$f_t : \mathcal{X}^t \times \mathcal{Y}^{(1),t-1} \times \mathcal{Y}^{(2),t-1} \times \mathcal{S}_{\mathcal{E}}^t \rightarrow \mathcal{B}_t^{(1)} \times \mathcal{B}_t^{(2)}, \quad t \in \mathbb{N}_0, \quad (4.2)$$

and at each time step  $t \in \mathbb{N}_0$ , the encoder produces

$$(B_t^{(1)}, B_t^{(2)}) = f_t(X^t, Y^{(1),t-1}, Y^{(2),t-1}, S_{\mathcal{E}}^t) \quad (4.3)$$

with  $B_t^{(i)} \in \mathcal{B}_t^{(i)}$  where  $\ell_t^{(i)}$  is the length of the codeword in bits. For the encoding of the first source symbol, no past reconstructions are available, hence  $(B_0^{(1)}, B_0^{(2)}) = f_0(X_0, S_{\mathcal{E},0})$ . The three decoders are specified by three sequences of functions  $\{g_t^{(i)} : t \in \mathbb{N}_0\}$ , where the side decoders are given by

$$g_t^{(i)} : \mathcal{B}^{(i),t} \times \mathcal{S}^{(i),t} \rightarrow \mathcal{Y}_t^{(i)}, \quad t \in \mathbb{N}_0, \quad i = 1, 2 \quad (4.4)$$

and the central decoder is given by

$$g_t^{(0)} : \mathcal{B}^{(1),t} \times \mathcal{B}^{(2),t} \times \mathcal{S}^{(1),t} \times \mathcal{S}^{(2),t} \rightarrow \mathcal{Y}_t^{(0)}, \quad t \in \mathbb{N}_0, \quad (4.5)$$

and at time step  $t \in \mathbb{N}_0$ , the decoders produce

$$Y_t^{(i)} = g_t^{(i)}(B^{(i),t}, S^{(i),t}), \quad i = 1, 2 \quad (4.6a)$$

$$Y_t^{(0)} = g_t^{(0)}(B^{(1),t}, B^{(2),t}, S^{(1),t}, S^{(2),t}), \quad (4.6b)$$

under the assumption that  $Y^{(i),t-1}$ ,  $i = 0, 1, 2$  have already been produced.

The rates associated with a ZDMD coding scheme is given by the asymptotic average of the expected codeword length for each description.

#### Definition 4.2 (Rate Pair for ZDMD Code [8])

Let  $\ell_t^{(i)}$  be the length of the  $i$ th description,  $i = 1, 2$  to time step  $t \in \mathbb{N}_0$  for a ZDMD code, then the rate pair  $(R_1, R_2)$  for the ZDMD code is defined by

$$R_i = \lim_{n \rightarrow \infty} \frac{1}{n+1} \sum_{t=0}^n \mathbb{E} \left[ \ell_t^{(i)} \right]. \quad (4.7)$$

In [8], the following asymptotic MSE distortion constraint is considered.

#### Definition 4.3 (Asymptotic MSE Distortion Constraint [8])

An  $(R_1, R_2)$  rate pair is said to be achievable with respect to the MSE distortion constraints  $D_i > 0$ ,  $i = 0, 1, 2$  if there exist a  $(R_1, R_2)$ -rate ZDMD code satisfying

$$\lim_{n \rightarrow \infty} \frac{1}{n+1} \sum_{t=0}^n \mathbb{E} \left[ \left( X_t - Y_t^{(i)} \right)^2 \right] \leq D_i, \quad i = 0, 1, 2. \quad (4.8)$$

As for the general non-causal MD coding, we wish to characterize the region of achievable rate pairs for ZDMD codes.

**Definition 4.4 (ZDMD Region [8])**

For a stationary source  $\{X_t\}$ , the ZDMD region  $\mathcal{R}_X^{ZD}(R_1, R_2, D_0, D_1, D_2)$  is the convex closure of all achievable ZDMD rate pairs  $(R_1, R_2)$  satisfying the MSE distortion constraints  $(D_0, D_1, D_2)$ .

A full characterization of the ZDMD region can be given by determining the bound between the sets of achievable and non-achievable rate-pairs, i.e., determining the fundamental smallest rates for given distortion constraints [8]. As mentioned in Chapter 2, the region can be partitioned into regions of degenerate and non-degenerate distortions. The distortion constraints we are interested in are the non-degenerative distortion constraints, i.e., distortion triplets  $(D_0, D_1, D_2)$  satisfying

$$D_1 + D_2 - \sigma_X^2 \leq D_0 \leq \left( \frac{1}{D_1} + \frac{1}{D_2} - \frac{1}{\sigma_X^2} \right)^{-1}, \quad (4.9)$$

where  $\sigma_X^2$  is the variance of the stationary source. Also, we restrict the distortions to be less than the source variance, i.e.,  $D_i \leq \sigma_X^2$ .

We will in this thesis mainly consider the symmetric case of ZDMD coding, i.e.,  $R_1 = R_2 = R$  and  $D_1 = D_2 = D_S$ . In this case the ZDMD region can be characterized by an MD equivalent to the RDF.

**Definition 4.5 (Symmetric ZDMD RDF [8])**

The ZDMD rate-distortion function for a stationary source  $\{X_t\}$  subject to MSE distortion constraints  $D_S, D_0 \geq 0$  is the infimum of achievable rates  $R$  per description with respect to  $(D_0, D_S)$ , i.e.,

$$\begin{aligned} R_{ZD}^{op}(D_0, D_S) &= \inf R \\ &\text{s.t. } (R, R) \in \mathcal{R}_X^{ZD}(R, R, D_0, D_S, D_S), \end{aligned} \quad (4.10)$$

where the infimum is over all ZDMD codes.

The operational symmetric ZDMD RDF can be characterized in terms of the sum-rate,  $R_1 + R_2$ , as  $R = \frac{1}{2}(R_1 + R_2)$  as follows:

**Definition 4.6 (Operational Symmetric ZDMD RDF)**

For the scalar stationary source  $\{X_t\}$  and non-degenerative MSE distortion constraints  $D_0, D_S > 0$ , the operational symmetric ZDMD RDF is given by

$$\begin{aligned}
 R_{ZD}^{op}(D_0, D_S) = & \inf \lim_{n \rightarrow \infty} \frac{1}{2(n+1)} \left( \mathbb{E} \left[ L_n^{(1)} \right] + \mathbb{E} \left[ L_n^{(2)} \right] \right) \\
 \text{s.t. } & \lim_{n \rightarrow \infty} \frac{1}{n+1} \sum_{t=0}^n \mathbb{E} \left[ \left( X_t - Y_t^{(0)} \right)^2 \right] \leq D_0, \\
 & \lim_{n \rightarrow \infty} \frac{1}{n+1} \sum_{t=0}^n \mathbb{E} \left[ \left( X_t - Y_t^{(i)} \right) \right] \leq D_S, \quad i = 1, 2,
 \end{aligned} \tag{4.11}$$

where  $L_n^{(i)} = \sum_{t=0}^n l_t^{(i)}$ ,  $i = 1, 2$ , and where the infimum is over all symmetric ZDMD encoder and decoder sequences, i.e., sequences  $\{f_t\}_{t \in \mathbb{N}_0}$ ,  $\{g_t^{(i)}\}_{t \in \mathbb{N}_0}$ ,  $i = 0, 1, 2$  given by Definition 4.1.

The operational symmetric ZDMD RDF is the infimum of the mean of the marginal rates over all possible ZDMD codes. This infimum is hard to find, since the minimization is over all possible ZDMD codes. As described in Chapter 3, the general non-causal RDF is a lower bound on the operational ZD RDF. Likewise, the MD region for non-causal codes is an outer bound on the ZDMD region. However, the ZDMD region does not in general span the MD region due to spacefilling losses, memoryless entropy coding, and causal filters at the ZD decoders as described in Chapter 3 for the single description case [8].

Therefore, in [8], they developed a novel information theoretic lower bounds on the operational ZDMD coding rates.

## 4.2 Lower Bounds on Average Rates

In this section, we present the information theoretic lower bounds on the ZDMD coding rates developed in [8] where the lower bounds are provided in the general non-symmetric case, but they are used to develop the information theoretic counterpart to the operational symmetric Gaussian ZDMD RDF.

We will first present the assumptions on the distribution of the source and the reconstructions which are considered in [8] and which we will consider in this worksheet.

### 4.2.1 Distributions

We consider the reconstruction of a stationary source sequence  $X_t = x_t$ ,  $t \in \mathbb{N}_0$ , with reconstructions  $Y_t^{(i)} = y_t^{(i)}$ ,  $t \in \mathbb{N}_0$ ,  $i = 0, 1, 2$ . On the source, we assume that the

current source symbol is not related to the previous reconstructions, i.e., the source satisfies the conditional independence given by

$$P\left(x_t|x^{t-1}, y^{(0),t-1}, y^{(1),t-1}, y^{(2),t-1}\right) = P\left(x_t|x^{t-1}\right), \quad t \in \mathbb{N}_0. \quad (4.12)$$

Hence the source is unaffected by the feedback from the reconstructions. For the AR(1) source in (4.1), the conditional independence of the past reconstructions in (4.12) implies that  $W_t$  is independent of the past reconstructions  $Y^{(i),t-1}$ ,  $i = 0, 1, 2$ ,  $t \in \mathbb{N}_0$  [7].

We assume that  $X_0 \sim P(x_0)$  and by Bayes rule, we the joint distribution of the  $n + 1$  first symbols is given by [7]

$$P(x^n) = \prod_{t=0}^n P(x_t|x^{t-1}). \quad (4.13)$$

Since we work under the constraint of zero-delay, the MD encoder-decoder pairs  $(f_t, g_t^{(i)})$ ,  $i = 0, 1, 2$  must be causal [7]. The MD encoder-decoder pairs are causal if and only if the following Markov chain holds [8], [20]

$$X_{t+1}^n - X^t - \left(Y^{(0),t}, Y^{(1),t}, Y^{(2),t}\right), \quad \forall t \in \{0, \dots, n-1\}. \quad (4.14)$$

Hence, we assume that the first  $n + 1$  reconstructions are randomly generated according to the collection of conditional distributions

$$P\left(y_t^{(0)}, y_t^{(1)}, y_t^{(2)}|y^{(0),t-1}, y^{(1),t-1}, y^{(2),t-1}, x^t\right), \quad t \in \{0, \dots, n\}. \quad (4.15)$$

If causality was not required, the reconstructions could be generated from the collection of conditional distributions

$$P\left(y_t^{(0)}, y_t^{(1)}, y_t^{(2)}|y^{(0),t-1}, y^{(1),t-1}, y^{(2),t-1}, x^n\right) \quad t \in \{0, \dots, n\} \quad (4.16)$$

where the current reconstruction can depend on future source samples. However, as we require causality, we assume that reconstructions are generated from (4.15), where for  $t = 0$  the distribution reduces to

$$P\left(y_0^{(0)}, y_0^{(1)}, y_0^{(2)}|y^{(0),-1}, y^{(1),-1}, y^{(2),-1}, x^0\right) = P\left(y_0^{(0)}, y_0^{(1)}, y_0^{(2)}|x_0\right). \quad (4.17)$$

### 4.2.2 Lower Bounds

In this subsection, the information theoretic lower bounds on the general non-symmetric ZDMD codes developed in [8] are presented.

One of the assumptions made in [8] is that the decoders are invertible.

**Definition 4.7 (Invertible Decoder [8], [23])**

The decoders  $g_t^{(i)}$ ,  $i = 0, 1, 2$ ,  $t \in \mathbb{N}_0$  defined in (4.4) and (4.5) is said to be invertible if and only if  $\forall t \in \mathbb{N}_0$  there exist deterministic mappings  $\tilde{g}_t^{(i)}$ ,  $i = 0, 1, 2$  such that

$$\begin{aligned} B^{(i),t} &= \tilde{g}_t^{(i)} \left( Y_t^{(i)}, S^{(i),t} \right), \quad i = 1, 2 \\ \left( B^{(1),t}, B^{(2),t} \right) &= \tilde{g}_t^{(0)} \left( Y_t^{(0)}, S^{(1),t}, S^{(2),t} \right). \end{aligned}$$

When the decoders are invertible, knowledge about the message and side information at each of the side decoders, e.g.  $(B^{(1),t}, S^{(1),t})$  is equivalent to knowledge about the reconstruction and the side information, i.e.,  $(Y_t^{(1)}, S^{(1),t})$  [8], [23]. In [23] it was shown that we without loss of generality can restrict our attention to invertible decoders in the single description case. Furthermore, it is optimal to use invertible decoders when minimizing the average data-rate in causal source coding schemes [8], [23].

As mentioned, both lower bounds on the marginal rates and the sum-rate are needed in order to establish the outer bound on the ZDMD rate-region. The lower bounds on the marginal rates can be established by considering the side reconstructions as single descriptions ZD coding. These are therefore derived from the results of [7], [23]. In the following theorem we state the lower bounds on the marginal rates together with the lower bound on the sum-rate as developed in [8].

**Theorem 4.8 (Lower Bounds on ZDMD rates [7], [8])**

Consider the ZDMD coding of a discrete-time stationary scalar source process  $\{X_t\}$  with non-degenerative MSE distortion constraints  $D_0, D_1, D_2 > 0$ . If the systems  $f, g^{(i)}$   $i = 0, 1, 2$  are causal, described by Definition 4.1, the side information is independent of the source, i.e.,  $(\{S^{(1)}\}, \{S^{(2)}\}) \perp \{X_t\}$ , the decoder side information is mutually independent, and the decoders are invertible, then the achievable rates  $R_1$  and  $R_2$  for any ZDMD code is lower bounded by

$$R_i \geq \lim_{n \rightarrow \infty} \frac{1}{n+1} I \left( X^n \rightarrow Y^{(i),n} \right), \quad i = 1, 2, \quad (4.19a)$$

$$R_1 + R_2 \geq \lim_{n \rightarrow \infty} \frac{1}{n+1} I \left( X^n \rightarrow Y^{(1),n}, Y^{(2),n} \right) + I \left( Y^{(1),n}; Y^{(2),n} \right) \quad (4.19b)$$

*Proof.*

For the marginal rates, the result follows from [23, Theorem 4.1] by considering the side reconstructions as individual systems. For a proof of the lower bound on the sum-rate, we refer to [8, Appendix A]. ■

### 4.2.3 Gaussian Lower Bound for Scalar Gaussian Sources

As mentioned in Chapter 3, Gaussian reconstructions minimizes the information theoretic ZD RDF. A similar result was shown in [8] for the ZDMD region under some technical assumptions. i.e., for a Gaussian source, Gaussian reconstructions minimizes (4.19b). The result is derived under the assumptions that sequential greedy coding is used and that the reconstructions satisfies conditional prediction residual independence. In this section we will define sequential greedy coding and conditional prediction residual independence and afterwards present the result from [8]. Finally, we will consider the symmetric case of ZDMD coding with Gaussian reconstructions.

#### Definition 4.9 (Sequential Greedy Coding [8])

Consider the ZDMD source coding problem in Fig. 4.1. The problem is said to be solved using sequential greedy coding if for each  $t \in \mathbb{N}_0$ , we minimize the bit-rate such that the MSE distortion constraints  $D_i > 0$ ,  $i = 0, 1, 2$  are satisfied for each  $t \in \mathbb{N}_0$ .

Specifically, for each  $t \in \mathbb{N}_0$ , choose the codewords  $B_t^{(i)}$ ,  $i = 1, 2$  with the minimum codeword length  $\ell_t^{(i)}$ ,  $i = 1, 2$  such that

$$\mathbb{E} \left[ \left( X_t - Y_t^{(i)} \right)^2 \right] \leq D_i, \quad i = 0, 1, 2. \quad (4.20)$$

When we assume sequential greedy coding, we find the reconstruction distributions that minimizes (4.19b) for each time step  $t \in \mathbb{N}_0$  and fix this distribution for all following  $t' > t$ .

It is reasonable to assume sequential greedy coding for the ZDMD coding problem since at each time step, the optimum description that minimizes the rate while achieving the desired distortion must be transmitted. The downside of assuming sequential greedy coding is a potential increase in rate, as the desired performance must be achieved in each time step and not just in an asymptotic average [8]. However, the assumption is necessary in proof given in [8] for the result that Gaussian reconstructions minimizes the sum-rate.

We will now define conditional prediction residual independence for the MMSE predictors.

#### Definition 4.10 (Conditional Prediction Residual Independence [8])

Let  $\{X_t\}$  be a stationary source process and let  $\{Y_t^{(1)}\}$  and  $\{Y_t^{(2)}\}$  be stationary arbitrarily distributed MMSE reconstruction processes. The MMSE reconstruction processes is said to have conditional prediction residual independence if, for all

$t \in \mathbb{N}_0$ , the MMSE prediction residuals satisfy

$$Y_t^{(i)} - \mathbb{E} \left[ Y_t^{(i)} | Y^{(1),t-1}, Y^{(2),t-1} \right] \perp \left( Y^{(1),t-1}, Y^{(2),t-1} \right), \quad i = 1, 2 \quad (4.21)$$

$$Y_t^{(i)} - \mathbb{E} \left[ Y_t^{(i)} | Y^{(i),t-1} \right] \perp Y^{(i),t-1}, \quad i = 1, 2 \quad (4.22)$$

$$Y_t^{(i)} - \mathbb{E} \left[ Y_t^{(i)} | Y^{(j),t-1} \right] \perp Y^{(j),t-1}, \quad i \neq j, i, j \in \{1, 2\}, \quad (4.23)$$

that is, the residuals are independent of the conditioning prediction variables.

If  $\{Y_t^{(i)}\}$ ,  $i = 1, 2$  is jointly Gaussian, then by the orthogonality principle [24, p. 45], the conditional prediction residual independence is satisfied by the MMSE predictors [8].

We now state the result derived in [8] that Gaussian reconstructions minimizes the sum-rate. For a proof, we refer to [8, Appendix B].

#### Theorem 4.11 (Gaussian Lower Bound [8])

Let  $\{X_t\}$  be a stable stationary scalar Gauss-Markov process (4.1) with non-degenerative MSE distortion constraints  $D_i > 0$ ,  $i = 0, 1, 2$ . Then, under the assumption of sequential greedy coding Definition 3.4 and the assumption that the reconstruction sequences  $\{Y_t^{(i)}\}$ ,  $i = 1, 2$  satisfies conditional prediction residual independence Definition 4.10, the following inequality holds

$$\begin{aligned} & \lim_{n \rightarrow \infty} \frac{1}{n+1} \left( I \left( X^n \rightarrow Y^{(1),n}, Y^{(2),n} \right) + I \left( Y^{(1),n}; Y^{(2),n} \right) \right) \\ & \geq \lim_{n \rightarrow \infty} \frac{1}{n+1} \left( I \left( X^n \rightarrow Y_G^{(1),n}, Y_G^{(2),n} \right) + I \left( Y_G^{(1),n}; Y_G^{(2),n} \right) \right), \end{aligned} \quad (4.24)$$

where  $Y_G^{(i)}$ ,  $i = 1, 2$  are jointly Gaussian random variables with first and second moment equal to those of  $Y^{(i)}$ ,  $i = 1, 2$ .

#### Symmetric Case

Using the result on the sum-rate in Theorem 4.8, we now define the information-theoretic symmetric ZDMD RDF in terms of directed information and mutual information.

**Definition 4.12 (Information Theoretic Symmetric ZDMD RDF [8])**

The information theoretic symmetric ZDMD RDF for a stationary Gaussian source process  $\{X_t\}$ , with MSE distortion constraints  $D_0, D_S > 0$ , is

$$\begin{aligned}
R_{ZD}^I(D_0, D_S) &= \inf \lim_{n \rightarrow \infty} \frac{1}{2(n+1)} \left( I(X^n \rightarrow Y^{(1),n}, Y^{(2),n}) + I(Y^{(1),n}; Y^{(2),n}) \right) \\
\text{s.t. } &\lim_{n \rightarrow \infty} \frac{1}{n+1} \sum_{t=0}^n \mathbb{E} \left[ \left( X_t - Y_t^{(0)} \right)^2 \right] \leq D_0 \\
&\lim_{n \rightarrow \infty} \frac{1}{n+1} \sum_{t=0}^n \mathbb{E} \left[ \left( X_t - Y_t^{(i)} \right)^2 \right] \leq D_S, \quad i = 1, 2,
\end{aligned} \tag{4.25}$$

where the infimum is over all processes  $\{Y_t^{(i)}\}$ ,  $i = 0, 1, 2$  that satisfy the Markov chain

$$X_{t+1}^\infty - X^t - \left( Y^{(0),t}, Y^{(1),t}, Y^{(2),t} \right), \quad \forall t \in \mathbb{N}_0. \tag{4.26}$$

Note, that the minimization over all processes that satisfy (4.26) is equivalent to the minimization over all sequences of conditional test-channel distributions [8]

$$\{P(Y_t^{(0)}, Y_t^{(1)}, Y_t^{(2)} | Y^{(0),t-1}, Y^{(1),t-1}, Y^{(2),t-1}, x^t) : t \in \mathbb{N}\}. \tag{4.27}$$

If we restrict the reconstructions to be Gaussian, the solution to (4.25) is the Gaussian symmetric information theoretic ZDMD RDF,  $R_{ZD,GM}^I(D_0, D_S)$ .

It follows by Theorems 4.8 and 4.11, that the Gaussian symmetric ZDMD RDF is a lower bound to the operational symmetric ZMDM RDF in Definition 4.6.

**Corollary 4.13 ([8])**

Let  $\{X_t\}$  be a stationary scalar Gaussian process (4.1) with MSE distortion constraints  $D_S \geq D_0 > 0$ . Then, under the assumption of sequential greedy coding (Definition 4.9) and the assumption that the reconstruction processes  $\{Y_t^{(i)}\}$ ,  $i = 1, 2$ , satisfy conditional prediction residual independence (Definition 4.10), the following inequalities hold:

$$R_{ZD,GM}^I(D_0, D_S) \leq R_{ZD}^I(D_0, D_S) \leq R_{ZD}^{op}(D_0, D_S). \tag{4.28}$$

In [8], they derived an optimal test-channel realization scheme that achieves the Gaussian symmetric ZDMD RDF for stationary scalar AR(1) sources and MSE distortion constraints, thus characterizing the symmetric ZDMD RDF for this source and distortion. We will in the following present this characterization.

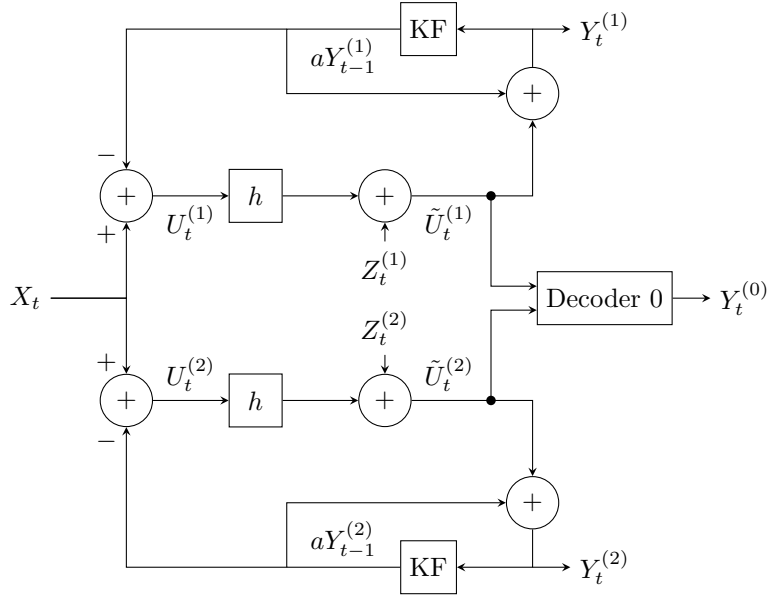


**Figure 4.2:** Overall feedback realization of the optimum test-channel for  $R_{ZD,GM}^I(D_0, D_S)$ . [8]

### 4.3 Characterization of Symmetric ZDMD RDF

The test-channel derived in [8] is an extension of the feedback realization scheme derived in [7], which is presented in Chapter 3 to the MD setup depicted in Fig. 4.1. In Figs. 4.2 and 4.3, the feedback realization of the test-channel is illustrated. We will first discuss the side reconstructions and thereafter the central decoder.

#### 4.3.1 Side Reconstructions

We consider the stationary scalar AR(1) source given by (4.1). For both side reconstructions, the test-channel realization follows the feedback realization scheme in [7]. That is, the reconstruction process for the optimum test-channel realized by

$$Y_t^{(i)} = hX_t + (1-h)aY_{t-1}^{(i)} + Z_t^{(i)}, \quad i = 1, 2, \quad (4.29)$$

where  $Z_t^{(i)} \sim \mathcal{N}(0, \sigma_Z^2)$  and

$$h = 1 - \pi_S \lambda^{-1}, \quad (4.30)$$

$$\sigma_Z^2 = \pi_S h, \quad (4.31)$$

$$\lambda = a^2 \pi_S + \sigma_W^2. \quad (4.32)$$

Furthermore,  $\pi_S$  is the MSE of the side reconstructions of  $X_t$ , i.e.,

$$\pi_S = \mathbb{E} \left[ \left( X_t - Y_t^{(i)} \right)^2 \right] \quad i = 1, 2. \quad (4.33)$$

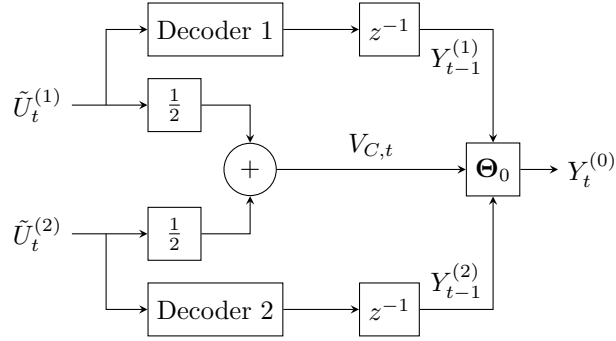


**Figure 4.3:** Central decoder of the optimum test-channel for  $R_{ZD,GM}^I(D_0, D_S)$ . [8]

As is the case of feedback realization scheme in [7], it is not the source which is directly encoded, but it is the error processes

$$\begin{aligned} U_t^{(i)} &= X_t - \mathbb{E} [X_t | Y^{(i), t-1}] \\ &= X_t - aY_{t-1}^{(i)}, \quad i = 1, 2, \end{aligned} \quad (4.34)$$

which has variance  $\lambda$ . The decoders observe the two innovation processes

$$\tilde{U}_t^{(i)} = hU_t^{(i)} + Z_t^{(i)}, \quad i = 1, 2, \quad (4.35)$$

and these can be seen as the side decoder estimate of  $U_t^{(i)}$ . Both processes have variance

$$\sigma_{\tilde{U}}^2 = h^2\lambda + \sigma_Z^2 = h^2\lambda + \pi_S h = h\lambda. \quad (4.36)$$

The side reconstructions are then obtained by

$$Y_t^{(i)} = \tilde{U}_t^{(i)} + aY_{t-1}^{(i)}, \quad i = 1, 2 \quad (4.37)$$

Considering the additive noise processes  $\{Z^{(i)}\}$ ,  $i = 1, 2$ , we have the following independence assumptions:

$$Z_t^{(1)} \perp\!\!\!\perp Z_{t'}^{(2)} \quad \forall t \neq t' \quad (4.38a)$$

$$Z_t^{(i)} \perp\!\!\!\perp Z_{t'}^{(i)} \quad \forall t \neq t', \quad i = 1, 2 \quad (4.38b)$$

$$Z_t^{(i)} \perp\!\!\!\perp U_{t'}^{(j)} \quad \forall t \geq t', \quad i, j \in \{1, 2\}. \quad (4.38c)$$

As described in Chapter 2, the quantization noise samples  $Z_t^{(i)}$ ,  $i = 1, 2$  must be correlated such that the central decoder can refine the reconstruction of  $X$ . Therefore, the test-channel noises are jointly distributed as

$$\begin{bmatrix} Z_t^{(1)} \\ Z_t^{(2)} \end{bmatrix} \sim \mathcal{N}(\mathbf{0}, \mathbf{\Sigma}_Z), \quad \forall t \in \mathbb{N}_0, \quad (4.39)$$

where

$$\mathbf{\Sigma}_Z = \begin{bmatrix} \pi_S h & \rho \pi_S h \\ \rho \pi_S h & \pi_S h \end{bmatrix}. \quad (4.40)$$

In contrast to the test-channel for non-causal MD coding, the correlated test-channel noise is added to the two prediction error samples  $U_t^{(i)}$ ,  $i = 1, 2$ , rather than the source directly. For  $t > 0$ , the two prediction error samples  $U_t^{(1)}$ ,  $U_t^{(2)}$  are correlated since the reconstructions  $Y_{t-1}^{(1)}$ ,  $Y_{t-1}^{(2)}$  are correlated. Therefore, the correlated noise is added to two correlated variables rather than the same variable  $X_t$ .

### 4.3.2 Central Decoder

As it figures from Fig. 4.2, the two innovation processes are produced by prescaling the two prediction error processes and adding Gaussian noise to these prescaled processes, i.e., the encoder output consists of two descriptions created by prescaling and adding noise to  $U_t^{(i)}$ ,  $i = 1, 2$ . The two noise processes  $Z_t^{(1)}$ ,  $Z_t^{(2)}$  are correlated as it figures from (4.40). Since the two noise processes are correlated, we can provide a better estimate of  $X_t$  by using both innovation processes  $\tilde{U}_t^{(1)}$ ,  $\tilde{U}_t^{(2)}$ . Therefore, the central decoder takes both innovation processes as input. An illustration of the central decoder is shown in Fig. 4.3.

At each time step  $t \in \mathbb{N}_0$ , the central decoder takes  $\tilde{U}_t^{(1)}$ ,  $\tilde{U}_t^{(2)}$  as input and creates the central description  $V_{C,t}$  by averaging the innovation samples, i.e.,

$$V_{C,t} = \frac{1}{2} \left( \tilde{U}_t^{(1)} + \tilde{U}_t^{(2)} \right). \quad (4.41)$$

Since the system works with zero delay, the previous side reconstructions  $Y_{t-1}^{(1)}$  and  $Y_{t-1}^{(2)}$  are available when the central decoder produces  $Y_t^{(0)}$ . These are therefore used together with  $V_{C,t}$  to produce  $Y_t^{(0)}$ . Let  $\mathbf{\Omega}_t = \left[ V_{C,t}, Y_{t-1}^{(1)}, Y_{t-1}^{(2)} \right]^T$ , then the central MMSE estimate of  $X_t$  is given by

$$\begin{aligned} Y_t^{(0)} &= \mathbb{E} [X_t | \mathbf{\Omega}_t] = \mathbf{\Theta}_0 \mathbf{\Omega}_t \\ &= \mathbf{\Sigma}_{X\mathbf{\Omega}} \mathbf{\Sigma}_{\mathbf{\Omega}}^{-1} \mathbf{\Omega}_t, \end{aligned} \quad (4.42)$$

where

$$\mathbf{\Sigma}_{X\mathbf{\Omega}} = \mathbb{E} [X \mathbf{\Omega}^T] \in \mathbb{R}^{1 \times 3} \quad (4.43)$$

$$\mathbf{\Sigma}_{\mathbf{\Omega}} = \mathbb{E} [\mathbf{\Omega} \mathbf{\Omega}^T] \in \mathbb{R}^{3 \times 3}. \quad (4.44)$$

The covariances can be computed using the definition of  $\mathbf{\Omega}$  and the covariances listed in [8, Lemma 2].

With this central reconstruction, the central distortion is

$$\pi_0 = \sigma_X^2 - \mathbf{\Sigma}_{X\mathbf{\Omega}} \mathbf{\Sigma}_{\mathbf{\Omega}}^{-1} \mathbf{\Sigma}_{X\mathbf{\Omega}}^T, \quad (4.45)$$

### 4.3.3 Rates

Finally, the achievable sum-rate for the test-channel is computed. By definition of directed information rate,  $R_{ZD,GM}^I(D_0, D_S)$  is given as

$$R_{ZD,GM}^I(D_0, D_S) = \inf \frac{1}{2} \lim_{n \rightarrow \infty} \frac{1}{n+1} \sum_{t=0}^n \left[ I\left(X^t; Y_t^{(1)}, Y_t^{(2)} | Y^{(1),t-1}, Y^{(2),t-1}\right) + I\left(Y_t^{(2)}; Y^{(1),t} | Y^{(2),t-1}\right) + I\left(Y_t^{(1)}; Y^{(2),t-1} | Y^{(1),t-1}\right) \right] \quad (4.46)$$

Each summand can be expressed in terms of differential entropy as [8]

$$\begin{aligned} & I\left(X^t; Y_t^{(1)}, Y_t^{(2)} | Y^{(1),t-1}, Y^{(2),t-1}\right) + I\left(Y_t^{(2)}; Y^{(1),t} | Y^{(2),t-1}\right) + I\left(Y_t^{(1)}; Y^{(2),t-1} | Y^{(1),t-1}\right) \\ &= h\left(Y_t^{(2)} | Y^{(2),t-1}\right) + h\left(Y_t^{(1)} | Y^{(1),t-1}\right) - h\left(Y_t^{(1)}, Y_t^{(2)} | Y^{(1),t-1}, Y^{(2),t-1}, X^t\right) \end{aligned}$$

We can express

$$h\left(Y_t^{(i)} | Y^{(i),t-1}\right) = h\left(\tilde{U}_t^{(i)}\right) = \frac{1}{2} \log(2\pi e \lambda h), \quad (4.47)$$

where the first equality follows from (4.37), translation invariance of differential entropy [12, Theorem 8.6.3], and conditional prediction residual independence Definition 4.10, and where the second equality follows from the differential entropy of a Gaussian random variable. Likewise, using (4.29) and the independence assumptions on  $Z_t^{(1)}$  and  $Z_t^{(2)}$ , we have that

$$\begin{aligned} h\left(Y_t^{(1)}, Y_t^{(2)} | Y^{(1),t-1}, Y^{(2),t-1}, X^t\right) &= h\left(Z_t^{(1)}, Y_t^{(2)}\right) \\ &= \frac{1}{2} \log\left((2\pi e)^2 |\Sigma_{\mathbf{Z}}|\right) \\ &= \frac{1}{2} \log\left((2\pi e)^2 \pi_S^2 h^2 (1 - \rho^2)\right). \end{aligned} \quad (4.48)$$

Since neither of (4.47) and (4.48) depend on the time  $t$ , the achievable symmetric sum-rate is

$$\begin{aligned} R_1 + R_2 &= \frac{1}{2} \log(2\pi e \lambda h) + \frac{1}{2} \log(2\pi e \lambda h) - \frac{1}{2} \log\left((2\pi e)^2 \pi_S^2 h^2 (1 - \rho^2)\right) \\ &= \log\left(\frac{2\pi e \lambda h}{2\pi e \pi_S h \sqrt{1 - \rho^2}}\right) \\ &= \log\left(\frac{\lambda}{\pi_S}\right) - \frac{1}{2} \log(1 - \rho^2). \end{aligned} \quad (4.49)$$

Summarizing the above derivations, the characterization of symmetric ZDMD RDF is given by the following theorem:

**Theorem 4.14 (Characterization of Symmetric ZDMD RDF [8])**

Consider the stationary scalar AR(1) source given by (4.1) and non-degenerate MSE distortion constraints  $(D_0, D_S)$  where  $0 < D_0 \leq D_S \leq \sigma_X^2$ . The Gaussian information theoretic symmetric ZDMD RDF  $R_{ZD,GM}^I(D_0, D_S)$  is characterized by the following minimization problem:

$$\begin{aligned} \min_{\{\pi_S, \rho\}} \quad & \frac{1}{2} \log\left(\frac{\lambda}{\pi_S}\right) - \frac{1}{4} \log(1 - \rho^2) \\ \text{s.t.} \quad & -1 \leq \rho \leq 0 \\ & 0 \leq \pi_S \leq \lambda \\ & 0 \leq \pi_i \leq D_i, \quad i = 0, S \end{aligned} \tag{4.50}$$

where

$$\lambda = a^2 \pi_S + \sigma_W^2 \tag{4.51}$$

$$\pi_0 = \sigma_X^2 - \Sigma_{X\Omega} \Sigma_{\Omega}^{-1} \Sigma_{X\Omega}^T, \tag{4.52}$$

and  $\Sigma_{X\Omega}$ ,  $\Sigma_{\Omega}$  are defined in (4.43) and (4.44).

We will in the following chapters design operational ZDMD coding schemes and simulate the performance. The symmetric ZDMD RDF will provide a lower bound for the operational ZDMD coding schemes, which assumes AR(1) sources.



## 5. Operational ZDMD coding

In this chapter, we present operational ZDMD coding schemes. In [8], they presented the scheme developed in [9], and showed that this scheme can be used as an operational ZDMD coding scheme. The scheme assume AR(1) sources, and thus the developed operational ZDMD scheme is restricted to assume this model order. In this chapter we will present novel ZDMD coding schemes, which are able to assume AR( $p$ ) sources of any order  $p$ .

We will consider encoding of a stationary scalar AR( $p$ ) source, i.e.

$$X_t = \sum_{i=1}^p a_i X_{t-i} + W_t, \quad t = p, p+1, \dots, \quad (5.1)$$

where  $W_t \sim \mathcal{N}(0, \sigma_W^2)$ . We can compactly write (5.1) as

$$X_t = \mathbf{a}^T \mathbf{X}_{t-1} + W_t, \quad t = p, p+1, \dots, \quad (5.2)$$

where  $\mathbf{a} = [a_1, \dots, a_p]^T \in \mathbb{R}^p$  and  $\mathbf{X}_{t-1} = [X_{t-1}, \dots, X_{t-p}]^T \in \mathbb{R}^p$ . We present schemes that assume AR( $p$ ) sources and therefore uses that the source is AR( $p$ ), but we will also present a scheme assuming an AR(1) source. To obtain the parameters, we use the Yule-Walker equation as described in e.g. [25, pp. 69-70].

As described in Chapter 4, the quantization noise of the two descriptions must be correlated such that a smaller MSE distortion can be obtained when combining the two descriptions in the central reconstruction. It is however not a straight-forward task to construct descriptions with correlated noises [16]. We will present two approaches to obtain correlated noises. The first one is based on staggered quantization as described in [9], and the second one is based on index assignment as described in [16]. Furthermore, all schemes presented in this chapter is based on differential pulse code modulation (DPCM) quantization.

In a DPCM encoder of the source in (5.1), the source sample at time  $t$  is predicted by  $\mathbf{a}^T \mathbf{Y}_{t-1}$ , where  $\mathbf{Y}_{t-1} = [Y_{t-1}, \dots, Y_{t-p}]^T \in \mathbb{R}^p$  and  $Y_{t-i}$  is the reconstructions of  $X_{t-i}$  for  $i = 1, 2, \dots, p$ . In stead of quantizing the source directly, the prediction error  $U_t = X_t - \mathbf{a}^T \mathbf{Y}_{t-1}$  is quantized and transmitted to the decoder. The reconstruction of  $X_t$  at the decoder is then  $Y_t = \mathcal{Q}(U_t) + \mathbf{a}^T \mathbf{Y}_{t-1}$ , where  $\mathcal{Q}(U_t)$  is the quantitation of  $U_t$ .

The use of DPCM encoders in the ZDMD schemes is motivated by the test-channel realization described in Chapter 4. As described, the optimal test-channel realization is based on the innovations approach, where the prediction error sequence is quantized, which is exactly the idea behind DPCM encoding.

Note, that we assume feedback from the decoder. This is done in order to synchronize the encoder and decoder.

## 5.1 Schemes Based on Staggered Quantizers

In this section, we present schemes based on staggered quantization. The schemes varies in how the predictor is defined. We present a scheme using the optimal predictor under the AR( $p$ ) assumption and a scheme using a sub-optimal predictor. The scheme using the sub-optimal predictor is only applicable when assuming AR(1) sources, whereas the scheme using the optimal predictor can be applied for any model order,  $p$ . The optimal and sub-optimal schemes are described in [9] and [8] for AR(1) sources.

Before we present the ZDMD coding schemes, we will introduce to staggered quantization.

### 5.1.1 Staggered Quantization

The main idea behind the use of staggered quantizers for a MD coding scheme, is to use two identical uniform quantizers, which are shifted compared to each other. In this way, when the output of both quantizers are combined, a finer quantization is accomplished. For now, consider a white Gaussian source process  $\{X_t\}$ , with  $X_t \sim N(0, \sigma_X^2)$ . The two staggered scalar uniform quantizers are given by

$$\mathcal{Q}_{1,\Delta}(x) = \text{Round}\left(\frac{x}{\Delta}\right) \Delta \quad (5.3a)$$

$$\mathcal{Q}_{2,\Delta}(x) = \text{Round}\left(\frac{x + \delta}{\Delta}\right) \Delta - \delta, \quad (5.3b)$$

where the Round( $\cdot$ ) function rounds to the nearest integer,  $\Delta$  is the bin size of the quantizers and  $\delta$  is the shift or stagger between the two quantizers. When  $\mathcal{Q}_{1,\Delta}$  and  $\mathcal{Q}_{2,\Delta}$  is applied to the source  $X_t$  with sufficiently high rates, corresponding to small  $\Delta$ , then the source is approximately uniformly distributed within each quantizer bin [12]. Therefore the optimal reconstruction of  $X_t$  given the output of the staggered quantizers is the mean of the outputs [9]. To minimize the MSE of the central reconstruction, the shift should be half the quantizer bin size, i.e.,  $\delta = \Delta/2$ , which ensures that  $\mathcal{Q}_{1,\Delta}(X_t) - \mathcal{Q}_{2,\Delta}(X_t) = \pm\Delta/2$  [9]. Using staggered quantizers, the central reconstruction has 6 dB better MSE performance compared to the side reconstructions, i.e., the output of each staggered quantizer [26].

### 5.1.2 Staggered DPCM Quantization

We will now present the staggered DPCM quantization schemes. As mentioned, we consider DPCM quantization as this resembles the test-channel realization scheme in the way that the a prediction error process is quantized instead of the source samples directly. We will first consider the schemes presented in [9] for AR(1) sources, and then extend the approach to AR( $p$ ) sources.

The general approach of the staggered ZDMD schemes is use two DPCM encoders with staggered quantizers  $\mathcal{Q}_{1,\Delta_S}$  and  $\mathcal{Q}_{2,\Delta_S}$ , referred to as the first stage quantizers, together with a refinement quantizer  $\mathcal{Q}_{0,\Delta_0}$  in a second layer. Let  $\hat{X}_t^{(i)}$ ,  $i = 1, 2$  denote the predictors of  $X_t$  used to obtain the prediction error samples in the DPCM encoders. Then at each time step  $t$ , the prediction error sample for each of the first stage quantizers is obtained by

$$U_t^{(i)} = X_t - \hat{X}_t^{(i)}. \quad (5.4)$$

Then the prediction error at each side is quantized using staggered quantizers, i.e.,

$$U_t^{\Delta_S,(1)} = \mathcal{Q}_{1,\Delta_S} \left( U_t^{(1)} \right) = \text{Round} \left( \frac{U_t^{(1)}}{\Delta_S} \right) \Delta_S \quad (5.5a)$$

$$U_t^{\Delta_S,(2)} = \mathcal{Q}_{2,\Delta_S} \left( U_t^{(2)} \right) = \text{Round} \left( \frac{U_t^{(2)} + \delta}{\Delta_S} \right) \Delta_S - \delta. \quad (5.5b)$$

The quantized prediction error samples are encoded using lossless entropy coding, and the codeword is included in packet  $i$ ,  $i = 1, 2$ .

In addition to the entropy coded output of the quantizers  $\mathcal{Q}_{1,\Delta_S}$  and  $\mathcal{Q}_{2,\Delta_S}$ , the packets also include information from the refinement quantizer  $\mathcal{Q}_{0,\Delta_0}$ . First the central prediction error sample  $E_{C,t}$  is computed by

$$E_{C,t} = X_t - \frac{1}{2} \left( Y_t^{(1)} + Y_t^{(2)} \right), \quad (5.6)$$

where  $Y_t^{(i)}$ ,  $i = 1, 2$  are the side reconstructions at time  $t$ . The prediction error sample is then quantized using  $\mathcal{Q}_{0,\Delta_0}$  with quantization step size  $\Delta_0$  followed by lossless entropy coding. The bits of codeword is separated into two sub-codewords, and one of these is included in each of the packets.

The packets are transmitted over erasure channels with packet loss probability  $p_l$  on both channels.

Assuming that both packets are received at the decoder, the central reconstruction serves as the estimate of  $X_t$ . If a packet is lost on either of the two channels,  $Y_t^{(1)}$  or  $Y_t^{(2)}$  will be used as the estimate for  $X_t$ . The side reconstructions are obtained by

$$Y_t^{(i)} = U_t^{\Delta_S,(i)} + \hat{X}_{t-1}^{(i)}, \quad i = 1, 2 \quad (5.7)$$

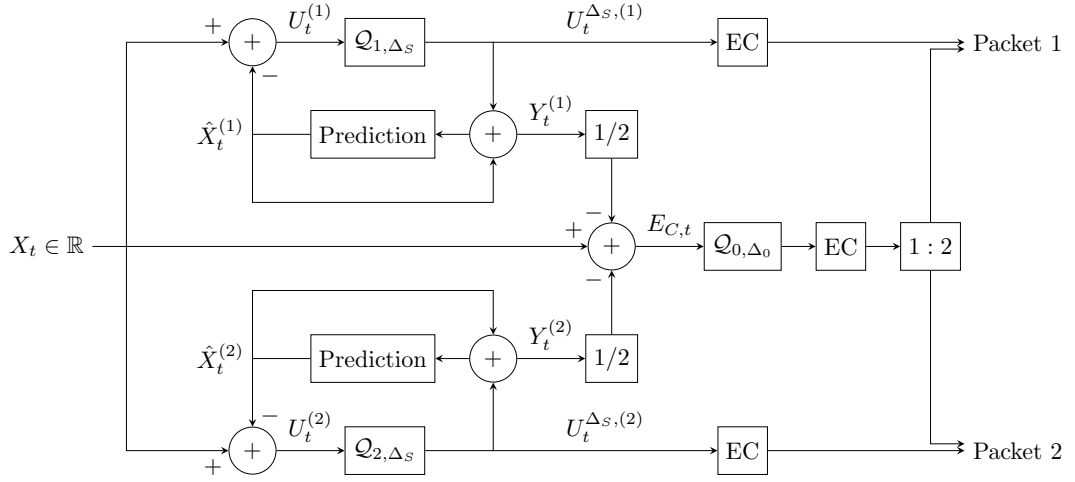


**Figure 5.1:** Illustration of the DPCM scheme using staggered quantizers. Here EC denotes lossless entropy coding and 1 : 2 means that the bits of the codeword for the refinement quantizer is split in two such that each packet contains half of the bits of this codeword.

while the central reconstruction is obtained using the side reconstructions as

$$Y_t^{(0)} = E_{C,t}^{\Delta_0} + \frac{1}{2} \left( Y_t^{(1)} + Y_t^{(2)} \right). \quad (5.8)$$

The scheme is depicted in Fig. 5.1.

The schemes presented in this section differs in how the predictors  $\hat{X}_t^{(i)}$ ,  $i = 1, 2$  are defined. The considerations when defining the predictors include the optimality of the predictors as well the resulting quantizer partitions. As mentioned in Section 5.1.1, the desired quantizer partitions should imply  $Y_t^{(1)} - Y_t^{(2)} = \pm \Delta_S/2$ . However, since we use the prediction error samples as input to the staggered quantizers, the quantizer partitions for  $X_t$  and  $U_t^{(i)}$  are shifted by  $\hat{X}_t^{(i)}$ . Thus, the optimal shift between the quantizers  $\delta$  depends on how the predictors are defined. One way to guarantee  $Y_t^{(1)} - Y_t^{(2)} = \pm \Delta_S/2$ , is to let  $\hat{X}_t^{(1)} - \hat{X}_t^{(2)} = \pm \Delta_S/2$ . [9]

Later in this section, we will cover the difference between the cases of optimal predictors for AR(1) and AR( $p$ ) as well as a sub-optimal predictor for AR(1).

## Rates and Distortion

We will in the following assess the rate and distortion performance of the staggered ZDMD scheme.

To each of the quantizers in the scheme, a rate is associated and this rate is related to the quantizer step size. Let  $R_S$  be the rate of the quantizers  $Q_{1, \Delta_S}$  and  $Q_{2, \Delta_S}$  in the first stage and let  $R_0$  be the rate of  $Q_{0, \Delta_0}$ . Then the sum-rate per sample of the scheme is given by

$$R = 2R_S + R_0. \quad (5.9)$$

If the rate of the quantizers is sufficiently high, the input to the quantizer is approximately uniformly distributed within each quantizer bin [27]. Therefore, we can model the quantization error as a sample of white process with uniformly distributed samples. The quantization error of the first stage quantizers is therefore modeled as

$$U_t^{(i)} - U_t^{\Delta_S, (i)} = Z_t^{(i)} \sim \mathcal{U}\left(-\frac{\Delta_S}{2}, \frac{\Delta_S}{2}\right) \quad (5.10)$$

which means that the variance of the first stage quantizers is approximately

$$\sigma_{Z_S}^2 \approx \frac{\Delta_S^2}{12}. \quad (5.11)$$

By modeling the quantization as uniformly distributed noise, we can analyze the variance of the input to the quantizer, which is relevant in relation to determining the rates and distortion of the scheme. First we note that

$$\begin{aligned} Y_t^{(i)} &= U_t^{\Delta_S, (i)} + \hat{X}_t \\ &= U_t^{(i)} - Z_t^{(i)} + \hat{X}_t \\ &= X_t - \hat{X}_t + \hat{X}_t - Z_t^{(i)} \\ &= X_t - Z_t^{(i)}, \quad i = 1, 2, \end{aligned} \quad (5.12)$$

which means that the side distortion is

$$D_S = \mathbb{E} \left[ \left( X_t - Y_t^{(i)} \right)^2 \right] = \mathbb{E} \left[ \left( Z_t^{(i)} \right)^2 \right] \approx \frac{\Delta_S^2}{12}, \quad i = 1, 2. \quad (5.13)$$

In the high-rate case, the coding rate is approximated by,

$$\begin{aligned} R_S &= H \left( U_t^{\Delta_S, (i)} \right) \approx h \left( U_t^{(i)} \right) - \log(\Delta_S) \\ &= \frac{1}{2} \log(2\pi e \lambda) - \log(\Delta_S), \end{aligned} \quad (5.14)$$

where the approximation follows from [12, Theorem 8.3.1] and where the last equation follows from the differential entropy of a Gaussian random variable with  $\lambda$  being the variance of  $U_t^{(i)}$ ,  $i = 1, 2$ . The rate of the second stage decoder is likewise given as

$$R_0 = H \left( E_{C,t}^{\Delta_0} \right) \approx h(E_{C,t}) - \log(\Delta_0), \quad (5.15)$$

where  $E_{C,t}$  is given by (5.6). As mentioned, the error in the first stage quantizers is approximately uniform for high rates. Furthermore, for high rates, the central prediction error  $E_{C,t}$  is also uniformly distributed with variance  $\sigma_{E_C}^2 = D_S/4$  [9]. Therefore, the differential entropy of  $E_{C,t}$  is

$$h(E_{C,t}) = \log\left(\sqrt{12}\sigma_{E_C}^2\right) = \log\left(\sqrt{3D_S}\right). \quad (5.16)$$

by isolating  $\Delta_0$  in (5.15), we obtain

$$\Delta_0 \approx 2^{-R_0} \sqrt{12\sigma_{EC}^2} = 2^{-R_0} \sqrt{3D_S}. \quad (5.17)$$

The central distortion in the high rate scenario is therefore

$$D_0 = \frac{\Delta_0^2}{12} = 2^{-2R_0} \frac{D_S}{4}. \quad (5.18)$$

### Sub-Optimal AR(1) Predictor

In [9] and [8], they consider a sub-optimal predictor for an AR(1) source. Specifically, they let  $\hat{X}_t^{(i)} = Y_{t-1}^{(i)}$ ,  $i = 1, 2$ , thus the prediction error sample at time step  $t$  is

$$U_t^{(i)} = X_t - Y_{t-1}^{(i)}, \quad i = 1, 2, \quad (5.19)$$

and the reconstructions are given by

$$Y_t^{(i)} = U_t^{\Delta_S, (i)} + Y_{t-1}^{(i)}, \quad i = 1, 2. \quad (5.20)$$

In order to minimize the MSE, the predictors must be offset by  $\Delta_S/2$ , i.e.  $\hat{X}_t^{(1)} - \hat{X}_t^{(2)} = \pm\Delta_S/2$ , which in this case requires  $Y_{t-1}^{(1)} - Y_{t-1}^{(2)} = \pm\Delta_S/2$ . Hence, if  $Y_{t-1}^{(1)} - Y_{t-1}^{(2)} = \pm\Delta_S/2$ , then  $Y_t^{(1)} - Y_t^{(2)} = \pm\Delta_S/2$ . Therefore, to achieve the optimal offset for all samples, it is only necessary to ensure the offset for  $t = 0$ . Letting the reconstructions for  $t < 0$  be zero, we have that

$$U_0^{(i)} = X_0 \quad (5.21)$$

and we use the staggered quantizers of (5.3) with step size  $\Delta_S$  and with a shift of  $\delta = \Delta_S/2$  for  $t = 0$ , and for  $t > 0$ ,  $\mathcal{Q}_{1, \Delta_S}$  and  $\mathcal{Q}_{2, \Delta_S}$  are two identical uniform quantizers with step size  $\Delta_S$ . [9]

Finally, the variance of  $U_t^{(i)}$ ,  $i = 1, 2$  using these predictors is

$$\begin{aligned} \lambda &= \text{Var} \left( U_t^{(i)} \right) = \text{Var} \left( X_t - Y_{t-1}^{(i)} \right) \\ &= \text{Var} \left( X_t - X_{t-1} + Z_{t-1}^{(i)} \right) \\ &= \text{Var} \left( a_1 X_{t-1} + W_t - X_{t-1} + Z_{t-1}^{(i)} \right) \\ &= (a_1 - 1)^2 \sigma_X^2 + \sigma_W^2 + \sigma_{Z_S}^2 \\ &= \frac{2}{1 + a_1} \sigma_W^2 + \frac{\Delta_S^2}{12}, \quad i = 1, 2, \end{aligned} \quad (5.22)$$

where the last equality follows from the stationary variance of an AR(1), which is  $\sigma_X^2 = \frac{\sigma_W^2}{1 - a_1^2}$ .

### Optimal AR(1) Predictor

The variance of  $U_t^{(i)}$ ,  $i = 1, 2$  can be decreased by using another definition for the predictors  $\hat{X}_t^{(i)}$ ,  $i = 1, 2$ . When assuming an AR(1) source, the optimal predictor is [10, p. 276]

$$\hat{X}_t^{(i)} = a_1 Y_{t-1}^{(i)}, \quad i = 1, 2. \quad (5.23)$$

Using the optimal predictors, the prediction error samples are given by

$$U_t^{(i)} = X_t - a_1 Y_{t-1}^{(i)}, \quad i = 1, 2, \quad (5.24)$$

and the reconstructions are given by

$$Y_t^{(i)} = U_t^{\Delta_S, (i)} + a_1 Y_{t-1}^{(i)}, \quad i = 1, 2. \quad (5.25)$$

The variance of  $U_t^{(i)}$ ,  $i = 1, 2$  using this predictor is

$$\begin{aligned} \lambda &= \text{Var} \left( U_t^{(i)} \right) = \text{Var} \left( X_t - a_1 Y_{t-1}^{(i)} \right) \\ &= \text{Var} \left( X_t - a_1 \left( X_{t-1} + Z_{t-1}^{(i)} \right) \right) \\ &= \text{Var} \left( a_1 X_{t-1} + W_t - a_1 \left( X_{t-1} + Z_{t-1}^{(i)} \right) \right) \\ &= \text{Var} \left( W_t - a_1 Z_{t-1}^{(i)} \right) \\ &= a_1^2 \sigma_{Z_S}^2 + \sigma_W^2 \\ &= a_1^2 \frac{\Delta_S^2}{12} + \sigma_W^2, \quad i = 1, 2. \end{aligned} \quad (5.26)$$

Comparing the variance of  $U_t^{(i)}$  using the optimal predictor to using the sub-optimal predictor, it is also apparent, that the optimal predictor yields a smaller variance of  $U_t^{(i)}$ . Let  $\lambda_{sub}$  denote the variance in (5.22) and let  $\lambda_{op}$  denote the variance using the optimal predictor, then

$$\begin{aligned} \lambda_{sub} - \lambda_{op} &= \frac{2}{1 + a_1} \sigma_W^2 + \sigma_{Z_S}^2 - a_1^2 \sigma_{Z_S}^2 - \sigma_W^2 \\ &= \frac{1 - a_1}{1 + a_1} \sigma_W^2 + (1 - a_1^2) \sigma_{Z_S}^2 \\ &> 0, \end{aligned} \quad (5.27)$$

since,  $\sigma_{Z_S}^2 > 0$ ,  $\sigma_W^2 > 0$ , and  $|a_1| < 1$  for a stationary AR(1) source, and it follows that  $\lambda_{sub} > \lambda_{op}$ . Hence for the same  $\Delta_S$ , the optimal predictor obtains a smaller rate  $R_S$  compared to the sub-optimal predictor.

However, using the optimal predictor, we have to use some bits on information about the shift between the first stage quantizers  $\mathcal{Q}_{1, \Delta_S}$  and  $\mathcal{Q}_{2, \Delta_S}$ . When an AR(1) source is assumed, the shift between the first stage quantizers at time  $t$  must be

$$\delta_t = \text{sign} \left( Y_{t-1}^{(1)} - Y_{t-1}^{(2)} \right) (1 - a) \frac{\Delta_S}{2}. \quad (5.28)$$

This can be seen from the difference between the two reconstructions in (5.25). We want this difference to be  $\pm \frac{\Delta_S}{2}$ . Assuming that  $Y_{t-1}^{(1)} - Y_{t-1}^{(2)} = \text{sign} \left( Y_{t-1}^{(1)} - Y_{t-1}^{(2)} \right) \frac{\Delta_S}{2}$ , we have that

$$\begin{aligned} \pm \frac{\Delta_S}{2} = Y_t^{(1)} - Y_t^{(2)} &= U_t^{\Delta_S, (1)} + aY_{t-1}^{(1)} - U_t^{\Delta_S, (2)} - aY_{t-1}^{(2)} \\ &= U_t^{\Delta_S, (1)} - U_t^{\Delta_S, (2)} + a \left( Y_{t-1}^{(1)} - Y_{t-1}^{(2)} \right) \\ &= \delta_t + a \left( \text{sign} \left( Y_{t-1}^{(1)} - Y_{t-1}^{(2)} \right) \frac{\Delta_S}{2} \right) \end{aligned} \quad (5.29)$$

where the last equality follows since the difference between prediction error samples is the shift between the staggered quantizers and since we assume that the previous difference between the predictions is  $\text{sign} \left( Y_{t-1}^{(1)} - Y_{t-1}^{(2)} \right) \frac{\Delta_S}{2}$ . Isolating  $\delta_t$  yields (5.28).

As pointed out in [9], an extra bit indicating the sign of  $Y_t^{(1)} - Y_t^{(2)}$  must be transmitted at every time step over the second channel, since this information is needed if the packet transmitted over the first channel is lost. At low rates, this will reduce the efficiency.

### Optimal AR( $p$ ) Predictor

We now extend the scheme to use the optimal predictors when assuming an AR( $p$ ) source. When assuming an AR( $p$ ) source, the optimal predictor is [10, p. 276]

$$\hat{X}_t^{(i)} = \mathbf{a}^T \mathbf{Y}_{t-1}^{(i)}, \quad i = 1, 2 \quad (5.30)$$

where  $\mathbf{a} = [a_1, \dots, a_p]^T \in \mathbb{R}^p$  are the  $p$  source coefficients and  $\mathbf{Y}_{t-1}^{(i)} = [Y_{t-1}^{(i)}, \dots, Y_{t-p}^{(i)}]^T \in \mathbb{R}^p$  are the  $p$  previous reconstructions. The extension of the staggered ZDMD scheme to use this predictor is straight forward. The prediction error samples are given by

$$U_t^{(i)} = X_t - \mathbf{a}^T \mathbf{Y}_{t-1}^{(i)}, \quad i = 1, 2, \quad (5.31)$$

and the reconstructions are given by

$$Y_t^{(i)} = U_t^{\Delta_S, (i)} + \mathbf{a}^T \mathbf{Y}_{t-1}^{(i)}, \quad i = 1, 2. \quad (5.32)$$

Letting  $\mathbf{Z}_{t-1}^{(i)} = [Z_{t-1}^{(i)}, \dots, Z_{t-p}^{(i)}]^T \in \mathbb{R}^p$ ,  $i = 1, 2$  be the collection of the quantization errors (5.10), the variance of the prediction error  $U_t^{(i)}$  is given by

$$\begin{aligned}
\lambda &= \text{Var} \left( U_t^{(i)} \right) = \text{Var} \left( X_t - \mathbf{a}^T \mathbf{Y}_{t-1}^{(i)} \right) \\
&= \text{Var} \left( X_t - \mathbf{a}^T \left( \mathbf{X}_{t-1} + \mathbf{Z}_{t-1}^{(i)} \right) \right) \\
&= \text{Var} \left( \mathbf{a}^T \mathbf{X}_{t-1} + W_t - \mathbf{a}^T \left( \mathbf{X}_{t-1} + \mathbf{Z}_{t-1}^{(i)} \right) \right) \\
&= \text{Var} \left( W_t - \mathbf{a}^T \mathbf{Z}_{t-1}^{(i)} \right) \\
&= \mathbf{a}^T \sigma_{Z_S}^2 \mathbf{I} \mathbf{a} + \sigma_W^2 \\
&= \frac{\Delta_S^2}{12} \|\mathbf{a}\|_2^2 + \sigma_W^2, \quad i = 1, 2,
\end{aligned} \tag{5.33}$$

When we assume an AR(2) source, the shift between the two first stage quantizers depends on the sign of the difference between the predictions of the  $p$  previous time steps. For  $p = 2$ , this is can be seen by

$$\begin{aligned}
\frac{\Delta_S}{2} &= U_t^{\Delta, (1)} + \mathbf{a}^T \mathbf{Y}_{t-1}^{(1)} - U_t^{\Delta, (2)} - \mathbf{a}^T \mathbf{Y}_{t-1}^{(2)} \\
&= \delta_t + \mathbf{a}^T \left( \mathbf{Y}_{t-1}^{(1)} - \mathbf{Y}_{t-1}^{(2)} \right) \\
&= \delta_t + \frac{\Delta_S}{2} \mathbf{a}^T \begin{bmatrix} \text{sign} \left( Y_{t-1}^{(1)} - Y_{t-1}^{(2)} \right) \\ \text{sign} \left( Y_{t-2}^{(1)} - Y_{t-2}^{(2)} \right) \end{bmatrix}.
\end{aligned} \tag{5.34}$$

Isolating  $\delta_t$  yields

$$\delta_t = \left( 1 - \mathbf{a}^T \begin{bmatrix} \text{sign} \left( Y_{t-1}^{(1)} - Y_{t-1}^{(2)} \right) \\ \text{sign} \left( Y_{t-2}^{(1)} - Y_{t-2}^{(2)} \right) \end{bmatrix} \right) \frac{\Delta_S}{2}. \tag{5.35}$$

In the worst case we, first lose two samples from the second quantizer and then we lose the next sample from the first quantizer. This means that any information sent over the second channel regarding the sign of the differences of the predictions for the two previous steps are lost. We therefore need to include  $\text{sign} \left( Y_{t-1}^{(1)} - Y_{t-1}^{(2)} \right)$  and  $\text{sign} \left( Y_{t-2}^{(1)} - Y_{t-2}^{(2)} \right)$  in the packet for the second quantizer at time  $t$  in order to decode  $Y_t^{(2)}$ . This is two bits of extra information we must include for every sample over the second channel. For general  $p$ , we need  $p$  bits of extra information.

We can reduce the extra information per sample by letting the packets include multiple samples. If a packet includes  $T$  samples, we need  $T+p-1$  bits of information regarding the sign difference of the predictions in each packet, which means we have and extra  $\frac{T+p-1}{T} > 1$  bits per sample of information regarding the sign.

As a final remark about the rates, it should be noted, that due to the necessity of transmitting the information of the sign of the difference of the side reconstructions,

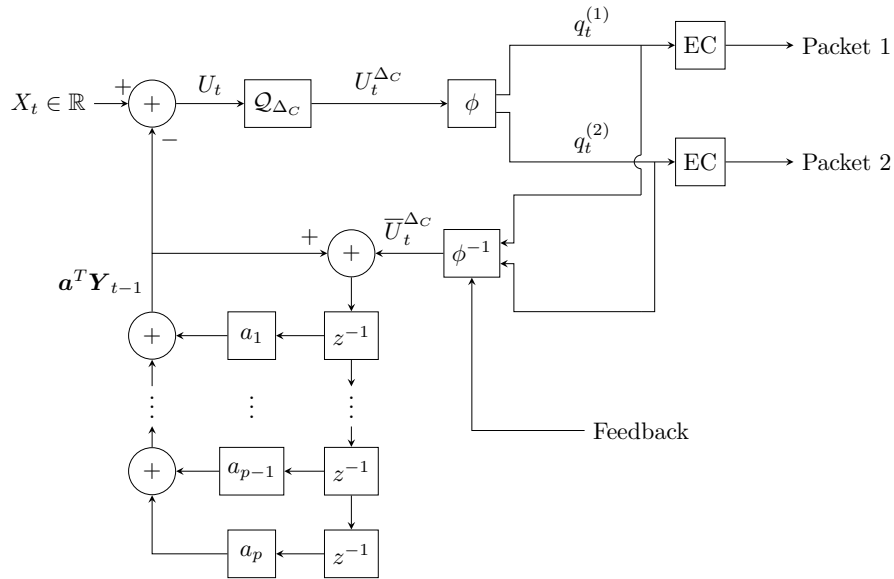


**Figure 5.2:** Illustration of DPCM index assignment scheme. Here EC denotes lossless entropy coding and ED denotes entropy decoding. The inverse index assignment symbol denotes the recovery of  $U_t^{\Delta_c}$  and the feedback is information from the receiver about which descriptions are received.

the setup is not balanced in the sense that the rates over the two channels are not the same. As mentioned, we need a rate of  $R_2 = R_S + \frac{T+1}{T} > R_S + 1$  on the second channel to transmit the necessary information of the sign. This means that the average rate per description is about 0.5 larger, compared to a scheme which does not need to send this extra information, for example the scheme in [9].

## 5.2 DPCM Index Assignment

In this section we present a index assignment scheme assuming AR( $p$ ) sources based on DPCM. In Chapter 6, we simulate the performance of the scheme when assuming both AR(1) and AR(2). Consider the AR( $p$ ) in (5.1). The main idea is to apply the index assignment method described in [16, Section IV-C] to the prediction error process

$$U_t = X_t - \mathbf{a}^T \mathbf{Y}_{t-1}, \quad t = \mathbb{N}_0, \quad (5.36)$$

where  $\mathbf{a} = [a_1, \dots, a_p]^T \in \mathbb{R}^p$  is a vector collecting the AR coefficients and

$$\mathbf{Y}_{t-1} = [Y_{t-1} \ \dots \ Y_{t-p}]^T \in \mathbb{R}^p \quad (5.37)$$

is a vector collecting the reconstructions of  $X_t$  to the  $p$  previous time steps. We choose  $Y_t = 0$  for  $t < 0$ . The scheme is illustrated in Fig. 5.2.

At each time step  $t$ , first the prediction error sample  $U_t$  is determined by (5.36). Then the prediction error sample is quantized using the central quantizer  $Q_{\Delta_c}$  which

is a fine-grained scalar uniform quantizer with step size  $\Delta_C$ . That is

$$U_t^{\Delta_C} = \mathcal{Q}_{\Delta_C}(U_t) = \text{Round}\left(\frac{U_t}{\Delta_C}\right)\Delta_C \in \Delta_C\mathbb{Z}. \quad (5.38)$$

Then, a one-to-many index assignment map  $\phi : \Delta_C\mathbb{Z} \rightarrow \Delta_S\mathbb{Z}^2$  is applied to  $U_t^{\Delta_C}$  to obtain the tuple

$$\mathbf{q}_t = \left(q_t^{(1)}, q_t^{(2)}\right) = \phi\left(U_t^{\Delta_C}\right) \in \Delta_S\mathbb{Z} \times \Delta_S\mathbb{Z}, \quad (5.39)$$

where  $\Delta_S/\Delta_C \in \mathbb{N}$  denotes the nesting ratio. Note, that each element  $q_t^{(i)}$ ,  $i = 1, 2$  of the tuple is a coarser quantization of  $U_t$  than  $U_t^{\Delta_C}$ . The two quantized values  $q_t^{(i)}$ ,  $i = 1, 2$  are individually entropy coded and transmitted over separate erasure channels [16].

By separate entropy decoding, we recover  $\bar{\mathbf{q}}_t$ . If both descriptions are received,  $\bar{\mathbf{q}}_t = \mathbf{q}_t$ , but if only the  $i$ 'th description is received,  $\bar{\mathbf{q}}_t = q_t^{(i)}$  and if none of the descriptions are received,  $\bar{\mathbf{q}}_t = \emptyset$ . We denote by  $\bar{U}_t^{\Delta_C}$  the recovery of  $U_t^{\Delta_C}$ . If both descriptions are received,  $U_t^{\Delta_C}$  can be recovered from  $\mathbf{q}_t$  using the inverse index-assignment map  $\phi^{-1}$ , i.e.,

$$\bar{U}_t^{\Delta_C} = U_t^{\Delta_C} = \phi^{-1}\left(q_t^{(1)}, q_t^{(2)}\right). \quad (5.40)$$

If only one of the descriptions is received, we use the received value  $\bar{U}_t^{\Delta_C} = q_t^{(i)}$  and if non of the descriptions are received, we use  $\bar{U}_t^{\Delta_C} = \mathbb{E}[U_t] = 0$  as the estimate of  $U_t$ . When the estimate of  $U_t$  is obtained, we reconstruct  $X_t$  by adding  $\mathbf{a}^T\mathbf{Y}_{t-1}$ . Hence, the central and side reconstructions are given by

$$Y_t^{(0)} = \phi^{-1}\left(q_t^{(1)}, q_t^{(2)}\right) + \mathbf{a}^T\mathbf{Y}_{t-1} = U_t^{\Delta_C} + \mathbf{a}^T\mathbf{Y}_{t-1} \quad (5.41a)$$

$$Y_t^{(i)} = q_t^{(i)} + \mathbf{a}^T\mathbf{Y}_{t-1}, \quad i = 1, 2. \quad (5.41b)$$

The used reconstruction  $Y_t$  depends on which descriptions are received. That is,

$$Y_t = \begin{cases} Y_t^{(0)} & \text{if both descriptions are received} \\ Y_t^{(i)} & \text{if only the } i\text{'th description is received} \\ \mathbf{a}^T\mathbf{Y}_{t-1} & \text{if no descriptions are received.} \end{cases} \quad (5.42)$$

### 5.2.1 Design of Index Assignment Map

With the approach described, what remains is to design the index assignment map  $\phi$ . This can be done by solving a bipartite graph matching problem [16], [28]. We will in the following describe this, based on the description in [16].

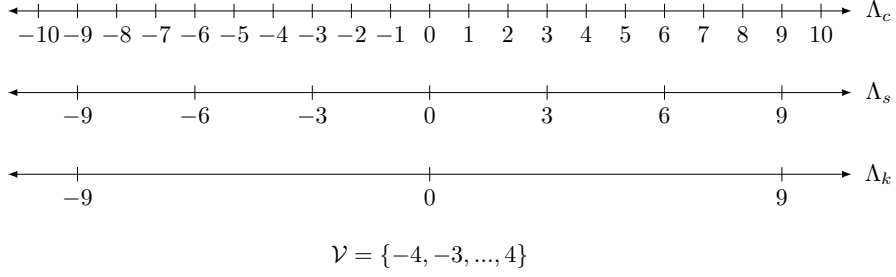


**Figure 5.3:** Illustration of the sets used in the definition of the index assignment map.

Let the nesting ratio  $r = \Delta_S/\Delta_C$  be a non-negative odd integer and define the three sets

$$\Lambda_c = \Delta_C \mathbb{Z}, \quad (5.43a)$$

$$\Lambda_s = \Delta_S \mathbb{Z}, \quad (5.43b)$$

$$\Lambda_k = r^2 \mathbb{Z}. \quad (5.43c)$$

Then it follows that  $\Lambda_k \subseteq \Lambda_s \subseteq \Lambda_c$ . As an example, consider the sets when  $\Delta_C = 1$  and  $\Delta_S = 3$  as depicted in Fig. 5.3. Now, define the set

$$\mathcal{V} = \{q \in \Lambda_c : |q| \leq |q - q'|, \forall q' \in \Lambda_k\}. \quad (5.44)$$

The set  $\mathcal{V}$  contains the  $r^2$  points in  $\Lambda_c$  which are closer to 0 compared to any other point in  $\Lambda_k$ .

Let  $(q^{(1)}, q^{(2)}) \in \Lambda_s^2$  be a tuple with  $q^{(i)} \in \Lambda_s$ ,  $i = 1, 2$ . Then, let the set  $\mathcal{S}(q^{(1)})$  be defined as

$$\mathcal{S}(q^{(1)}) = \{(q^{(1)}, q^{(2)}) \in \Lambda_s^2 : |q^{(1)} - q^{(2)}| \leq \varphi_r\}, \quad (5.45)$$

that is, the set of all distinct tuples in  $\Lambda_s^2$ , where the first element is  $q^{(1)}$  and the distance between  $q^{(1)}$  and  $q^{(2)}$  is less than  $\varphi_r$ . The value of  $\varphi_r$  depends on  $r$  and it is chosen such that  $|\mathcal{S}(q^{(1)})| \geq r$ . Using  $\mathcal{S}(q^{(1)})$ , construct the superset

$$\mathcal{S} = \{S(q^{(1)}) : q^{(1)} \in \mathcal{V} \cap \Lambda_s\}. \quad (5.46)$$

Since  $|\mathcal{V} \cap \Lambda_s| = r$ ,  $\mathcal{S}$  contains at least  $r^2$  tuples, where the first element belongs to  $\mathcal{V}$ .

The index assignment map  $\phi$  is defined by assigning the  $r^2$  elements in  $\mathcal{V}$  to tuples of the set  $\mathcal{S}$  such that the mapping is invertible and such that a cost function is minimized. As the elements of the tuple  $(q^{(1)}, q^{(1)})$  serves as estimates of  $U_t$  when only one of the descriptions is received and since we want to minimize the MSE, we define the cost function as

$$c(\mathbf{q}, \lambda) = \frac{1}{2} \sum_{i=1}^2 (\lambda - q^{(i)})^2. \quad (5.47)$$

The optimal index assignment map is the map that minimizes

$$\min_{\phi} \sum_{\lambda \in \mathcal{V}} c(\phi(\lambda), \lambda), \quad (5.48)$$

where the minimization is over all possible one-to-many maps  $\phi : \mathcal{V} \rightarrow \mathcal{S}$  where  $\phi^{-1}(\phi(\lambda)) = \lambda, \forall \lambda \in \mathcal{V}$ .

### Example 5.1 (Index Assignment Map)

As an example, let  $\Delta_C = 1$  and  $\Delta_S = 3$ , thus  $r = 3$ . Then the set  $\mathcal{V}$  contains the  $r^2 = 9$  points in the column with the title  $B$  in Table 5.1. The two last columns of Table 5.1 show the tuples assigned to each of the points in  $\mathcal{V}$ . The assignment is found using the method described in [28].

$U^{\Delta_C}$	$q^{(1)}$	$q^{(2)}$
-4	-3	-6
-3	-3	-3
-2	0	-3
-1	-3	0
0	0	0
1	0	3
2	3	0
3	3	3
4	3	6

**Table 5.1:** Index assignment map for  $\Delta_C = 1$  and  $\Delta_S = 3$ .

We conclude this section about the index assignment map design with a couple of useful properties of the index assignment map. First, the tuples are shift-invariant with respect to translations by  $\lambda_k \in \Lambda_k$ , i.e.,  $\phi(\lambda + \lambda_k) = \phi(\lambda) + \lambda_k, \forall \lambda_k \in \Lambda_k$  [16]. This means, that we only need to construct and store the table corresponding the  $r^2$  points closest to 0, e.g. Table 5.1 for  $r = 3$ . When  $U^{\Delta_C}$  is not in  $\mathcal{V}$ , we find the required shift  $s$ , e.g. by dividing  $U^{\Delta_C}$  by  $r^2$  and rounding to the nearest integer and then multiplying by  $r^2$ . Then we can find the index assignment by

$$\left( q^{(1)}, q^{(2)} \right) = \phi(U^{\Delta_C} - s) + s, \quad s \in \Lambda_k, \quad (5.49)$$

where the addition is understood as  $s$  is added to all elements of the index assignment tuple. As an example, let  $U^{\Delta_C} = 7$  and  $r = 3$ , then the shift is

$$s = \text{Round} \left( \frac{7}{9} \right) \cdot 9 = 9. \quad (5.50)$$

We then have that

$$\left( q^{(1)}, q^{(2)} \right) = \phi(7 - 9) + 9 = \phi(-2) + 9 = (0, -3) + 9 = (9, 6). \quad (5.51)$$

If we want  $\Delta_C$  to be different from 1, we can multiply the table in Table 5.1 with the desired  $\Delta_C$  [16]. In this way, the nesting ratio stays the same and the shift-invariance property is still maintained, but with  $\lambda_k \in \Delta_C \Lambda_k$ .

### 5.2.2 Rates and Distortion Performance

Since the quantization in the index assignment scheme is deterministic, it is only possible to analyze the rate and quantization noise in the asymptotic limit of  $\Delta_C, \Delta_S \rightarrow 0$  and  $\Delta_S/\Delta_C \rightarrow \infty$ . However, good estimates of the rate and the quantization error variance can be obtained for moderate to high rates [16].

First, let us consider the distortion induced by the central reconstructions,  $Y_t^{(0)}$ . The central reconstruction sample at time step  $t$  is given by (5.41a). For sufficiently high rates, the quantization error samples

$$Z_t = U_t - U_t^{\Delta_C}, \quad t \in \mathbb{N}_0 \quad (5.52)$$

can be modeled as a white process with uniformly distributed samples [10, p. 158], i.e.  $Z_t \sim \mathcal{U}\left(\frac{-\Delta_C}{2}, \frac{\Delta_C}{2}\right)$ . Hence, the central reconstruction sample can be modeled as

$$\begin{aligned} Y_t^{(0)} &= U_t^{\Delta_C} + \mathbf{a}^T \mathbf{Y}_{t-1} \\ &= U_t - Z_t + \mathbf{a}^T \mathbf{Y}_{t-1} \\ &= X_t - \mathbf{a}^T \mathbf{Y}_{t-1} + \mathbf{a}^T \mathbf{Y}_{t-1} - Z_t \\ &= X_t - Z_t \end{aligned} \quad (5.53)$$

and the central distortion is

$$D_0 = \mathbb{E} \left[ \left( X_t - Y_t^{(0)} \right)^2 \right] = \mathbb{E} [Z_t^2] \approx \frac{\Delta_C^2}{12}. \quad (5.54)$$

Next, we consider the side distortion. Recall, that the quantization of  $U_t$  is  $q_t^{(i)}$  for the  $i$ 'th side description. Therefore, the quantization error for the  $i$ 'th side description is

$$Z_t^{(i)} = U_t - q_t^{(i)}, \quad t \in \mathbb{N}_0, \quad i = 1, 2. \quad (5.55)$$

By [16, Eq. (39)], the variance of  $Z_t^{(i)}$  is approximately

$$\text{var} \left( Z_t^{(i)} \right) \approx \frac{\Delta_C^2}{12} + \frac{\Delta_C^2}{48} \left( \frac{\Delta_S}{\Delta_C} \right)^4 = \frac{\Delta_C^2}{12} + \frac{\Delta_S^4}{48\Delta_C^2}. \quad (5.56)$$

Like for the central reconstruction, we can write the side reconstruction as

$$\begin{aligned} Y_t^{(i)} &= q_t^{(i)} + \mathbf{a}^T \mathbf{Y}_{t-1} \\ &= U_t - Z_t^{(i)} + \mathbf{a}^T \mathbf{Y}_{t-1} \\ &= X_t - \mathbf{a}^T \mathbf{Y}_{t-1} + \mathbf{a}^T \mathbf{Y}_{t-1} - Z_t^{(i)} \\ &= X_t - Z_t^{(i)}, \end{aligned} \quad (5.57)$$

and we obtain the following side distortion approximation

$$D_S = \mathbb{E} \left[ \left( X_t - Y_t^{(i)} \right)^2 \right] = \mathbb{E} \left[ \left( Z_t^{(i)} \right)^2 \right] \approx \frac{\Delta_C^2}{12} + \frac{\Delta_S^4}{48\Delta_C^2}. \quad (5.58)$$

Finally, by [16, Eq. (40)], the sum-rate of the index assignment scheme can be approximated by

$$R \approx 2h(U_t) - 2\log(\Delta_S) = \log(2\pi e\sigma_U^2) - 2\log(\Delta_S), \quad (5.59)$$

where  $h(U_t)$  is the differential entropy of  $U_t$  and the last equality follows from the differential entropy of a Gaussian random variable [16]. If we assume that  $Y_t$  in (5.42) is always the central reconstruction  $Y_t^{(i)}$ , then we can determine the variance of  $U_t$  as

$$\begin{aligned} \text{var}(U_t) &= \text{var} \left( X_t - \mathbf{a}^T \mathbf{Y}_{t-1} \right) \\ &= \text{var} \left( \mathbf{a}^T \mathbf{X}_{t-1} + W_t - \mathbf{a}^T (\mathbf{X}_{t-1} - \mathbf{Z}_{t-1}) \right) \\ &= \text{var} \left( W_t - \mathbf{a}^T \mathbf{Z}_{t-1} \right) \\ &\stackrel{(a)}{=} \sigma_Z^2 \|\mathbf{a}\|_2^2 + \sigma_W^2 \\ &= \frac{\Delta_C^2}{12} \|\mathbf{a}\|_2^2 + \sigma_W^2, \end{aligned} \quad (5.60)$$

where  $\mathbf{X}_{t-1} = [X_{t-1}, \dots, X_{t-p}]^T$ ,  $\mathbf{Z}_{t-1} = [Z_{t-1}, \dots, Z_{t-p}]^T$ , and where (a) follows from independence between  $W_t$  and  $\mathbf{Z}_{t-1}$ .

### 5.3 Theoretical Rate-Distortion Performance

In this section, we will compare the theoretical rate-distortion performance for the schemes presented in this chapter. To this end we plot side distortion against central distortion for different choices of fixed sum-rates  $R = 8, 10, 12$  bits. The curves will be referred to as distortion trade-off curves. We compare the distortion trade-off curves for both an AR(1) and AR(2) source. The AR(2) source has the parameters

$$a_1 = 1.421, \quad a_2 = -0.579, \quad \sigma_W^2 = 0.126. \quad (5.61)$$

and the AR(1) source parameters are obtained by the Yule-Walker equations using the autocorrelation function (ACF) of the AR(2) source. This is described in more details in Chapter 6. The distortion trade-off curves for the AR(1) source is the distortion trade-off curve for assuming an AR(1) source, when the source is actually AR(2). Therefore, the difference between the distortion trade-off curves for AR(1) and AR(2) sources is the theoretical loss of assuming an AR(1) source when it is actually AR(2).

If the schemes e.g. were to be used for transmission of audio signals, we would have to transmit the source coefficients  $a_1, a_2$ . However, we will assume that the source parameters are known to both the encoder and decoder, thus no rate is spent on communicating the source parameters.

### 5.3.1 Theoretical Lower Bound

We compare the performance of the schemes to the theoretical lower bound on the performance of ZDMD coding schemes assuming AR(1) sources given by (4.50). For a fixed sum-rate  $R$ , we let

$$R = \log\left(\frac{a_1^2 \pi_S + \sigma_W^2}{\pi_S}\right) - \frac{1}{2} \log(1 - \rho^2) \quad (5.62)$$

and determine the corresponding side distortion  $\pi_S$  for a grid of correlations  $\rho$ , with  $\rho \in (-1; 0)$ . We then calculate  $\pi_0$  using (4.52).

Within the time frame of the project, it has not been possible to develop the lower bound of ZDMD coding schemes assuming AR(2) sources. Therefore, we cannot lower bound the performance of the AR(2) schemes.

### 5.3.2 Schemes Using Staggered Quantizers

First we consider the theoretical performance of schemes using staggered quantization. For the schemes using staggered quantizers, the curves are obtained by varying the first stage rate  $R_S$  and the refinement rate  $R_0$  such that (5.9) is satisfied. Then  $\Delta_S$  is determined by isolating it in (5.14) using the relevant expression of  $\lambda$  depending on the predictor. We then compute the side and central distortion by

$$D_S = \frac{\Delta_S^2}{12} \quad (5.63)$$

$$D_0 = 2^{-2R_0} \frac{D_S}{4}. \quad (5.64)$$

As mentioned, for the scheme using the optimal predictors, at least 1 bit must be spent on the sign of the difference of the previous predictions. Therefore, we subtract 1 from the sum-rate when computing the distortion trade-off curve when using the optimal predictors.

In Fig. 5.4, the distortion trade-off curves are shown for the staggered quantization schemes. From the figure, it is seen that the scheme using the sub-optimal predictors obtains the best performance for a given sum-rate. Hence, no gain in performance is achieved by using the optimal predictors. The reason is the extra 1 bit used for the sign. This is seen by comparing Fig. 5.4 with Fig. 5.5, which shows the performance assuming that we do not need to spend 1 bit on the sign. Due to the superiority of the scheme using sub-optimal predictors in the staggered scheme, we will not consider the use of the optimal predictors further.

### 5.3.3 Index Assignment Schemes

For the scheme using index assignment, we vary the side and central distortion for each sum-rate by varying the nesting ratio  $r = \Delta_S/\Delta_C$ . For each sum-rate we

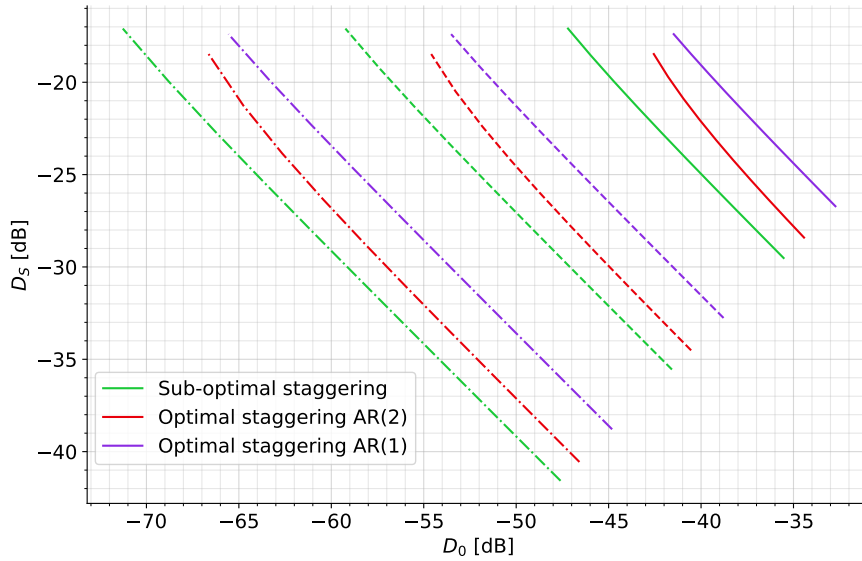


**Figure 5.4:** Central distortion  $D_0$  versus side distortion  $D_S$  for the ZDMD coding scheme using staggered quantization with sub-optimal predictor (green), optimal AR(1) predictor (purple), and optimal AR(2) predictor (red). The different line styles represent different sum-rates. Specifically solid is  $R = 8$ , dashed is  $R = 10$  and dashdotted (-.-) is  $R = 12$ . It is assumed that one bit is used for communicating the sign of the difference between side reconstructions.

compute  $\Delta_C$  by (5.59), using that  $\Delta_S = r\Delta_C$ . Then we compute the central and side distortion by

$$D_0 = \frac{\Delta_C^2}{12} \quad (5.65)$$

$$D_S = \frac{\Delta_C^2}{12} + \frac{\Delta_S^4}{48\Delta_C^2}. \quad (5.66)$$

In Fig. 5.6, the distortion trade-off curves are shown for the index assignment scheme assuming AR(1) and AR(2) as well as the staggered scheme using the sub-optimal predictor. It is seen that, the index assignment scheme assuming AR(1) source has a small gain in performance compared to the scheme using staggered quantization. Furthermore, it is seen that when assuming an AR(2) source, the performance of the index assignment scheme increases by roughly 3.5 dB. It is also worth noting, that for this source, the index assignment scheme achieve performance below the lower bound for AR(1) sources when an AR(2) source is assumed. Therefore, when we consider an AR(2) source, we can obtain better performance using the index assignment scheme for AR(2) sources than for any ZDMD coding scheme assuming AR(1) source.

In the next chapter, we will by simulations further investigate the performance of the ZDMD schemes presented in this chapter.

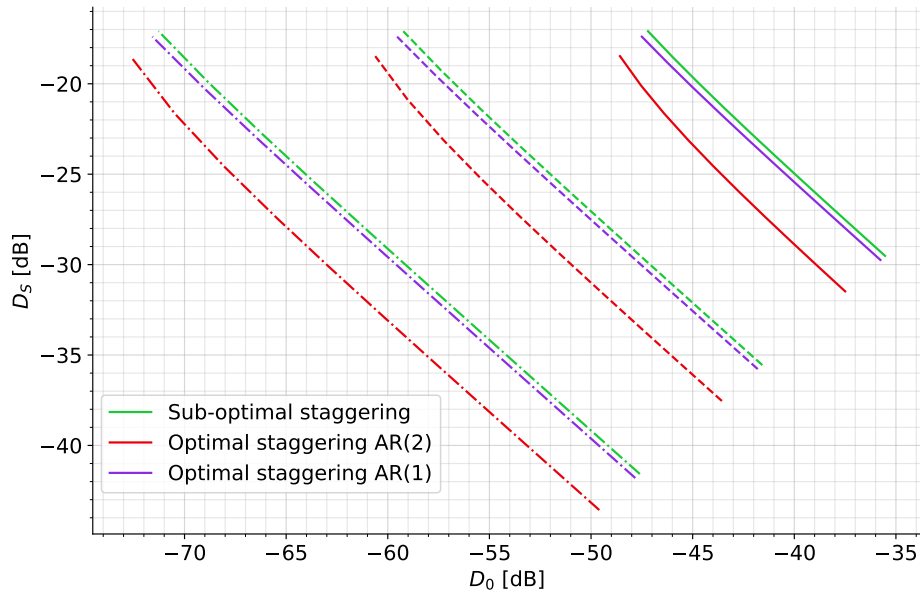


**Figure 5.5:** Side distortion  $D_S$  versus central distortion  $D_0$  for the ZDMD coding scheme using staggered quantization with sub-optimal predictor (green), optimal AR(1) predictor (purple), and optimal AR(2) predictor (red). The different line styles represent different sum-rates. Specifically solid is  $R = 8$ , dashed is  $R = 10$  and dashdotted (-.-) is  $R = 12$ .

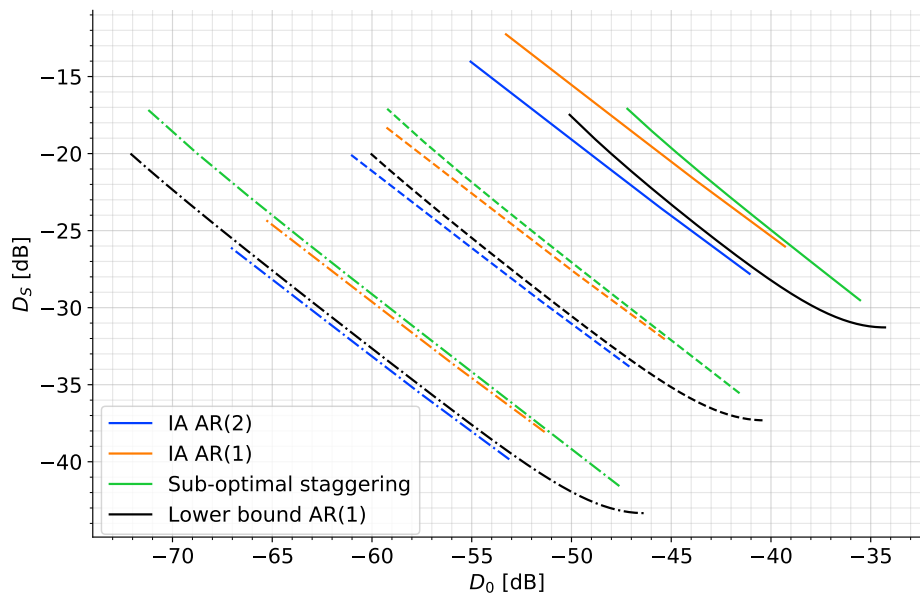


**Figure 5.6:** Side distortion  $D_S$  versus central distortion  $D_0$  for the ZDMD coding scheme using staggered quantization with sub-optimal predictor (green) as well as using index assignment assuming AR(1) (orange), and AR(2) (blue). The different line styles represent different sum-rates. Specifically solid is  $R = 8$ , dashed is  $R = 10$  and dashdotted (-.-) is  $R = 12$ . The black curve represents the theoretic lower bound assuming AR(1).

## 6. Simulation Study

In this chapter, we will present simulated results regarding the performance of the schemes presented in Chapter 5. The performance is evaluated realizations of an AR(2) source. We will use the ZDMD coding schemes assuming both the source is AR(1) and AR(2). Recall that we assume feedback from the decoder, in order to synchronize the encoding and decoding.

We will simulate the performance of the developed schemes in terms of the average MSE of the central and side reconstructions to different rates. The performance will be compared to the theoretical lower bound on the MSE distortion for ZDMD coding assuming an AR(1) source.

Before we present the simulation results, we cover the setup for the simulations. Afterwards, we present results with zero packet loss probability followed by results with non-zero packet loss probability. The simulation results are discussed in Chapter 7.

### 6.1 Simulation Setup

In all simulations, we consider scalar stationary AR(2) sources of the form

$$X_t = \sum_{i=1}^2 a_i X_{t-i} + W_t, \quad t = 2, 3, \dots, \quad (6.1)$$

where  $W_t \sim \mathcal{N}(0, \sigma_W^2)$ . The parameters of the source is chosen such that the stationary variance of the source  $\sigma_X^2 = 1$  and such that the parameters resembles linear predictive coding (LPC) parameters of an AR(2) modeling of an audio signal. Therefore, the source parameters used in all simulations are

$$a_1 = 1.421, \quad a_2 = -0.579, \quad \sigma_W^2 = 0.126. \quad (6.2)$$

When the source is assumed to be AR(2), we use the parameters in (6.2) in schemes. When an AR(1) source is assumed, we calculate the AR(1) source parameters using the Yule-Walker equations for an AR(1) source. First, the first three samples of the autocorrelation function (ACF)  $R_X(k)$  can be computed using the AR(2) source

parameters by solving the set of equations

$$R_X(0) = \sum_{i=1}^2 a_i R_X(i) + \sigma_W^2 \quad (6.3)$$

$$R_X(k) = \sum_{i=1}^2 a_i R_X(k-i), \quad k = 1, 2. \quad (6.4)$$

Using the parameters in (6.2), the first three samples of the ACF is

$$R_X(0) = 1, \quad R_X(1) = 0.9, \quad R_X(2) = 0.7, \quad (6.5)$$

and the source parameters when assuming AR(1) is

$$a_1 = R_X(1)/R_X(0) = 0.9, \quad \sigma_W^2 = 0.19. \quad (6.6)$$

For all simulations we use  $N = 100000$  time samples and average the performance over  $M = 4$  Monte-Carlo simulations. That is, we generate 4 realizations of the AR(2) source, apply the ZDMD coding schemes each of the realizations, and average the performance for each schemes over the 4 realizations.

In all simulations we fix the sum-rate  $R$  and determine the respective step sizes of the quantizers in the schemes. For each sum-rate we then calculate the operational distortions for each scheme. We simulate the sum-rates  $R \in \{5, 5.5, \dots, 12\}$ . Due to the fact, that the rates in (5.14) and (5.59) are only approximations, the operational rates will be larger than  $R$ , especially for small rates. When we compare the performance for different rates, we will use the operational rates and we will compute the theoretical lower bound to rates close to the operational rates of the schemes.

We will describe the setup in detail for both types of schemes in the following.

### 6.1.1 Index Assignment Scheme

When simulating the performance of the index assignment scheme, we fix the sum-rate  $R$  and the nesting ratio  $r$  and determine the corresponding step size of the central quantizer by isolating  $\Delta_C$  in (5.59), i.e.,

$$\Delta_C \approx \frac{\sqrt{12 \cdot 2\pi e \sigma_W^2}}{\sqrt{12 \cdot 2^R \cdot r^2 - 2\pi e \|\mathbf{a}\|_2^2}}. \quad (6.7)$$

The operational rates are obtained from estimates of the entropy of the elements of the index assignment tuples  $(q_t^{(1)}, q_t^{(2)})$ . The estimates are determined by estimates of the distributions of  $q_t^{(i)}$ ,  $i = 1, 2$ , which are obtained from histograms of  $\{q_t^{(i)}\}_{t=0}^{N-1}$ ,  $i = 1, 2$ . The operational sum-rate is the sum of the estimated entropies of  $q_t^{(i)}$ ,  $i = 1, 2$ .

$U^{\Delta_C}$	$q^{(1)}$	$q^{(2)}$
1	0	3
2	3	0
3	3	3
4	3	6
-4	-3	-6
-3	-3	-3
-2	0	-3
-1	-3	0
0	0	0

**Table 6.1:** Index assignment map for  $\Delta_C = 1$  and  $\Delta_S = 3$ .

$U^{\Delta_C}$	$q^{(1)}$	$q^{(2)}$	$U^{\Delta_C}$	$q^{(1)}$	$q^{(2)}$
0	0	0	-12	-15	-10
1	-5	5	-11	-5	-15
2	5	0	-10	-15	-5
3	0	5	-9	-10	-10
4	5	5	-8	-10	-5
5	0	10	-7	-5	-10
6	10	0	-6	-5	-5
7	10	5	-5	0	-10
8	5	10	-4	-10	0
9	10	10	-3	-5	0
10	5	15	-2	0	-5
11	15	5	-1	5	-5
12	15	10			

**Table 6.2:** Index assignment map for  $\Delta_C = 1$  and  $\Delta_S = 5$ .

As mentioned, we will simulate the performance of the schemes for different packet loss probabilities. When the packet loss probability is zero, we calculate the central and side distortions as

$$D_i = \frac{1}{N} \sum_{t=0}^{N-1} \left( X_t - Y_t^{(i)} \right)^2 \quad i = 0, 1, 2 \quad (6.8)$$

$$D_S = \frac{D_1 + D_2}{2}, \quad (6.9)$$

where  $Y_t^{(i)}$ ,  $i = 0, 1, 2$  are the reconstructions of the source sample  $X_t$  given by (5.41a) and (5.41b).

When the packet loss probability is non-zero, we determine the average MSE distortion of the used reconstruction samples, i.e.,

$$D = \frac{1}{N} \sum_{t=0}^{N-1} (X_t - Y_t)^2, \quad (6.10)$$

where  $Y_t$  is the used reconstruction given the received packets and it is given by (5.42).

We simulate the performance using nesting ratios of  $r = 3, 5, 7$ . The tables for the index assignment mappings for each nesting ratio is determined using the procedure described in [28], using the cost function in (5.47). The resulting index assignment maps are shown in Tables 6.1 to 6.3.

$U^{\Delta_C}$	$q^{(1)}$	$q^{(2)}$	$U^{\Delta_C}$	$q^{(1)}$	$q^{(2)}$	$U^{\Delta_C}$	$q^{(1)}$	$q^{(2)}$
0	-7	7	17	21	14	-15	-7	-21
1	7	-7	18	14	21	-14	-21	-7
2	14	-7	19	7	28	-13	-14	-14
3	7	0	20	14	28	-12	-21	0
4	-7	14	21	28	14	-11	-14	-7
5	0	7	22	21	21	-10	-7	-14
6	0	14	23	14	35	-9	0	-21
7	14	0	24	28	21	-8	0	-14
8	7	7	-24	-14	-35	-7	-14	0
9	21	0	-23	-28	-21	-6	-7	-7
10	14	7	-22	-28	-14	-5	7	-14
11	7	14	-21	-21	-21	-4	-7	0
12	0	21	-20	-14	-28	-3	-14	7
13	7	21	-19	-7	-28	-2	0	-7
14	21	7	-18	-21	-14	-1	0	0
15	14	14	-17	-14	-21			
16	28	7	-16	-28	-7			

**Table 6.3:** Index assignment map for  $\Delta_C = 1$  and  $\Delta_S = 7$ .

### 6.1.2 Staggered Quantization Schemes

As we saw in Section 5.3, the best performance using the staggered quantization scheme is obtained using the sub-optimal predictors. Therefore, we will only simulate the performance using the sub-optimal predictor assuming an AR(1) source. For each fixed sum-rate  $R$ , we vary  $R_S, R_0$  such that  $R = 2R_S + R_0$ . Specifically, we for a given sum-rate  $R$ , we let  $R_S \in [1.5; R/2]$  and  $R_0 \in [0; R - 3]$ . For each rate pair  $R_S, R_0$ , we determine the corresponding quantizer step sizes by isolating  $\Delta_S$  in (5.14), using the prediction error variance for in (5.22), and by using (5.17) for  $\Delta_0$ .

The operational rates are obtained from estimates of the entropy of the quantizer outputs  $U_t^{\Delta_S, (i)}$ ,  $i = 1, 2$  and  $E_{C_t}^{\Delta_0}$ , which are based on histograms of  $\{U_t^{\Delta_S, (i)}\}_{t=0}^{N-1}$ ,  $i = 1, 2$  and  $\{E_{C_t}^{\Delta_0}\}_{t=0}^{N-1}$ . Let  $R_i^{op}$ ,  $i = 1, 2$ , and  $R_0^{op}$  be the estimated entropy of  $U_t^{\Delta_S, (i)}$ ,  $i = 1, 2$  and  $E_{C_t}^{\Delta_0}$ , respectively. Then the operational sum-rate is the sum of the estimated entropies,  $R^{op} = \sum_{i=0}^2 R_i^{op}$ .

For the distortions, we calculate the central and side distortions as

$$D_i = \frac{1}{N} \sum_{t=0}^{N-1} \left( X_t - Y_t^{(i)} \right)^2 \quad i = 0, 1, 2 \quad (6.11)$$

$$D_S = \frac{D_1 + D_2}{2}, \quad (6.12)$$

when the packet loss probability is zero, where  $Y_t^{(i)}$ ,  $i = 0, 1, 2$  are the reconstructions of the source sample  $X_t$  given by (5.8) and (5.20).

When the packet loss probability is non-zero, we determine the average MSE distortion of the used reconstruction samples, i.e.,

$$D = \frac{1}{N} \sum_{t=0}^{N-1} (X_t - Y_t)^2, \quad (6.13)$$

where  $Y_t$  is the used reconstruction given the received packets and it is given by

$$Y_t = \begin{cases} Y_t^{(0)} & \text{if both descriptions are received} \\ Y_t^{(i)} & \text{if only the } i\text{'th description is received} \\ \frac{1}{2}(Y_{t-1}^{(1)} + Y_{t-1}^{(2)}) & \text{if no descriptions are received.} \end{cases} \quad (6.14)$$

### 6.1.3 Lower bound

We compare the performance of the schemes to the theoretical lower bound on the performance of ZDMD coding schemes assuming AR(1) sources given by (4.50). As described in Section 5.3.1, for each fixed sum-rate  $R$ , we let

$$R = \log\left(\frac{a_1^2 \pi_S + \sigma_W^2}{\pi_S}\right) - \frac{1}{2} \log(1 - \rho^2) \quad (6.15)$$

and determine the corresponding side distortion  $\pi_S$  for a grid of correlations  $\rho$ , with  $\rho \in (-1; 0)$ . We then calculate  $\pi_0$  using (4.52). For each rate, we can then plot the side distortion against the central distortion.

We will also consider the smallest possible central distortion for a given sum-rate. To this end, for each fixed sum-rate we find the minimum of the obtained central distortions  $\pi_0$  by the determination described above.

When we simulate packet losses, it is possible that both packets are lost. Specifically, if the probability of losing a packet over either channel is  $p_l$ , we have the following four possible cases

$$\begin{cases} \text{Both descriptions received} & \text{with probability } (1 - p_l)^2 \\ \text{Only packet } i \text{ received, } i = 1, 2 & \text{with probability } p_l - p_l^2 \\ \text{Both packets lost} & \text{with probability } p_l^2, \end{cases} \quad (6.16)$$

where it is assumed that packet losses on each channel is independent of packet losses on the other.

When both packets are lost, we use the MMSE estimate of  $X_t$  given the previous side reconstructions, i.e.

$$Y_t = \mathbb{E}\left[X_t | Y_{t-1}^{(1)}, Y_{t-1}^{(2)}\right] = \Theta_l \mathbf{Y}_{t-1}, \quad (6.17)$$

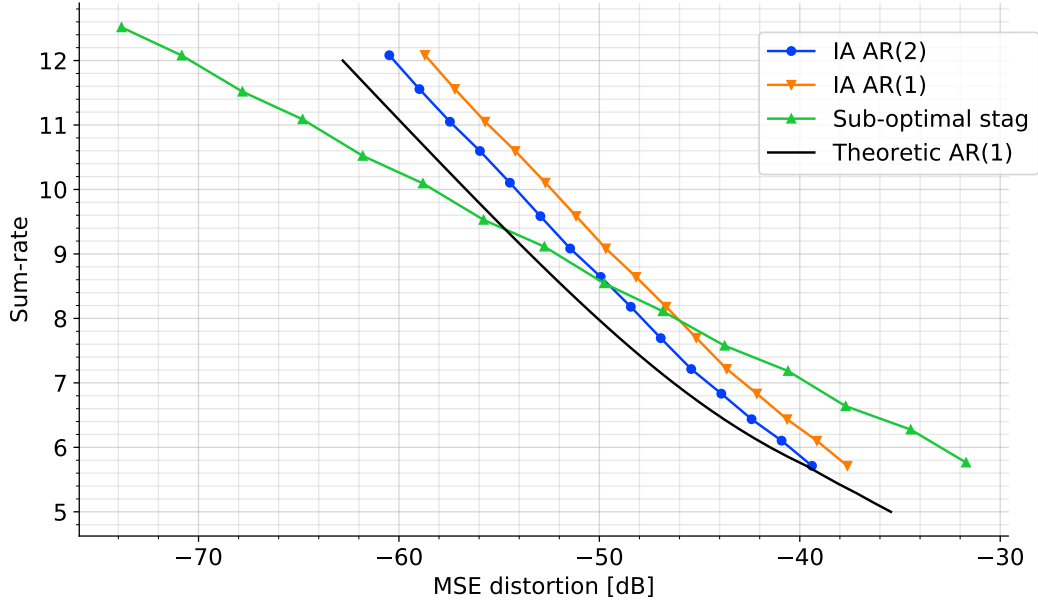


**Figure 6.1:** Sum-rate versus minimum central distortion.

where  $\mathbf{Y}_{t-1} = [Y_{t-1}^{(1)}, Y_{t-1}^{(2)}]^T$  and

$$\Theta_l = \Sigma_{XY} \Sigma_Y^{-1} \quad (6.18)$$

with  $\Sigma_{XY} = \mathbb{E}[X_t \mathbf{Y}_{t-1}^T]$  and  $\Sigma_Y = \mathbb{E}[\mathbf{Y}_t \mathbf{Y}_t^T]$ . The distortion when no packets are received be expressed as

$$\pi_l = \mathbb{E}[(X_t - \Theta_l \mathbf{Y}_{t-1})^2] = \sigma_X^2 - \Sigma_{XY} \Sigma_Y^{-1} \Sigma_{XY}^T. \quad (6.19)$$

The distortion associated to a given packet loss probability is then the weighted sum of the four cases, i.e.,

$$D(p_l) = (1 - p_l)^2 \pi_0 + 2(p_l - p_l^2) \pi_S + p_l^2 \pi_l. \quad (6.20)$$

## 6.2 Rate-Distortion Performance with no Packet Loss

First we consider the rate-distortion performance of the schemes when packet loss probability is zero. In Fig. 6.1 the sum-rate is plotted against the smallest central distortion obtained for the specific sum-rate. Notice, that the scheme using staggering achieves distortions below the theoretical lower bound. This is due to the refinement quantization in scheme. Specifically, for all sum-rates  $R$ , the maximum possible rate is used in the refinement quantizer. This means that staggered quantization

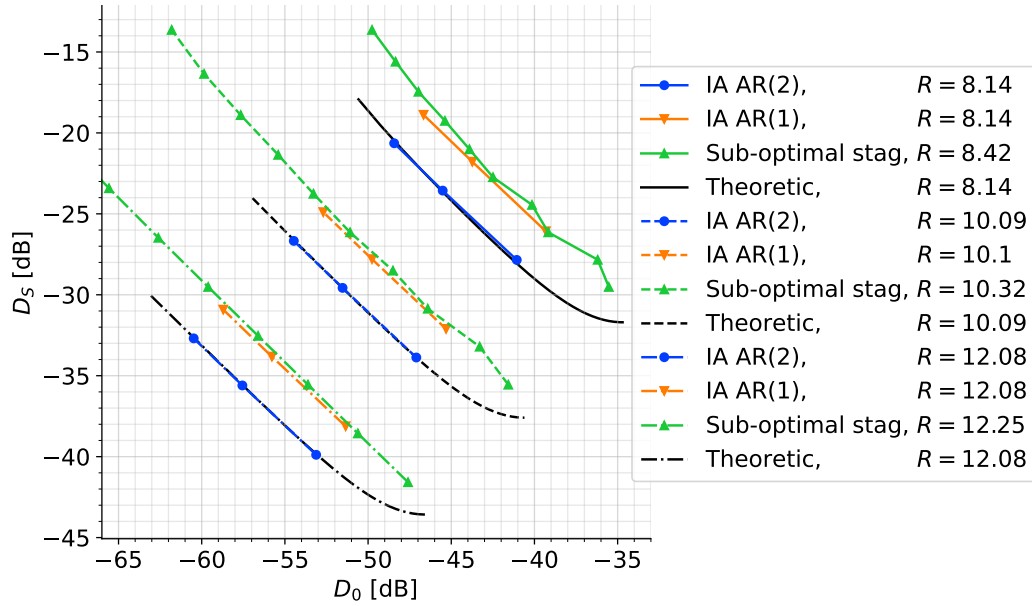


**Figure 6.2:** Side distortion  $D_S$  versus central distortion  $D_0$  for the ZDMD coding scheme using staggered quantization with sub-optimal predictor (green) as well as using index assignment assuming AR(1) (orange), and AR(2) (blue). The black curve represents the theoretical lower bound assuming AR(1). The different line styles represent different sum-rates.

scheme approaches a single description quantization, since most of the rate is used on quantizing  $E_{C,t}$ .

For the index assignment schemes, the nesting ratio that minimizes the central distortion for a given sum-rate is  $r = 7$  of the used nesting ratios. It is seen, that we obtain a gain in performance of when using the AR(2) predictor compared to the AR(1) predictor. In particular, the average gain is 3.5 dB.

The plots in Fig. 6.1 only tells half of the story about the performance of the schemes, since the side distortions does not figure from these plots. Therefore, consider Fig. 6.2 where the side distortion is plotted against the central distortion for three different rates. From, Fig. 6.2 we see, that for all the simulated cases, the index assignment scheme using assuming AR(1) sources obtains a slightly better performance compared to the scheme using staggering. Both schemes assuming AR(1) sources has about 3.5 to 4 dB larger central distortion for a given side distortion compared to the theoretical lower bound. The index assignment scheme assuming AR(2) achieves a performance near the lower bound for a ZDMD scheme assuming AR(1) sources. This is in line with what was seen in Section 5.3.

	IA $r = 3$	IA $r = 5$	IA $r = 7$	Staggering
$\rho$	-0.73	-0.91	-0.96	-0.5

**Table 6.4:** Quantization noise correlations for different nesting ratio  $r$  in the index assignment scheme (IA) and for the scheme using staggering.

	IA AR(1)	Sub-optimal stag.	IA AR(2)
$D - D_{\text{theo}}$ [dB]	0.38	0.68	-1.33

**Table 6.5:** Average deviation from the theoretical lower bound for ZDMD coding of AR(1) sources for the different schemes.

### 6.2.1 Correlation of Quantization Noise

As presented in Chapter 2, it is desirable to have quantization noises which are highly negatively correlated. The correlations between the quantization noises over the two channels are shown in Table 6.4. It is seen that we get a higher correlation between the quantization noises when using the index assignment scheme compared to the scheme using staggering. Actually, the correlation for scheme using staggering is the minimum quantization noise correlation for a scheme using staggering [15]. Furthermore, it is seen that the correlation goes towards  $-1$  when increasing the nesting ratio for the index assignment schemes.

## 6.3 Performance Versus Packet Loss Probability

In this section, we investigate the performance of the ZDMD schemes in terms of MSE distortion against packet loss probability. The MSE distortion is the average distortion of used reconstruction which depends on how many packets are received. In Figs. 6.3 and 6.4, the average MSE distortion is plotted against packet loss probability for the different schemes with a operational sum-rate of about 10 bits.

It is seen, that the scheme using staggering and the index assignment scheme assuming AR(1) has similar performance, and that the average distortion is close to the theoretic achievable distortion. In Table 6.5, the average deviation from the theoretical lower bound for ZDMD coding of AR(1) sources for the different schemes is shown, where the average is over packet loss probabilities  $p_l \geq 1\%$ .

Furthermore, the index assignment scheme assuming AR(2) achieves a better average MSE distortion than the AR(1) schemes. On average, the average MSE of the AR(2) scheme is 1.7 and 2.0 bits smaller than the index assignment scheme assuming AR(1) and the scheme using staggering, respectively.

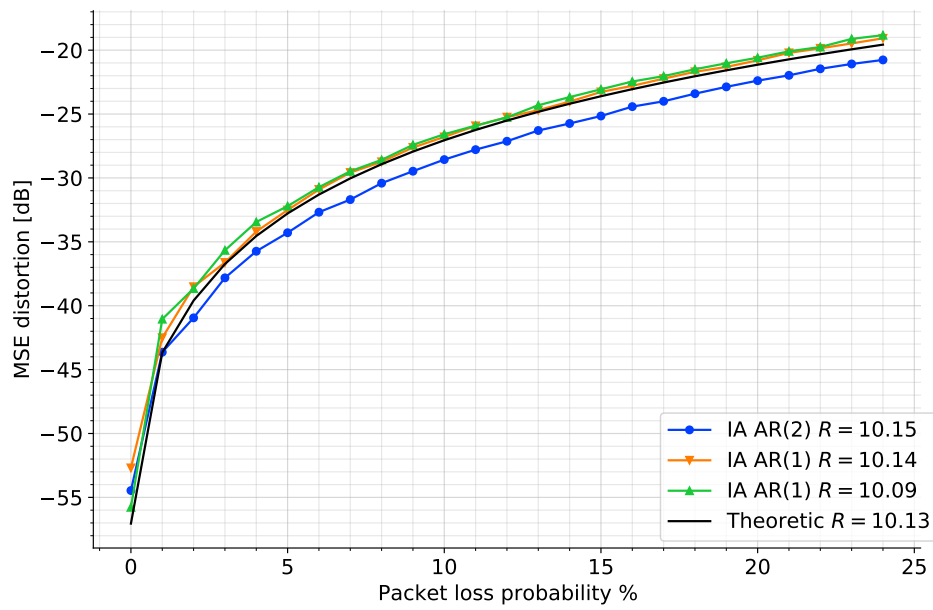


**Figure 6.3:** Average MSE performance for the different ZDMD schemes as a function of packet loss probability.

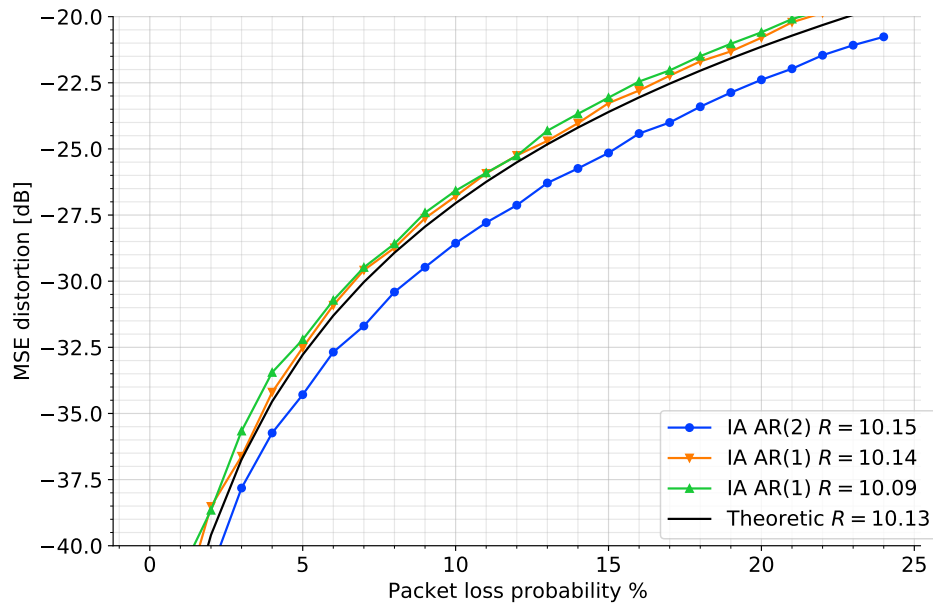


**Figure 6.4:** Average MSE performance for the different ZDMD schemes as a function of packet loss probability.



## 7. Discussion

In this chapter we discuss the design of the operational ZDMD schemes as well as the simulation results presented in Chapter 6.

### 7.1 Operational ZDMD Coder Design

In Chapter 5, we presented a quantization scheme based on staggered quantizers, which was described in [8], [9] for AR(1) sources. The design of the staggered quantization scheme resembles the structure of the test-channel for ZDMD coding, which can be seen by comparing Fig. 5.1 to Figs. 4.2 and 4.3. As the test-channel adds Gaussian noise to two prediction error sequences, the similarity lies in the fact the staggered quantization scheme uses staggered quantizers on two prediction error samples.

We have extended the scheme to use the optimal predictor for an AR(2) source, such that the scheme could exploit the source structure. However, as pointed out in [8], [9], when using the optimal predictor, bits must be used on communicating the sign of the difference between the previous reconstruction samples, which increases the sum-rate. This is necessary, since the difference cannot be computed at the decoder, if one of the packets was lost in the previous time step. It turns out, as can be seen in Section 5.3, that the gain of using the optimal predictor is no greater than the loss of having to transmit the sign bit. Hence, the best rate-distortion performance is obtained by using the sub-optimal predictor when using the staggered quantization scheme.

To overcome the difficulty in using the optimal predictor in a DPCM quantizer for ZDMD coding, we have developed a novel ZDMD quantization scheme using index assignment. With the index assignment scheme, we are able to use the optimal predictor of any model order without having to spend bits on information not regarding the prediction error sequence directly. In contrast to the staggered quantization scheme, the index assignment scheme does not resemble the test-channel by quantizing two prediction error samples. Rather, a single prediction error sample is quantized, and this quantized value is mapped to two coarser quantizations of the prediction error sample.

Even though, the index assignment scheme does not resemble the test-channel,

we have seen from the theoretical rate-distortion performance in Section 5.3 and in the simulations that the index assignment scheme assuming AR(1) achieves a better performance compared to the staggered quantization scheme using the sub-optimal predictor. The slight gain in rate-distortion performance can be attributed to the use of the optimal predictor. This can be seen if we compare the plots in Fig. 5.5 and Fig. 5.6. In Fig. 5.5, the distortion performance is shown for staggered quantization assuming that the sign bit is not necessary. For both the index assignment scheme and the staggered quantization scheme using the optimal AR(1), it is seen that a similar gain is achieved compared to staggered scheme using the sub-optimal predictor.

Since we assume that the source parameters are known to the decoder, no rate has been used on transmitting information about the source parameters. However, if schemes should be used for encoding of speech signals, we would have to estimate the parameters from small segments of the source samples assuming an AR model order  $p$ . This means that the source parameters are not known at the decoder and bits have to be used on communicating the parameters to the decoder.

To reduce the overhead when transmitting the source parameters, we can transmit packets including more samples. This will naturally introduce a delay. Thus, there would be a trade-off between the rate used for the source parameters per packet and the delay.

### 7.1.1 Trade-off between Central and Side Distortion

A key feature for MD coding, is the trade-off between the central and side distortion. For the ZDMD test-channel, this trade-off is controlled by the quantization noise correlation  $\rho$ . This does also apply to the index assignment scheme. In particular, choosing a higher nesting ratio implies that the quantization noise correlation gets closer to  $-1$ . As seen in Section 5.3, a higher nesting ratio is associated with a lower central distortion but a higher side distortion.

In contrast, for the staggered quantization scheme, the distortion trade-off is controlled by the amount of the sum-rate used in the central quantizer. Allocating more or less of the sum-rate to the central quantizer does not change the correlation between the side description quantization noises. In this regard, the staggered quantization scheme differs from the test-channel. Furthermore, the bits used for the refinement is only used if both packets are received. Thus, if one of the packets is lost, the bits spend on refinement in the received packet cannot be used.

### 7.1.2 Feedback Assumption

In both the scheme using staggering and the scheme using index assignment we assume that the encoder receives information about which packets are received at the decoder. This is assumed, such that the reconstructions at the encoder are identical to the reconstructions at the decoder, or in other words, the encoder and decoder reconstruct the source samples in synchrony. The feedback is essential when packet

losses occur, since the decoder cannot produce the same reconstructions as the encoder if packets are lost. However, the reconstruction of the previous time step is required to generate the reconstruction to the current time step. By letting the encoder know which packets are lost, the encoder can produce prediction error samples using the reconstructions that the decoder produce in the event of a packet loss.

The synchronicity is obtained through a noiseless feedback channel with 1 sample delay. Such a feedback channel may not be feasible in a practical setup of wireless transmission of speech or audio. Therefore, in order to make these schemes practical applicable, it is desirable investigate whether the synchronicity between the encoder and decoder can be removed.

Naively removing the feedback channel without modification of the schemes may result in a huge degradation in performance under packet losses, since at a time step following a packet loss, the encoder and decoder does not use the same prediction in the prediction error and the reconstruction. In order to facilitate the use of ZDMD coding for speech or audio transmission, designing ZDMD schemes without the feedback channel is a topic for future research.

## 7.2 Simulation Results

### 7.2.1 Using AR(1) Predictors

From the simulations, it is seen that the best rate-distortion performance using AR(1) predictors is obtained by the index assignment scheme. For the rates plotted in Fig. 6.2, the loss in MSE distortion of the AR(1) index assignment scheme compared to the theoretical lower bound is about 3.5 dB. Some of this loss can be attributed to the space-filling loss of uniform quantization, which is about 1.5 dB [8].

### 7.2.2 Using AR(2) Predictors

The proposed design for a ZDMD scheme using index assignment has made it possible to use the optimal predictor for an AR( $p$ ) source of any order  $p$  without having to spend bits not related directly to the source. When comparing the rate-distortion performance of the index assignment scheme using the optimal AR(2) predictor to the schemes using AR(1) predictors, we see that a better rate-distortion performance is obtained. This is due to the fact that the AR(2) predictor minimizes the MSE of the prediction, when the source is an AR(2) source, hence the variance of the prediction error samples are minimized when using the AR(2) predictor. Since rates are directly related to the variance of the prediction error samples, we can achieve a smaller sum-rate using the same quantizer step sizes, or equivalently, we can use smaller quantizer step sizes for the same rate, thus achieving a smaller MSE distortion.

### 7.2.3 Packet Loss

When different packet loss probabilities are experienced, different levels of central and side distortion is optimal. E.g., when the packet loss probability is zero, we always use the central decoder. For the staggered quantizer this means that the maximum amount of rate is spend on the central quantizer and for the index assignment scheme it means that the highest possible nesting ratio is chosen. When the packet loss probability increases, the side reconstructions are used more often. Therefore, for higher packet loss probabilities we require smaller side distortions.

From the simulation results concerning packet loss, it is seen from Figs. 6.3 and 6.4, that the performance of the schemes assuming AR(1) are similar to the lower bound with an average deviation from the lower bound of 0.38 dB and 0.68 dB for the index assignment scheme and scheme using staggered quantization, respectively. Thus we have demonstrated the robustness against packet loss of the operational ZDMD coding scheme.

## 8. Conclusion

We have in this work studied ZDMD coding for the two-descriptions case with perfect feedback from the decoder as well as the design of operational ZDMD coding schemes. We have considered the symmetric case of ZDMD coding. To this end, we have developed a novel operational ZDMD coding scheme for stationary scalar AR( $p$ ) sources based on index assignment and DPCM quantization under the assumption of feedback from the decoder.

The proposed index assignment scheme uses the MMSE predictor of the source sample  $X_t$  given the previous reconstructions  $Y_{t-1}$  under the assumption of an stationary scalar AR( $p$ ) source. The trade-off between central and side distortion is controlled varying the so-called nesting ratio  $r = \Delta_S/\Delta_C$ .

In addition, we studied the generalization of the scheme developed in [9] which uses staggered quantization and sub-optimal prediction of  $X_t$  assuming model order  $p = 1$  in the DPCM quantization. We generalized the scheme to use the MMSE predictor of any order  $p$ . By the theoretical central and side distortion of the staggered ZDMD scheme, it was shown that the scheme using sub-optimal predictors has the best performance among schemes of this structure. This is due to the necessity of spending a bit on the sign of the difference between previous reconstructions when using the MMSE predictor.

Using the MMSE predictor to for order  $p = 1$ , the operational MSE performance of the index assignment scheme achieves a gain of 0.5 dB in MSE performance compared to the scheme developed in [9]. We argue that the gain can be attributed to the use of the MMSE prediction instead of the sub-optimal.

Compared to the theoretical lower bound for ZDMD coding of AR(1) sources with MSE distortion constraints, simulations showed a loss in MSE distortion of about 3.5 dB for the index assignment scheme assuming model order  $p = 1$ .

By analysis of the of the operational coding scheme, we have showed that for a stationary scalar AR(2) source, a gain in MSE error performance of about 3.5 dB is obtained when using the MMSE predictor for the AR(2) compared to the MMSE predictor for the corresponding AR(1) modeling of source.

Finally, by simulation of the average MSE distortion under i.i.d. packet losses, we

have demonstrated the robustness of the operational ZDMD coding schemes compared to the theoretical lower bound on the average MSE distortion.

## 8.1 Future Work

We have studied the design of operational ZDMD coders, but further research about ZDMD coding still remains.

We compare the performance of the operational ZDMD coding schemes to the theoretical lower bound for an AR(1) source and MSE distortion constraints developed in [8]. During the time frame of the project, it has not been possible to extend the theoretical lower bound to scalar AR( $p$ ) sources for  $p > 0$ . Since the information theoretic symmetric ZDMD RDF Theorems 4.8 and 4.11 holds for any stationary source, we speculate that the extension to scalar AR( $p$ ) sources for  $p > 0$  can be obtained by expressing the scalar AR( $p$ ) source as a vector AR(1) source following the approach in [29].

It may also be possible to generalize Theorems 4.8 and 4.11 to vector AR(1) sources using the results of [30] and [7] and then obtain a characterization similar to Theorem 4.14. Then similar to [29], express the scalar AR( $p$ ) source as a vector AR(1) source and use the characterization of the symmetric ZDMD RDF for vector AR(1) sources as the lower bound on the scalar AR( $p$ ) source.

Since the feedback channel from the decoder is infeasible in e.g. practical wireless transmission of audio, it would be interesting to study ZDMD coding under packet loss without assuming feedback from the decoder. In particular, the design of operational ZDMD coding schemes would be relevant in this case.

# Bibliography

- [1] G. Schuller, J. Kovacevic, F. Masson, and V. Goyal, “Robust low-delay audio coding using multiple descriptions”, *IEEE Transactions on Speech and Audio Processing*, vol. 13, no. 5, pp. 1014–1024, 2005. DOI: 10.1109/TSA.2005.853205.
- [2] J. Østergaard, D. E. Quevedo, and J. Jensen, “Low delay moving-horizon multiple-description audio coding for wireless hearing aids”, in *2009 IEEE International Conference on Acoustics, Speech and Signal Processing*, 2009, pp. 21–24. DOI: 10.1109/ICASSP.2009.4959510.
- [3] V. Goyal, “Multiple description coding: Compression meets the network”, *IEEE Signal Processing Magazine*, vol. 18, no. 5, pp. 74–93, 2001. DOI: 10.1109/79.952806.
- [4] L. Ozarow, “On a source-coding problem with two channels and three receivers”, *The Bell System Technical Journal*, vol. 59, no. 10, pp. 1909–1921, 1980. DOI: 10.1002/j.1538-7305.1980.tb03344.x.
- [5] A. Gamal and T. Cover, “Achievable rates for multiple descriptions”, *IEEE Transactions on Information Theory*, vol. 28, no. 6, pp. 851–857, 1982. DOI: 10.1109/TIT.1982.1056588.
- [6] J. Østergaard, Y. Kochman, and R. Zamir, “Colored-gaussian multiple descriptions: Spectral and time-domain forms”, *IEEE Transactions on Information Theory*, vol. 62, no. 10, pp. 5465–5483, 2016. DOI: 10.1109/TIT.2015.2513773.
- [7] P. A. Stavrou, J. Østergaard, and C. D. Charalambous, “Zero-delay rate distortion via filtering for vector-valued gaussian sources”, *IEEE Journal of Selected Topics in Signal Processing*, vol. 12, no. 5, pp. 841–856, 2018. DOI: 10.1109/JSTSP.2018.2855046.
- [8] A. J. Fuglsig and J. Østergaard, “Zero-delay multiple descriptions of stationary scalar gauss-markov sources”, *Entropy*, vol. 21, no. 12, Dec. 2019, ISSN: 1099-4300. DOI: 10.3390/e21121185.
- [9] U. Samarawickrama and J. Liang, “A two-stage algorithm for multiple description predictive coding”, in *2008 Canadian Conference on Electrical and Computer Engineering*, 2008, pp. 000 685–000 688. DOI: 10.1109/CCECE.2008.4564622.

- [10] N. S. Jayant and P. Noll, *Digital coding of waveforms : principles and applications to speech and video*, eng, 3. printing., ser. Prentice-Hall signal processing series. Englewood Cliffs, N.J: Prentice-Hall, 1984, ISBN: 0132119137.
- [11] J. Chen, C. Tian, and S. Diggavi, “Multiple description coding for stationary gaussian sources”, *IEEE Transactions on Information Theory*, vol. 55, no. 6, pp. 2868–2881, 2009. DOI: 10.1109/TIT.2009.2018178.
- [12] T. M. Cover and J. A. Thomas, *Elements of Information Theory*, 2nd ed. John Wiley & Sons, 2006, ISBN: 978-0-471-24195-9.
- [13] S. M. Kay, *Intuitive Probability and Random Processes Using Matlab*, eng, Elektronisk udgave. Boston, MA: Steven M. Kay, 2006, ISBN: 9780387241579.
- [14] J. Chen, C. Tian, T. Berger, and S. S. Hemami, “Multiple description quantization via gram–schmidt orthogonalization”, *IEEE Transactions on Information Theory*, vol. 52, no. 12, pp. 5197–5217, 2006. DOI: 10.1109/TIT.2006.885498.
- [15] J. Østergaard, Y. Kochman, and R. Zamir, “An asymmetric difference multiple description gaussian noise channel”, in *2017 Data Compression Conference (DCC)*, 2017, pp. 360–369. DOI: 10.1109/DCC.2017.16.
- [16] J. Østergaard, “Stabilizing error correction codes for control over erasure channels”, *IEEE Transactions on Control of Network Systems*, pp. 1–1, 2022. DOI: 10.1109/TCNS.2022.3165514.
- [17] M. S. Derpich, E. I. Silva, and J. Østergaard, *Fundamental inequalities and identities involving mutual and directed informations in closed-loop systems*, 2013. arXiv: 1301.6427 [cs.IT].
- [18] J. L. Massey, “Causality, feedback and directed information”, *Proc. Int. Symp. Inf. Theory Appl.*, pp. 303–305, Nov. 1990. DOI: 10.1109/TIT.1982.1056552.
- [19] J. Massey and P. Massey, “Conservation of mutual and directed information”, in *Proceedings. International Symposium on Information Theory, 2005. ISIT 2005.*, 2005, pp. 157–158. DOI: 10.1109/ISIT.2005.1523313.
- [20] M. S. Derpich and J. Østergaard, “Improved upper bounds to the causal quadratic rate-distortion function for gaussian stationary sources”, *IEEE Transactions on Information Theory*, vol. 58, no. 5, pp. 3131–3152, 2012. DOI: 10.1109/TIT.2012.2184669.
- [21] T. Tanaka, K.-K. K. Kim, P. A. Parrilo, and S. K. Mitter, “Semidefinite programming approach to gaussian sequential rate-distortion trade-offs”, *IEEE Transactions on Automatic Control*, vol. 62, no. 4, pp. 1896–1910, 2017. DOI: 10.1109/TAC.2016.2601148.
- [22] T. Wiegand and H. Schwarz, “Source coding: Part i of fundamentals of source and video coding”, *Foundations and Trends® in Signal Processing*, vol. 4, no. 1–2, pp. 1–222, 2011, ISSN: 1932-8346. DOI: 10.1561/2000000010. [Online]. Available: <http://dx.doi.org/10.1561/2000000010>.

- [23] E. I. Silva, M. S. Derpich, and J. Østergaard, “A framework for control system design subject to average data-rate constraints”, *IEEE Transactions on Automatic Control*, vol. 56, no. 8, pp. 1886–1899, 2011. DOI: 10.1109/TAC.2010.2098070.
- [24] H. Madsen and P. Thyregod, *Introduction to general and generalized linear models*. eng, London, 2011.
- [25] S. Haykin and T. Prabhakar, *Adaptive Filter Theory*, ser. Always learning. Pearson, 2014, ISBN: 9780273764083. [Online]. Available: <https://books.google.dk/books?id=Tf6oZwEACAAJ>.
- [26] Y. Frank-Dayana and R. Zamir, “Dithered lattice-based quantizers for multiple descriptions”, *IEEE Transactions on Information Theory*, vol. 48, no. 1, pp. 192–204, 2002. DOI: 10.1109/18.971748.
- [27] R. Zamir, B. Nazer, Y. Kochman, and I. Bistriz, *Lattice Coding for Signals and Networks: A Structured Coding Approach to Quantization, Modulation and Multiuser Information Theory*. Cambridge University Press, 2014. DOI: 10.1017/CB09781139045520.
- [28] J. Østergaard, J. Jensen, and R. Heusdens, “N-channel entropy-constrained multiple-description lattice vector quantization”, *IEEE Transactions on Information Theory*, vol. 52, no. 5, pp. 1956–1973, 2006. DOI: 10.1109/TIT.2006.872847.
- [29] P. Stavrou and J. Østergaard, “A lower bound on causal and zero-delay rate distortion for scalar gaussian autoregressive sources”, English, in *Proceedings of the 2017 Symposium on Information Theory and Signal Processing in the Benelux*, R. Heusdens and J. Weber, Eds., ser. Symposium on Information Theory and Signal Processing in the Benelux (SITB), 2017 Symposium on Information Theory and Signal Processing in the Benelux ; Conference date: 11-05-2017 Through 12-05-2017, Delft University of Technology, 2017, pp. 207–214, ISBN: 978-94-6186-811-4. [Online]. Available: [http://www.w-i-c.org/CFP\\_SITB2017.pdf](http://www.w-i-c.org/CFP_SITB2017.pdf).
- [30] H. Wang and P. Viswanath, “Vector gaussian multiple description with individual and central receivers”, *IEEE Transactions on Information Theory*, vol. 53, no. 6, pp. 2133–2153, 2007. DOI: 10.1109/TIT.2007.896880.



# A. Information Theory

In this appendix, we will present the basic definitions and results regarding information and coding theory. The content of this chapter is based on [12].

## A.1 Entropy and Mutual Information

In this section, the notion of entropy and mutual information will be presented. We will initially present the definitions and results regarding discrete random variables. Let  $X$  be a discrete random variable with alphabet  $\mathcal{X}$  and probability mass function (PMF)  $p(x) = \mathcal{P}\{X = x\}$ , for  $x \in \mathcal{X}$ .

### Definition A.1 (Entropy [12])

The entropy  $H(X)$  of a discrete random variable  $X$  is defined as

$$H(X) = - \sum_{x \in \mathcal{X}} p(x) \log(p(x)). \quad (\text{A.1})$$

Unless otherwise stated, the logarithm is to base 2 and the entropy is expressed in bits. By convention, we let  $0 \log(0) = 0$ , which is justified by continuity since  $x \log(x) \rightarrow 0$  as  $x \rightarrow 0$ . This means, that adding terms of zero probability does not affect the entropy.

We denote by  $\mathbb{E}$  the expected value operator, e.g., for a random variable  $X \sim p(x)$ , the expected value of  $g(X)$  is

$$\mathbb{E}_p [g(X)] = \sum_{x \in \mathcal{X}} g(x)p(x). \quad (\text{A.2})$$

When the PMF is understood from the context, we write  $\mathbb{E} [g(X)]$  instead. From Definition A.1, it is seen that the entropy can be understood as the expected value of the random variable  $\log\left(\frac{1}{p(X)}\right)$ , where  $X \sim p(x)$ . Thus

$$H(X) = \mathbb{E}_p \left[ \log\left(\frac{1}{p(X)}\right) \right]. \quad (\text{A.3})$$

From the fact that  $\log\left(\frac{1}{p(x)}\right) \geq 0$  since  $0 \leq p(x) \leq 1$ , it follows that the entropy is non-negative, i.e.,  $H(X) \geq 0$ .

Additionally, it is possible to change the base of the logarithm in the definition of entropy by multiplying by an appropriate factor, as seen from

$$\begin{aligned}
 H_b(X) &= - \sum_{x \in \mathcal{X}} p(x) \log_b(p(x)) \\
 &= - \sum_{x \in \mathcal{X}} p(x) \log_b\left(a^{\log_a(p(x))}\right) \\
 &= - \sum_{x \in \mathcal{X}} p(x) \log_b(a) \log_a(p(x)) \\
 &= \log_b(a) H_a(X).
 \end{aligned} \tag{A.4}$$

The definition of entropy is extended to the entropy of two discrete random variables in the following definition.

**Definition A.2 (Joint Entropy [12])**

The joint entropy  $H(X, Y)$  of a pair of discrete random variables  $(X, Y) \sim p(x, y)$  is defined by

$$H(X, Y) = - \sum_{x \in \mathcal{X}} \sum_{y \in \mathcal{Y}} p(x, y) \log(p(x, y)) = -\mathbb{E}[\log(p(X, Y))]. \tag{A.5}$$

**Definition A.3 (Conditional Entropy [12])**

For  $(X, Y) \sim p(x, y)$ , the conditional entropy  $H(Y|X)$  is defined as

$$H(Y|X) = - \sum_{x \in \mathcal{X}} \sum_{y \in \mathcal{Y}} p(x, y) \log(p(y|x)) = -\mathbb{E}[\log(p(Y|X))]. \tag{A.6}$$

The joint entropy of the pair of random variables  $(X, Y)$  can be decomposed into the sum of the entropy of  $X$  and the conditional entropy of  $Y$  given  $X$ .

**Theorem A.4 (Chain Rule [12])**

$$H(X, Y) = H(X) + H(Y|X). \tag{A.7}$$

*Proof.*

$$\begin{aligned}
H(X, Y) &= - \sum_{x \in \mathcal{X}} \sum_{y \in \mathcal{Y}} p(x, y) \log(p(x, y)) \\
&= - \sum_{x \in \mathcal{X}} \sum_{y \in \mathcal{Y}} p(x, y) \log(p(x)p(y|x)) \\
&= - \sum_{x \in \mathcal{X}} \sum_{y \in \mathcal{Y}} p(x, y) \log(p(x)) - \sum_{x \in \mathcal{X}} \sum_{y \in \mathcal{Y}} p(x, y) \log(p(y|x)) \\
&= - \sum_{x \in \mathcal{X}} p(x) \log(p(x)) - \sum_{x \in \mathcal{X}} \sum_{y \in \mathcal{Y}} p(x, y) \log(p(y|x)) \\
&= H(X) + H(Y|X).
\end{aligned} \tag{A.8}$$

■

### Corollary A.5

$$H(X, Y|Z) = H(X|Z) + H(Y|X, Z). \tag{A.9}$$

The entropy of a random variable is a measure of the uncertainty of the random variable, thus it is a measure of the amount of information required on average to describe a random variable [12].

### Example A.6

Consider the two random variables

$$X = \begin{cases} a & \text{with probability } \frac{1}{4} \\ b & \text{with probability } \frac{1}{4} \\ c & \text{with probability } \frac{1}{4} \\ d & \text{with probability } \frac{1}{4} \end{cases} \quad Y = \begin{cases} a & \text{with probability } \frac{1}{2} \\ b & \text{with probability } \frac{1}{4} \\ c & \text{with probability } \frac{1}{8} \\ d & \text{with probability } \frac{1}{8} \end{cases}$$

The entropy of these random variables is

$$H(X) = -\frac{4}{4} \log\left(\frac{1}{4}\right) = -\log\left(\frac{1}{4}\right) = 2 \text{ bits} \tag{A.10}$$

and

$$H(Y) = -\frac{1}{2} \log\left(\frac{1}{2}\right) - \frac{1}{4} \log\left(\frac{1}{4}\right) - \frac{2}{8} \log\left(\frac{1}{8}\right) = \frac{7}{4} \text{ bits.} \tag{A.11}$$

The example suggests that when the distribution of a discrete random variable is uniform, the entropy is maximized. This can be interpreted as the uncertainty of the random variable  $X$  is greater than the uncertainty of  $Y$ . This means on average, fewer bits are required to describe  $Y$  than  $X$ . The fact that the uniform distribution maximizes the entropy will be shown later in Theorem A.12. But first we will introduce relative entropy and mutual information

The relative entropy is a measure of the distance between two distributions.

**Definition A.7 (Relative Entropy [12])**

The relative entropy between two PMF's  $p(x)$  and  $q(x)$  is defined as

$$D(p||q) = \sum_{x \in \mathcal{X}} p(x) \log \left( \frac{p(x)}{q(x)} \right) = \mathbb{E}_p \left[ \log \left( \frac{p(X)}{q(X)} \right) \right]. \quad (\text{A.12})$$

In the relative entropy, the convention is that  $0 \log \left( \frac{0}{0} \right) = 0$ ,  $0 \log \left( \frac{0}{q} \right) = 0$ , and  $p \log \left( \frac{p}{0} \right) = \infty$ . Thus the  $D(p||q) = \infty$  if there is any symbol  $x \in \mathcal{X}$  with  $p(x) > 0$  and  $q(x) = 0$ .

The relative entropy is always non-negative, but it is not a true distance since it is not symmetric and it does not satisfy the triangle inequality. However, it can be useful to think of relative entropy as the distance between distributions. [12]

**Theorem A.8 (Non-negativity of Relative Entropy [12])**

Let  $p(x)$ ,  $q(x)$ ,  $x \in \mathcal{X}$  be two PMF's. Then

$$D(p||q) \geq 0 \quad (\text{A.13})$$

with equality if and only if  $p(x) = q(x)$  for all  $x \in \mathcal{X}$ .

*Proof.*

Let  $A = \{x : p(x) > 0\}$  be the support set of  $p(x)$ . Then

$$\begin{aligned} -D(p||q) &= -\mathbb{E}_p \left[ \log \left( \frac{p(X)}{q(X)} \right) \right] \\ &= \mathbb{E}_p \left[ \log \left( \frac{q(X)}{p(X)} \right) \right]. \end{aligned} \quad (\text{A.14})$$

Since  $\log(t)$  is a strictly concave function, we have by Jensen's inequality [12, The-

orem 2.6.2] that  $\mathbb{E}_p[\log(X)] \leq \log(\mathbb{E}_p[X])$ . Hence

$$\mathbb{E}_p \left[ \log \left( \frac{q(X)}{p(X)} \right) \right] \leq \log \left( \mathbb{E}_p \left[ \frac{q(X)}{p(X)} \right] \right) \quad (\text{A.15})$$

$$= \log \left( \sum_{x \in A} p(x) \frac{q(x)}{p(x)} \right)$$

$$= \log \left( \sum_{x \in A} q(x) \right)$$

$$\leq \log \left( \sum_{x \in \mathcal{X}} q(x) \right) \quad (\text{A.16})$$

$$= \log(1)$$

$$= 0.$$

Again since  $\log(t)$  is strictly concave, we have by [12, Theorem 2.6.2] equality in (A.15) if and only if  $\frac{q(x)}{p(x)}$  is constant for all  $x$ , i.e.,  $q(x) = cp(x)$  for all  $x$ . Thus

$$\sum_{x \in A} q(x) = c \sum_{x \in A} p(x) = c. \quad (\text{A.17})$$

In (A.16), we have equality only if

$$\sum_{x \in A} q(x) = \sum_{x \in \mathcal{X}} q(x) = 1. \quad (\text{A.18})$$

This implies that  $c = 1$  and therefore  $D(p||q) = 0$  if and only if  $p(x) = q(x)$  for all  $x \in \mathcal{X}$ . ■

We now introduce mutual information as a special case of relative entropy. Mutual information is a measure of the reduction in uncertainty of one random variable due to knowledge of another.

### Definition A.9 (Mutual Information [12])

Let  $X$  and  $Y$  be two discrete random variables with joint PMF  $p(x, y)$  and marginal PMF's  $p(x)$  and  $p(y)$ . The mutual information  $I(X; Y)$  is the relative entropy

between the joint PMF and the product of the marginals, i.e.,

$$\begin{aligned}
 I(X; Y) &= D(p(x, y) \| p(x)p(y)) \\
 &= \sum_{x \in \mathcal{X}} \sum_{y \in \mathcal{Y}} p(x, y) \log \left( \frac{p(x, y)}{p(x)p(y)} \right) \\
 &= \mathbb{E}_{p(x, y)} \left[ \log \left( \frac{p(X, Y)}{p(X)p(Y)} \right) \right]
 \end{aligned} \tag{A.19}$$

As mutual information is a special case of the relative entropy, it is also non-negative.

**Corollary A.10 (Non-negativity of Mutual Information)**

For two random variables  $X$  and  $Y$ ,

$$I(X; Y) \geq 0, \tag{A.20}$$

with equality if and only if  $X$  and  $Y$  are independent.

*Proof.*

$I(X; Y) = D(p(x, y) \| p(x)p(y)) \geq 0$ , with equality if and only if  $p(x, y) = p(x)p(y)$ , which is only the case if  $X$  and  $Y$  are independent. ■

Mutual information is related to the entropy of the random variables through the following relations.

**Theorem A.11**

For the random variables  $X$  and  $Y$ , we have the following relations:

$$I(X; Y) = H(X) - H(X|Y) \tag{A.21}$$

$$I(X; Y) = H(Y) - H(Y|X) \tag{A.22}$$

$$I(X; Y) = H(X) + H(Y) - H(X, Y) \tag{A.23}$$

$$I(X; Y) = I(Y; X) \tag{A.24}$$

$$I(X; X) = H(X) \tag{A.25}$$

*Proof.*

By rewriting the mutual information we obtain (A.21)

$$\begin{aligned}
 I(X; Y) &= \sum_{x,y} p(x, y) \log \left( \frac{p(x, y)}{p(x)p(y)} \right) \\
 &= \sum_{x,y} p(x, y) \log \left( \frac{p(x|y)}{p(x)} \right) \\
 &= - \sum_{x,y} p(x, y) \log(p(x)) + \sum_{x,y} p(x, y) \log(p(x|y)) \\
 &= H(X) - H(X|Y).
 \end{aligned} \tag{A.26}$$

Since  $p(x|y)p(y) = p(x, y) = p(y|x)p(x)$ , we obtain (A.22) with the same argument. The relation in (A.23) follows from (A.21) and  $H(X, Y) = H(X) + H(Y|X)$  as stated in Theorem A.4. The symmetry property in (A.24) follows from the definition of mutual information. For the last relation in (A.25), note that

$$I(X; X) = H(X) - H(X|X) = H(X). \tag{A.27}$$

■

With the definitions of relative entropy and mutual information we state that the uniform distribution over  $\mathcal{X}$  is the maximum entropy distribution over this range. Furthermore, we will show that conditioning reduces entropy.

**Theorem A.12 (Maximum Entropy Distribution is Uniform [12])**

Let  $|\mathcal{X}|$  denote the number elements in the range of the discrete random variable  $X$ , then

$$H(X) \leq \log(|\mathcal{X}|), \tag{A.28}$$

with equality if and only if  $X$  has uniform distribution over  $\mathcal{X}$ .

*Proof.*

Let  $u(x) = \frac{1}{|\mathcal{X}|}$  be the uniform PMF over  $\mathcal{X}$  and let  $p(x)$  be the PMF of  $X$ . Then

$$\begin{aligned}
 D(p||u) &= \sum_{x \in \mathcal{X}} p(x) \log \left( \frac{p(x)}{u(x)} \right) \\
 &= \sum_{x \in \mathcal{X}} p(x) \log(p(x)) - \sum_{x \in \mathcal{X}} p(x) \log \left( \frac{1}{|\mathcal{X}|} \right) \\
 &= \log(|\mathcal{X}|) - H(X),
 \end{aligned} \tag{A.29}$$

and by the non-negativity of relative entropy we have

$$0 \leq D(p||u) = \log(|\mathcal{X}|) - H(X). \quad (\text{A.30})$$

■

We conclude the treatment of entropy with a result on the conditional entropy.

**Theorem A.13 (Conditioning Reduces Entropy [12])**

$$H(X|Y) \leq H(X)$$

with equality if and only if  $X$  and  $Y$  are independent.

*Proof.*

$0 \leq I(X;Y) = H(X) - H(X|Y)$ , and with  $X \perp Y$ , the equality follows from Corollary A.10. ■

## A.2 Differential Entropy

The focus has until now been on discrete random variables, but in many cases we consider continuous random variables. In this section we therefore introduce the differential entropy, which is the entropy of a continuous random variable.

**Definition A.14 (Differential Entropy [12])**

The differential entropy  $h(X)$  of a continuous random variable  $X$  with density  $f(x)$  is defined as

$$h(X) = - \int_S f(x) \log(f(x)) dx, \quad (\text{A.31})$$

where  $S$  is the support of  $f(x)$ .

In contrast to the entropy of a discrete random variable, the differential entropy can be negative. Consider for example a random variable with density  $f(x) = \frac{1}{a}$  for  $x \in [0; a]$ , i.e, a uniformly distributed random variable. Then the differential entropy is

$$h(X) = - \int_0^a \frac{1}{a} \log\left(\frac{1}{a}\right) dx = \log(a). \quad (\text{A.32})$$

If  $0 < a < 1$ , then  $h(X) < 0$ . Another property of differential entropy is that for a given variance, the Gaussian distribution maximizes the entropy. As an indicative example let's consider the entropy of a zero-mean Gaussian random variable  $X \sim \phi(x) = \frac{1}{\sqrt{2\pi\sigma^2}} e^{-\frac{x^2}{2\sigma^2}}$  with variance  $\sigma^2 = \frac{a^2}{12}$ . We will calculate the entropy in nats.

$$\begin{aligned}
h(X) &= - \int \phi(x) \ln(\phi(x)) dx \\
&= - \int \phi(x) \left( -\frac{x^2}{2\sigma^2} - \frac{1}{2} \ln(2\pi\sigma^2) \right) dx \\
&= \mathbb{E} \left[ \frac{x^2}{2\sigma^2} + \frac{1}{2} \ln(2\pi\sigma^2) \right] \\
&= \frac{\mathbb{E}[X^2]}{2\sigma^2} + \frac{1}{2} \ln(2\pi\sigma^2) \\
&= \frac{1}{2} + \frac{1}{2} \ln(2\pi\sigma^2) \\
&= \frac{1}{2} \ln(e) + \frac{1}{2} \ln(2\pi\sigma^2) \\
&= \frac{1}{2} \ln(2\pi e\sigma^2), \tag{A.33}
\end{aligned}$$

where  $\ln(\cdot)$  denotes the logarithm to base  $e$ . Changing the base of the logarithm yields the entropy in bits given by

$$h(X) = \frac{1}{2} \frac{\ln(2\pi e\sigma^2)}{\ln(2)} = \frac{1}{2} \log(2\pi e\sigma^2). \tag{A.34}$$

Now if the variance is  $\sigma^2 = \frac{a^2}{12}$  we have that

$$h(X) = \frac{1}{2} \log\left(2\pi e \frac{a^2}{12}\right) = \frac{1}{2} \log\left(\frac{2\pi e}{12}\right) + \log(a), \tag{A.35}$$

which is larger than the entropy of the uniform distribution with the same variance since  $\frac{1}{2} \log\left(\frac{2\pi e}{12}\right) > 0$ . It will be shown later in Theorem A.21 that the Gaussian distribution maximizes the entropy over distributions with the same variance.

Before introducing joint differential entropy and mutual information for continuous random variables, we consider the relation between differential entropy and discrete entropy.

### Theorem A.15

Let  $X$  be a random variable with Riemann integrable density  $f(x)$ . Suppose the range of  $X$  is divided into bins of length  $\Delta$ . Let  $X^\Delta$  be the quantized random variable defined as

$$X^\Delta = x_i, \quad \text{if } i\Delta \leq X < (i+1)\Delta, \tag{A.36}$$

where  $x_i$  is the value in the  $i^{\text{th}}$  bin satisfying

$$f(x_i)\Delta = \int_{i\Delta}^{(i+1)\Delta} f(x) dx. \quad (\text{A.37})$$

Then

$$H(X^\Delta) + \log(\Delta) \rightarrow h(X), \quad \text{as } \Delta \rightarrow 0. \quad (\text{A.38})$$

Thus, the entropy of an  $n$ -bit quantization of a continuous random variable  $X$  is approximately  $h(X) + n$ .

We now extend the differential entropy to the differential entropy of several random variables.

**Definition A.16 (Joint Differential Entropy [12])**

The differential entropy of the set of random variables  $X^n = (X_1, X_2, \dots, X_n)$  with the joint density  $f(x_1, x_2, \dots, x_n)$  is defined by

$$h(X^n) = - \int f(x^n) \log(f(x^n)) dx^n. \quad (\text{A.39})$$

**Definition A.17 (Conditional Differential Entropy [12])**

For the random variables  $X$  and  $Y$  with joint density  $f(x, y)$ , the conditional differential entropy  $h(X|Y)$  is defined as

$$h(X|Y) = - \int f(x, y) \log(f(x|y)) dx dy. \quad (\text{A.40})$$

The chain rule of Theorem A.4 also apply for differential entropy, i.e.,

$$h(X, Y) = H(X) + H(Y|X) \quad (\text{A.41})$$

since by definition of conditional density  $f(y|x) = f(x, y)/f(x)$ .

As for discrete entropy we define the relative entropy and mutual information.

**Definition A.18 (Relative Entropy [12])**

The relative entropy  $D(f||g)$  between two densities  $f$  and  $g$  is defined by

$$D(f||g) = \int f(x) \log\left(\frac{f(x)}{g(x)}\right) dx. \quad (\text{A.42})$$

We let  $0 \log\left(\frac{0}{0}\right) = 0$ . Note that the relative entropy is only finite if the support set of  $f$  is contained in the support set of  $g$ .

**Definition A.19 (Mutual information [12])**

The mutual information between two random variables  $X$  and  $Y$  with joint density  $f(x, y)$  is defined as

$$I(X; Y) = D(f(x, y) \| f(x)f(y)) = \int f(x, y) \log\left(\frac{f(x, y)}{f(x)f(y)}\right) dx dy \quad (\text{A.43})$$

We will conclude the section about differential entropy by proving that the Gaussian distribution maximizes differential entropy.

**Theorem A.20 (Differential Entropy of Multivariate Gaussian [12])**

Let  $X^n = (X_1, X_2, \dots, X_n) \sim \mathcal{N}(\boldsymbol{\mu}, \boldsymbol{\Sigma})$ . Then

$$h(X^n) = \frac{1}{2} \log(2\pi e)^n |\boldsymbol{\Sigma}|, \quad (\text{A.44})$$

where  $|\boldsymbol{\Sigma}|$  denotes the determinant of  $\boldsymbol{\Sigma}$ .

*Proof.*

See [12, p. 250] ■

**Theorem A.21 (Maximum Differential Entropy, [12])**

Let the random vector  $\mathbf{X} \in \mathbb{R}^n$  have zero mean and covariance  $\mathbf{K} = \mathbb{E}[\mathbf{X}\mathbf{X}^T]$ . Then

$$h(\mathbf{X}) \leq \frac{1}{2} \log((2\pi e)^n |\mathbf{K}|), \quad (\text{A.45})$$

with equality if and only if  $\mathbf{X} \sim \mathcal{N}(0, \mathbf{K})$ .

*Proof.*

Let  $g(\mathbf{x})$  be any density satisfying  $\mathbb{E}_g[\mathbf{X}\mathbf{X}^T] = \mathbf{K}$ . Let  $\phi_{\mathbf{K}}$  be the density of  $\mathcal{N}(0, \mathbf{K})$ . Note that  $\log(\phi_{\mathbf{K}}(\mathbf{x}))$  is a quadratic form and by definition  $\mathbb{E}_{\phi_{\mathbf{K}}}(\mathbf{X}\mathbf{X}^T) =$

**K.** Then

$$\begin{aligned}
0 &\leq D(g\|\phi_{\mathbf{K}}) \\
&= \int g(\mathbf{x}) \log\left(\frac{g(\mathbf{x})}{\phi_{\mathbf{K}}(\mathbf{x})}\right) d\mathbf{x} \\
&= -h(\mathbf{X}) - \int g(\mathbf{x}) \log(\phi_{\mathbf{K}}(\mathbf{x})) d\mathbf{x} \\
&= -h(\mathbf{X}) - \int \phi_{\mathbf{K}}(\mathbf{x}) \log(\phi_{\mathbf{K}}(\mathbf{x})) d\mathbf{x} \\
&= \frac{1}{2} \log((2\pi e)^n |\mathbf{K}|) - h(\mathbf{X}), \tag{A.46}
\end{aligned}$$

where the substitution  $\int g(\mathbf{x}) \log(\phi_{\mathbf{K}}(\mathbf{x})) d\mathbf{x} = \int \phi_{\mathbf{K}}(\mathbf{x}) \log(\phi_{\mathbf{K}}(\mathbf{x})) d\mathbf{x}$  follows from the fact that

$$\mathbb{E}_g[\log(\phi_{\mathbf{K}}(\mathbf{X}))] = \mathbb{E}_{\phi_{\mathbf{K}}}[\log(\phi_{\mathbf{K}}(\mathbf{X}))]. \tag{A.47}$$

■

## B. WS: Source Coding

In this appendix, we will describe the basics of source coding. The primary task of source coding is to represent a source signal by the smallest possible number of bits while ensuring reconstruction with an acceptable level of distortion, which is application specific [22, p. 6]. In general, we distinguish between two types of source coding, namely lossless source coding and lossy source coding. As the names suggest, no distortion is introduced using lossless coding, while distortion is introduced using lossy coding. In this section we will focus on the lossless source coding and lossy coding will be introduced in Appendix C.

We begin with a formal definition of a source code.

### Definition B.1 (Source Code [12])

A source code  $C$  for a random variable  $X$  is a mapping from the range of  $X$  to a set  $\mathcal{D}^*$  of finite-length strings of symbols from a  $D$ -ary alphabet, i.e.,  $C : \mathcal{X} \rightarrow \mathcal{D}^*$ . Furthermore,  $C(x)$  denotes the codeword corresponding to  $x$  and  $\ell(x)$  denotes the length of  $C(x)$ .

We will in this thesis only focus on the source codes using the binary alphabet  $\mathcal{D} = \{0, 1\}$ .

In lossless coding, we must be able to uniquely decode a codeword  $C(x)$  to its corresponding source symbol  $x$ . Therefore it is necessary that the source code is non-singular.

### Definition B.2 (Non-singular Source Code [12])

A code is said to be non-singular if every element  $x \in \mathcal{X}$  maps to a different codeword in  $\mathcal{D}^*$ , i.e., for any  $x, x' \in \mathcal{X}$  with

$$x \neq x' \Rightarrow C(x) \neq C(x').$$

However, Non-singularity does not suffice for unique decodability if a sequence of codewords is sent, which is usually the case in many practical situations.

$X$	Code A	Code B	Code C	Code D
1	0	0	10	0
2	0	010	00	10
3	0	01	11	110
4	0	10	110	111

**Table B.1:** Examples of codes**Definition B.3 (Uniquely Decodability [12])**

The extension  $C^*$  of a code  $C$  is the mapping from finite-length strings of symbols from  $\mathcal{X}$  to finite-length strings of symbols from  $\mathcal{D}$ , defined by

$$C(x_1x_2 \dots x_n) = C(x_1)C(x_2) \dots C(x_n), \quad (\text{B.1})$$

where  $C(x_1)C(x_2) \dots C(x_n)$  indicates concatenation of the corresponding codewords.

A code is called uniquely decodable if its extension is non-singular.

If a code is uniquely decodable, then there is not two finite-length strings of source symbols which yields the same codeword. However, one may need the entire codeword in order to decode even first source symbol.

**Definition B.4 (Instantaneous Code [12])**

A code is called a prefix code or instantaneous code if no codeword is a prefix of any other codeword.

Since no codeword is a prefix of another in an instantaneous code, a source symbol can be decoded as soon as the end of the corresponding codeword is reached. Therefore, instantaneous codes are also categorized as self-punctuating codes. In Table B.1, four examples of codes are given. Here code A is singular, code B is non-singular but not uniquely decodable, code C is uniquely decodable but not instantaneous, and code D is an instantaneous code.

The goal when designing a lossless code is to minimize the expected length of the codeword while ensuring unique decodability [22, p. 22].

**Definition B.5 (Expected Length [12])**

The expected length  $L(C)$  of a source code  $C$  for a random variable  $X$  with PMF  $p(x)$  is given by

$$L(C) = \sum_{x \in \mathcal{X}} p(x)\ell(x), \quad (\text{B.2})$$

where  $\ell(x)$  denotes the length of  $C(x)$ .

The following inequality limits the set of codeword lengths possible for instantaneous codes.

**Theorem B.6 (Kraft Inequality [12])**

For any instantaneous code over the binary alphabet  $\mathcal{D} = \{0, 1\}$ , the codeword lengths  $l_1, l_2, \dots, l_m$  must satisfy the inequality

$$\sum_{i=1}^m 2^{-l_i} \leq 1.$$

Conversely, for any set of codeword lengths satisfying this inequality, there exists an instantaneous code with these codeword lengths.

*Proof.*

For a proof see [12, pp. 107-109] ■

Actually, the Kraft inequality must also be satisfied for any uniquely decodable code, as shown in [12, Theorem 5.5.1]. Thus, even though the set of uniquely decodable codes is larger than the set of instantaneous codes, we can always find a instantaneous code with the same codeword lengths as any uniquely decodable code. Hence, instantaneous codes are the ones used in practice [22, p. 27].

In the following we will find bounds on the expected codeword length for optimal instantaneous codes, where optimal refers to the instantaneous codes with minimum expected codeword length.

**Theorem B.7**

The expected length  $L$  of any instantaneous binary code for a random variable  $X$  is greater than or equal to the entropy  $H(X)$ , i.e.,

$$L \geq H(X), \tag{B.3}$$

with equality if and only if  $2^{-l_i} = p_i$ , where  $l_i$  and  $p_i$  is the length of the codeword and the probability, respectively, for the  $i^{\text{th}}$  symbol in  $\mathcal{X}$ .

*Proof.*

By Definition B.5

$$L = \sum p_i l_i = \sum p_i \log_2 \left( 2^{l_i} \right). \quad (\text{B.4})$$

We can now write the difference  $L - H(X)$  as

$$\begin{aligned} L - H(X) &= \sum p_i \log_2 \left( 2^{l_i} \right) + \sum p_i \log_2(p_i) \\ &= \sum p_i \log_2 \left( 2^{l_i} p_i \right) \\ &= \frac{1}{\ln(2)} \sum p_i \ln \left( 2^{l_i} p_i \right), \end{aligned} \quad (\text{B.5})$$

where the last equality follows from the same argument as in (A.4). By Lemma B.8

$$L - H(X) \geq \frac{1}{\ln(2)} \sum p_i \left( 1 - \frac{1}{2^{l_i} p_i} \right) \quad (\text{B.6})$$

$$\begin{aligned} &= \frac{1}{\ln(2)} \left( 1 - \sum 2^{-l_i} \right) \\ &\geq \frac{1}{\ln(2)} (1 - 1) = 0, \end{aligned} \quad (\text{B.7})$$

where the last inequality follows from Kraft inequality Theorem B.6.

In (B.6) equality is obtained if  $2^{l_i} p_i = 1$  by Lemma B.8 which equivalent to  $2^{-l_i} = p_i$ . If  $2^{-l_i} = p_i$ , (B.6) reduced to

$$\frac{1}{\ln(2)} \sum p_i \left( 1 - \frac{1}{2^{l_i} p_i} \right) = \frac{1}{\ln(2)} \sum p_i (1 - 1) = 0, \quad (\text{B.8})$$

thus  $L = H(X)$  if  $2^{-l_i} = p_i$ . ■

In Theorem B.7, the equality is obtained if and only if  $2^{-l_i} = p_i$ . The codeword lengths  $l_i$  must be integers, thus the lower equality is only obtained if  $p_i \in \{1/2, 1/4, 1/8 \dots\}$ . In this case we can choose the length of the codewords as  $l_i = -\log(p_i)$  and  $L$  will equal  $H(X)$ . When  $-\log(p_i)$  is not an integer, we can choose

$$l_i = \left\lceil \log \left( \frac{1}{p_i} \right) \right\rceil, \quad (\text{B.9})$$

where  $\lceil x \rceil$  is the smallest integer  $\geq x$ . With these lengths, the Kraft inequality is still satisfied as

$$\sum 2^{-\lceil \log(\frac{1}{p_i}) \rceil} \leq \sum 2^{-\log(\frac{1}{p_i})} = \sum p_i = 1. \quad (\text{B.10})$$

Furthermore, we can show that with these codeword lengths

$$H(X) \leq L < H(X) + 1 \quad (\text{B.11})$$

since when we round up to the nearest integer

$$\log\left(\frac{1}{p_i}\right) \leq l_i < \log\left(\frac{1}{p_i}\right) + 1. \quad (\text{B.12})$$

By multiplying by  $p_i$  and summing over  $i$ , we obtain the bounds on the expected length. Since the expected length of an instantaneous code with the minimum expected codeword length cannot be larger than  $L$  with this choice of codeword length, we can conclude that the optimal expected codeword length  $L^*$  satisfies [12, pp. 112-113]

$$H(X) \leq L^* < H(X) + 1. \quad (\text{B.13})$$

The upper bound can be lowered by encoding an  $n$ -length string of source symbols from  $\mathcal{X}$  instead of each source symbol. In fact, if  $L_n$  denotes the expected length per source symbol, then

$$H(X) \leq L_n < H(X) + \frac{1}{n} \quad (\text{B.14})$$

if the source symbols are drawn i.i.d with respect to  $p(x)$ . [12, p. 113]

## B.1 Bound on Natural Logarithm

### Lemma B.8

$$\ln(a) \geq 1 - \frac{1}{a}, \quad \forall a > 0, \quad (\text{B.15})$$

with equality if and only if  $a = 1$ .

*Proof.*

Let

$$f(x) = \ln(x) - 1 + \frac{1}{x}, \quad \forall x > 0. \quad (\text{B.16})$$

We want to show that  $f(x) \geq 0$  for all  $x > 0$ . First we find the derivative of  $f$

$$f'(x) = \frac{1}{x} - \frac{1}{x^2} = \frac{x-1}{x^2} \quad (\text{B.17})$$

which only is zero at  $x = 1$ . Evaluating  $f$  in  $x = 1$  yields  $f(1) = \ln(1) - 1 + \frac{1}{1} = 0$ , and since the derivative is negative for  $x \in (0; 1)$  and positive for  $x \in (1; \infty)$ , we can conclude that  $f(x) \geq 0$  for all  $x > 0$  with equality if and only if  $x = 1$ . ■



## C. WS: Rate-Distortion Theory

In many practical situations of communication where the source is the result of some physical event, the source take on a value from a continuous range. Therefore it is not possible to transmit such source with a finite amount of bits, since the description of an arbitrary real number requires an infinite amount of bits. To enable a finite rate, some distortion must be introduced to the representation of the continuous random variable. The distance from the source to the representation is measured by a so-called distortion measure. Given a source distribution and a distortion measure, in rate-distortion theory we seek to find the minimum expected distortion achievable for a specific rate. Or equivalently, find the minimum rate required to achieve a particular distortion. [12, p. 301]

In order to encode a continuous random variable into a finite set of codewords with a finite number of bits, quantization must be applied. As described in [12, pp. 301-303], quantization of blocks of  $n$  realizations of a random variable using  $nR$  bits achieves a lower distortion than quantization of each individual sample using  $R$  bits, even if the realizations are i.i.d. Therefore, we will consider the encoding of a sequence of source symbols  $X^n = (X_1, X_2, \dots, X_n)$  with  $X_i \stackrel{\text{i.i.d.}}{\sim} p(x)$  for  $x \in \mathcal{X}$ .

### Definition C.1 (Rate-Distortion Code [12])

Let  $X^n = (X_1, X_2, \dots, X_n)$  be a sequence of random variables with  $X_i \stackrel{\text{i.i.d.}}{\sim} p(x)$  for  $x \in \mathcal{X}$ . A  $(2^{nR}, n)$ -rate distortion code consists of an encoding function

$$f_n : \mathcal{X}^n \rightarrow \{1, 2, \dots, 2^{nR}\} \quad (\text{C.1})$$

and a decoding function

$$g_n : \{1, 2, \dots, 2^{nR}\} \rightarrow \mathcal{Y}^n \quad (\text{C.2})$$

where  $\mathcal{Y}$  is the reconstruction alphabet.

### C.1 Distortion

As mentioned, for continuous random variables, the encoding is not invertible, thus distortion is introduced. Distortion is also introduced when encoding discrete random

variables with a rate less than the entropy. We present the notion of distortion through the definitions in this section. We first introduce the distortion measure.

**Definition C.2 (Distortion Measure [12])**

A distortion function or distortion measure is a mapping from the pairs of source symbols and reconstruction symbols to the non-negative real numbers, i.e.,

$$d : \mathcal{X} \times \mathcal{Y} \rightarrow \mathbb{R}^+. \quad (\text{C.3})$$

The distortion  $d(x, y)$  is a measure of the cost of representing  $x$  by  $y$ .

Examples of commonly used distortion measures are the Hamming distortion given by

$$d(x, y) = \begin{cases} 0 & \text{if } x = y \\ 1 & \text{if } x \neq y \end{cases}, \quad (\text{C.4})$$

and the squared-error distortion given by

$$d(x, y) = (x - y)^2. \quad (\text{C.5})$$

The squared-error distortion is the most common used distortion measure for continuous source alphabets, and we will also use this distortion measure throughout this thesis. However, it is worth noting that the squared-error distortion is not an appropriate distortion measure for speech or sound coding, as two identical waveforms slightly shifted in time can result in a large squared-error distortion, even though these would sound identical to a human listener. [12, p. 305]

In order to extend the distortion measure to distortion between sequences, we use the following definition.

**Definition C.3 (Average Distortion Measure [12])**

The distortion between sequences  $x^n$  and  $y^n$  is given by

$$d(x^n, y^n) = \frac{1}{n} \sum_{i=1}^n d(x_i, y_i). \quad (\text{C.6})$$

That is, the distortion between sequences is the average per symbol distortion of the elements in the sequences. With this extension, using the squared-error distortion, the distortion between sequences is the mean squared error (MSE). Other appropriate extensions can be used, for example letting the distortion between sequences be the maximum per symbol distortion. However, we will restrict us to the the average per symbol distortion.

**Definition C.4 (Distortion [12])**

The distortion of a  $(2^{nR}, n)$ -code is defined as the expected value of the distortion measure between the source sequence and the reconstruction sequence, where the expectation is with respect to probability distribution on  $X$ , i.e.,

$$D = \mathbb{E}[d(X^n, g_n(f_n(X^n)))] \quad (\text{C.7})$$

## C.2 Rate-Distortion Function

As mentioned, the rate-distortion theory seeks to answer what is the minimum achievable rate for a given distortion.

**Definition C.5 (Rate-Distortion Region [12])**

A rate-distortion pair  $(R, D)$  is said to be achievable if there exist a sequence of  $(2^{nR}, n)$ -rate-distortion codes  $(f_n, g_n)$  such that

$$\lim_{n \rightarrow \infty} \mathbb{E}[d(X^n, g_n(f_n(X^n)))] \leq D. \quad (\text{C.8})$$

The closure of the set of achievable rate-distortion pairs is called the rate-distortion region.

**Definition C.6 (Rate-Distortion Function [12])**

The rate-distortion function  $R(D)$  is the infimum of all rates such that  $(R, D)$  is in the rate-distortion region of the source for a given  $D$ .

The infimum in Definition C.6 is over all rate-distortion codes and it is therefore not feasible to use the definition directly to find the rate-distortion function for a source and distortion measure. Instead, we can use the information rate-distortion function, which is equal to the operational rate-distortion function of Definition C.6.

**Theorem C.7**

For a source  $X$  with distribution  $p(x)$  and a distortion measure  $d$ , the information rate-distortion function is defined as

$$R^I(D) = \inf I(X; Y), \quad (\text{C.9})$$

where the infimum is over all conditional distributions  $p(y|x)$  such that

$$\sum_{(x,y)} p(x)p(y|x)d(x,y) \leq D. \quad (\text{C.10})$$

For an i.i.d source and bounded distortion measure

$$R(D) = R^I(D) = \inf I(X; Y). \quad (\text{C.11})$$

*Proof.*

For a proof see [12, pp. 316-318, 321-324] ■

As an example, the rate-distortion function of a white Gaussian source with variance  $\sigma_X^2$  is

$$R(D) = \begin{cases} \frac{1}{2} \log\left(\frac{\sigma_X^2}{D}\right) & 0 \leq D \leq \sigma_X^2 \\ 0 & D > \sigma_X^2 \end{cases} \quad (\text{C.12})$$

and it is achieved with the test-channel described in [12, pp. 310-311].